

A Model Problem for Nematic-Isotropic Transitions with Highly Disparate Elastic Constants

Dmitry Golovaty^{*1}, Michael Novack^{†3}, Peter Sternberg^{‡3}, and Raghavendra Venkatraman^{§4}

¹*Department of Mathematics, University of Akron, Akron, OH 44325*

^{2,3}*Department of Mathematics, Indiana University, Bloomington, IN 47405*

⁴*Department of Mathematical Sciences, Carnegie Mellon University, Pittsburgh, PA 15213*

December 3, 2018

Abstract: Continuing the program initiated in [17], we analyze a model problem based on highly disparate elastic constants that we propose in order to understand corners and cusps that form on the boundary between the nematic and isotropic phases in a liquid crystal. For a bounded planar domain Ω we investigate the $\varepsilon \rightarrow 0$ asymptotics of the variational problem

$$\inf \frac{1}{2} \int_{\Omega} \left(\frac{1}{\varepsilon} W(u) + \varepsilon |\nabla u|^2 + L_{\varepsilon} (\operatorname{div} u)^2 \right) dx$$

within various parameter regimes for $L_{\varepsilon} > 0$. Here $u : \Omega \rightarrow \mathbb{R}^2$ and W is a potential vanishing on the unit circle and at the origin. When $\varepsilon \ll L_{\varepsilon} \rightarrow 0$, we show that these functionals Γ -converge to a constant multiple of the perimeter of the phase boundary and the divergence penalty is not felt. However, when $L_{\varepsilon} \equiv L > 0$, we find that a tangency requirement along the phase boundary for competitors in the conjectured Γ -limit becomes a mechanism for development of singularities. We establish criticality conditions for this limit and under a non-degeneracy assumption on the potential we prove compactness of energy bounded sequences in L^2 . The role played by this tangency condition on the formation of interfacial singularities is investigated through several examples: each of these examples involves analytically rigorous reasoning motivated by numerical experiments. We argue that generically, “wall” singularities between \mathbb{S}^1 -valued states of the kind analyzed in [17] are expected near the defects along the phase boundary.

1 Introduction

Our purpose in this article is to propose and then initiate an analysis of a family of models inspired by phase transitions in liquid crystals. We have in mind the islands of phase known as tactoids, whose singular phase boundaries separate a locally well-ordered state of nematic liquid

^{*}dmitry@uakron.edu

[†]mrnovack@indiana.edu

[‡]sternber@indiana.edu

[§]rvenkatr@andrew.cmu.edu

crystals from a disordered isotropic state. Our models should be relevant more generally to other phase transition problems for which large disparity in the elastic constants is a salient feature. Our analysis is mainly rigorous, but also includes formal calculations as well as computational experiments.

Many models, of course, exist for nematic liquid crystals, including the Oseen-Frank energy, based on the elastic deformations of an \mathbb{S}^1 - or \mathbb{S}^2 -valued director n , and the Q -tensor based Landau-de Gennes model, whose energy density consists of a bulk potential favoring either a uniaxial nematic state, an isotropic state, or both, depending on temperature. What distinguishes our effort here is the attempt to capture the often singular structure of nematic/isotropic phase boundaries using a model reminiscent of Landau-de Gennes.

The modeling of phase transitions in thin liquid crystalline films has attracted the attention of materials scientists and physicists for some time, [13, 21, 35, 39]. In experiments, one observes thin liquid crystal samples separated into nematic and isotropic phases. The islands of phase, i.e. the ‘‘tactoids,’’ appear as planar regions, with boundaries consisting of two or more smooth curves. Depending on temperature and on the type of liquid crystals, these smooth boundary curves may meet each other at singular points, known as ‘‘boojums,’’ forming angles or perhaps even cusps.

Regarding the significance of tactoids as an object of study, we quote from the recent computational study of tactoids [11], ‘‘Tactoid structures have been shown to act as sensors via chirality amplification and can be used to guide motile bacteria. They are also valuable architectural elements of self assembly, for example providing nucleation sites for growth of the smectic phase.’’

In modeling these regions, the typical approach found in the materials science literature is to use a director theory and to postulate a surface energy that depends on the angle the director n makes with the normal ν to the phase boundary. Calling the region occupied by the phase of uniaxial nematic say Ω_N , and writing $n = (\cos \theta, \sin \theta)$ and $\nu = (\cos \phi, \sin \phi)$, this leads to minimization of a surface energy of the form

$$F_s(n) := \int_{\partial\Omega_N} \sigma(\theta - \phi) ds \quad (1.1)$$

where a typical choice for the function $\sigma : \mathbb{R} \rightarrow \mathbb{R}$, based on symmetries (and simplicity), is given by

$$\sigma(\theta - \phi) = c_1 + c_2 \cos 2(\theta - \phi),$$

a form referred to as a Rapini-Papoular type surface density, (see e.g. [28], section 3.4). In some studies within the physics literature the phase domain Ω_N is taken as a given region having a simple geometry such as a disk and then the minimization, taken over director fields $n : \Omega_N \rightarrow \mathbb{S}^1$, may involve coupling the surface term above to an elastic term such as $\int_{\Omega_N} |\nabla n|^2 dx$, corresponding to the so-called ‘equal constants’ form of elastic energy, see e.g. [39]. In other studies, the shape itself is an unknown, but then, due to the difficulty of the analysis, the director field is often ‘frozen,’ that is, taken to be a constant so that there is no elastic energy contribution and one minimizes (1.1) alone. Then the problem resembles somewhat the Wulff shape problem arising in the classical study of crystal morphology, see e.g. [14, 35].

Rather than postulating a specific surface energy, here we seek a model based on an order parameter, $u : \Omega \rightarrow \mathbb{R}^2$ defined on a planar domain Ω in which the singularities of the phase boundary emerge as a result of large disparity between the values of the elastic constants. We are

not alone in taking this viewpoint; see for example, [11], where the authors write “It is clear that significant shape deformation is only achieved with the introduction of elastic anisotropy.”

In [17], our first endeavor in this direction, we propose a model problem coupling the Ginzburg-Landau potential to an elastic energy density with large elastic disparity, namely

$$\inf_{u \in H^1(\Omega; \mathbb{R}^2)} \frac{1}{2} \int_{\Omega} \left(\frac{1}{\varepsilon} (1 - |u|^2)^2 + \varepsilon |\nabla u|^2 + L(\operatorname{div} u)^2 \right) dx. \quad (1.2)$$

The minimization is taken over competitors satisfying an \mathbb{S}^1 -valued Dirichlet condition on $\partial\Omega$ so as to avoid a trivial minimizer. Here one might view the positive constant $\varepsilon \ll 1$ as being comparable in size to the elastic constant L_1 in say a Landau-de Gennes elastic energy density while the positive constant L , independent of ε , is playing the role of L_2 , the coefficient of squared divergence in more standard elastic energy densities.

This choice of potential clearly favors \mathbb{S}^1 -valued states, which are a stand-in in our models for uniaxial nematic states. As such, the model (1.2) precludes any phase transitions between \mathbb{S}^1 -valued states and the isotropic state $u = 0$, and corresponds to the situation where the temperature—and therefore the potential—favor only the nematic state. Analysis of (1.2) in the $\varepsilon \rightarrow 0$ limit involves a ‘wall energy’ along a jump set J_u penalizing jumps of any \mathbb{S}^1 -valued competitor u , and bulk elastic energy favoring low divergence. The conjectured Γ -limit of (1.2) is

$$\frac{L}{2} \int_{\Omega} (\operatorname{div} u)^2 dx + \frac{1}{6} \int_{J_u \cap \Omega} |u_+ - u_-|^3 d\mathcal{H}^1, \quad (1.3)$$

where u_+ and u_- are the one-sided traces of u along J_u . The natural space for competitors for this limit should be some subset of $H_{\operatorname{div}}(\Omega; \mathbb{S}^1)$, the Hilbert space of L^2 vector fields having L^2 divergence. In order to make sense of the jump set we make the additional assumption in [17] that $u \in BV(\Omega; \mathbb{S}^1)$, though this is surely not optimal. As a simple consequence of the Divergence Theorem, it follows that allowable jumps for an H_{div} vector field must satisfy continuity of the normal component

$$u_+ \cdot \nu = u_- \cdot \nu \quad \text{along } J_u, \quad (1.4)$$

where ν denotes the normal to J_u . Hence the cubic jump cost is penalizing the jump in the tangential component only.

In the present paper, we allow for co-existence of both nematic and isotropic phases by replacing the Ginzburg-Landau potential in (1.2) with a potential $W : \mathbb{R}^2 \rightarrow [0, \infty)$ that still depends radially on u but that instead vanishes on $\mathbb{S}^1 \cup \{0\}$. This is reminiscent of the zero set of the Landau-de Gennes potential in the critical temperature regime within the thin film context, see e.g. [7]. A prototype for what we have in mind is a potential of the form $W(u) = W_{CSH}(u) := |u|^2 (|u|^2 - 1)^2$, or what is known in other physical contexts as the Chern-Simons-Higgs potential, see e.g. [23].

We thus arrive at two models based on this potential. In the first model, analyzed in Section 2, we examine the asymptotic limit in ε of the energy

$$F_{\varepsilon}(u) := \frac{1}{2} \int_{\Omega} \left(\frac{1}{\varepsilon} W(u) + \varepsilon |\nabla u|^2 + L_{\varepsilon} (\operatorname{div} u)^2 \right) dx,$$

where we assume $\varepsilon \ll L_{\varepsilon} \rightarrow 0$. Our main result for this model is Theorem 2.1, which states that in the L^1 -topology, this sequence of energies Γ -converges to a perimeter functional, measuring

the arclength of the phase boundary between the \mathbb{S}^1 -valued phase and the zero phase. In short, despite the much stronger penalty on divergence—think of say $L_\varepsilon = \frac{1}{|\log \varepsilon|}$ —this amount of ‘elastic disparity’ is too weak to be felt in the limit. In particular, minimizers of the limit, even under a boundary condition or area constraint to induce co-existence of \mathbb{S}^1 -valued and 0 phases, will have smooth phase boundaries. We mention that in [23], the authors study the Γ -convergence of $\frac{1}{\varepsilon}F_\varepsilon$ for $L_\varepsilon = 0$. In that scaling, vortices rather than perimeter contributes at leading order.

Our second model, and the main focus of our paper, involves the same type of potential W as in F_ε , but now we ‘ramp up’ the cost of divergence still further, leading us to the energy

$$E_\varepsilon(u) := \frac{1}{2} \int_{\Omega} \left(\frac{1}{\varepsilon} W(u) + \varepsilon |\nabla u|^2 + L(\operatorname{div} u)^2 \right) dx, \quad (1.5)$$

where L is a positive constant *independent of* ε . As $\varepsilon \rightarrow 0$ in this model, the jump set J_u features two distinct types of discontinuities: as in (1.3), there are what we will call ‘walls’ involving a jump discontinuity between two \mathbb{S}^1 -valued states that respect (1.4), and there are what we will call ‘interfaces’ involving a jump between an \mathbb{S}^1 -valued state and the isotropic 0 phase.

We mention that one can consider minimization of E_ε subject to a Dirichlet condition $g : \partial\Omega \rightarrow \mathbb{R}^2$, or a constraint such as $\int_{\Omega} |u|^2 = \text{const}$, or both in order to induce the co-existence of phases. The weak H_{div} convergence of energy bounded sequences, however, implies that the appropriate condition for the limiting functional E_0 is that it inherits only the condition

$$u \cdot n_{\partial\Omega} = g \cdot n_{\partial\Omega} \quad \text{along } \partial\Omega, \quad (1.6)$$

or simply $\operatorname{meas}(\{u = 0\}) = \text{const}$ in the case of the constraint.

In any event, it is the interfaces that represent the nematic/isotropic phase boundary and in light of the requirement (1.4), one sees that whatever form the Γ -limit takes, the competitors, being in H_{div} , must have \mathbb{S}^1 -valued traces *that are tangent to the phase boundaries*. As we will demonstrate through examples and numerics in Section 4, it is this tangency requirement that may induce singularities in the phase boundary. On this point, we mention that in this article we chose to penalize divergence more than other elastic energy terms, but had we replaced the term $L \int (\operatorname{div} u)^2$ in (1.5) by $L \int (\operatorname{div} R_\theta u)^2$ where R_θ is any rotation matrix, we would arrive at a limiting requirement on the nematic/isotropic interface in which tangency is replaced by u making some non-zero angle with the tangent to the phase boundary. In particular, for $\theta = \pi/2$ one penalizes the curl rather than the divergence and the resulting interface requirement is that the trace is orthogonal to the boundary.

In Fig. 1, we present an example of experimental nematic/isotropic configuration obtained in the laboratory of Oleg Lavrentovich along with a figure showing a numerically generated phase boundary based on gradient flow for E_ε . Both figures represent transient states but we point out the similar nature of the singular phase boundaries. Note that in the experimental picture, the phase boundary is singular only for the isotropic island whose surrounding nematic phase has degree 0 on the boundary of the isotropic tactoid, not for the island where the degree is 1. This distinction will come up frequently in our analysis.

Regarding a rigorous identification of the Γ -limit of E_ε , we only have partial results at this point. We present rigorous compactness results in $L^2(\Omega; \mathbb{R}^2)$ in Theorem 3.4 based on an adaptation of [12], but roughly put, it is easy to verify that any limit u of an energy bounded sequence, i.e. $\{u_\varepsilon\}$ such that $E_\varepsilon(u_\varepsilon) < C$, is a vector field $u \in H_{\operatorname{div}}(\Omega; \mathbb{S}^1 \cup \{0\})$ such that the isotropic phase $\{x : u(x) = 0\}$ is a set of finite perimeter. Then making the extra assumption that u is of

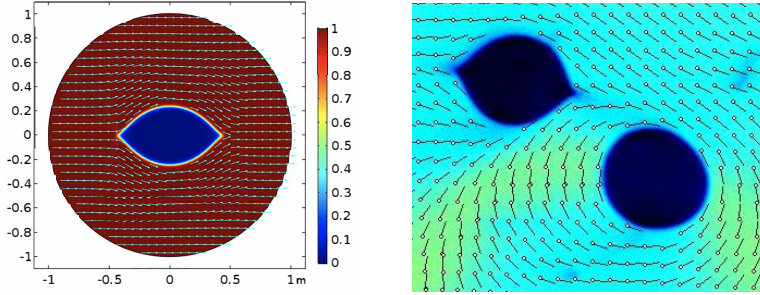


Figure 1: Tactoids observed in simulations (left) and the experiments (right). The figure on the right is courtesy of O. D. Lavrentovich.

bounded variation in the nematic phase where $u(x) \in \mathbb{S}^1$, one can invoke a combination of known techniques [17, 34] to establish a lower bound on the limit of the form

$$E_0(u) = \frac{L}{2} \int_{\Omega} (\operatorname{div} u)^2 dx + c_0 \operatorname{Per}_{\Omega}(\{|u| = 0\}) + \int_{J_u \cap \{|u|=1\}} K(u \cdot \nu) d\mathcal{H}^1, \quad (1.7)$$

where c_0 is the standard Modica-Mortola cost of an interface, cf. (2.3), and $K : \mathbb{R} \rightarrow [0, \infty)$ is a wall cost, arising through an abstractly defined solution to a certain cell problem. We wish to emphasize that, unlike for example (1.1), the limiting problem that arises involves both interfacial energy terms and a bulk term.

We strongly suspect that this wall cost K is in fact the cost associated with the heteroclinic connection between the states $(-u \cdot \tau, u \cdot \nu)$ and $(u \cdot \tau, u \cdot \nu)$ where τ is the approximate tangent to the jump set, see (3.8) and (3.9). The upper bound based on a recovery sequence for such a “one-dimensional” wall where only the tangential component varies across the boundary layer is the content of Theorem 3.1.

The optimality of one-dimensional walls is a delicate point that turns out to hold in the analysis of (1.2)-(1.3), cf. [17], as well as in the analysis of the divergence-free, or equivalently $L = \infty$, versions of these problems known as the Aviles-Giga problem, see e.g. [3, 5, 9, 12, 18, 25, 26, 33, 34]. However, for Aviles-Giga and in [17], the matching of lower bound to upper bound is achieved through the somewhat miraculous Jin-Kohn entropy, cf. [20] and (3.13). The divergence of this vector field on the one hand bounds the Aviles-Giga energy from below but at the same time yields a value for the cost of a wall that coincides with the one-dimensional upper bound construction described above. As far as we can tell, there is no analogous entropy that works similarly for (1.5).

In Section 3.3, in contrast to the partial results from Section 3.1, we establish a complete Γ -convergence analysis along with optimal compactness, in the case where Ω is an interval.

In Section 3.4, we turn to the derivation of criticality conditions for the proposed Γ -limit, E_0 . As in [17], we find that in the \mathbb{S}^1 -valued phase, away from walls, we can phrase criticality in terms of a system of conservation laws sharing characteristics, cf. Corollary 3.11. Characteristics turn out to be circular arcs along which divergence is constant with the curvature of the arc being given by the value of the divergence. We also explore criticality conditions for the wall and interface in

Theorems 3.9 and 3.12, as well as for possible junctions between walls and interfaces in Theorem 3.13, whose somewhat technical proof we delay until the appendix.

Section 4 is crucial to our paper in that we explore the possible morphology of vortices, interfaces and walls through a series of examples. We focus on constructing critical points to the formal $L \rightarrow \infty$ limit of E_0 which one might describe as the Aviles-Giga Γ -limit augmented by isotropic regions, see (4.1). These constructions are in particular divergence-free competitors for E_0 for L finite that should be close to optimal for L large. One might expect that when no area constraint on the size of the isotropic phase is imposed and \mathbb{S}^1 -valued Dirichlet data g is specified in (1.6) for E_0 , then only critical points that are nematic–i.e. \mathbb{S}^1 -valued– would emerge, with perhaps a certain number of defects in order to accommodate the degree of g , as in [8]. However, in Example 4.3, we take Ω to be the unit disk and g to have negative degree, and we show that, somewhat surprisingly, an $O(1)$ isotropic region opens up. We provide a possible explanation for this phenomenon in Theorem 4.1.

In Section 4.4, we construct a divergence-free example in all of \mathbb{R}^2 in which a singular phase boundary encloses an isotropic island and in which the infinite nematic complement of this island obeys a trivial degree zero condition at infinity, i.e. $u \rightarrow \vec{e}_1$ as $|x| \rightarrow \infty$. Unlike in the first example, this island is induced through an area constraint. This somewhat delicate calculation involves construction of both interfaces and walls with proper junction conditions holding at their intersection.

In this section we also comment on the following crucial feature of the model observed in several of our examples. At defects on the phase boundary, the director u often switches the sense of tangency. If a defect is a corner in the interior of the domain and a change in tangency occurs, then walls necessarily emanate from the defect in order to avoid infinite energy from the bulk divergence term; see Fig. 7 and the discussions at the end of Section 4.2 and preceding Example 4.4.

Needless to say, this article represents just the initial investigation of a problem which holds within it a rich array of phenomena yet to be understood and questions to be pursued. We also mention that upgrading this model to the setting of Q -tensors should not pose significant obstacles.

2 First try: A model whose elastic disparity is weak

In this section, we begin our examination of the effect of disparity in elastic energy. Throughout this section, we will consider a continuous potential $W : \mathbb{R}^2 \rightarrow [0, \infty)$ which vanishes on $\mathbb{S}^1 \cup \{0\}$. We assume that for some continuous function $V : \mathbb{R} \rightarrow [0, \infty)$, one has $W(u) = V(|u|)$ with then $V(0) = V(1) = 0$ and $V > 0$ elsewhere. The prototype for what we have in mind is the Chern-Simons-Higgs potential

$$W_{CSH}(u) := |u|^2 (|u|^2 - 1)^2. \quad (2.1)$$

Then for a sequence of positive numbers $L_\varepsilon \downarrow 0$, we consider the sequence of functionals

$$F_\varepsilon(u) := \begin{cases} \frac{1}{2} \int_\Omega \left(\frac{1}{\varepsilon} W(u) + \varepsilon |\nabla u|^2 + L_\varepsilon (\operatorname{div} u)^2 \right) dx & \text{if } u \in H^1(\Omega; \mathbb{R}^2), \\ +\infty & \text{otherwise.} \end{cases} \quad (2.2)$$

Though the Γ -convergence result below holds for any sequence $\{L_\varepsilon\}$ approaching zero, we are especially interested in the situation where

$$\frac{L_\varepsilon}{\varepsilon} \rightarrow \infty \text{ as } \varepsilon \rightarrow 0,$$

so that the divergence term in the elastic energy is heavily emphasized. Our goal is to explore whether or not this disparity can produce a Γ -limit whose minimizers possess the types of phase boundary singularities reminiscent of isotropic-nematic interfaces as described in the introduction. What we shall find is that this level of elastic disparity is in fact *not* sufficiently strong to achieve this goal.

To this end, we define our candidate for the Γ -limit:

$$F_0(u) := \begin{cases} c_0 \text{Per}_\Omega(\{|u| = 0\}) & \text{if } |u| \in BV(\Omega; \{0, 1\}), \\ +\infty & \text{otherwise.} \end{cases}$$

Here,

$$c_0 := \int_0^1 \sqrt{V(s)} ds. \quad (2.3)$$

The reader may well recognize this Γ -limit as precisely the well-known limit of the Modica-Mortola energies, an indication that to leading order in the energy, the divergence term has no effect on the asymptotic behavior of minimizers.

Our main result for this section is:

Theorem 2.1. *The sequence $\{F_\varepsilon\}$ Γ -converges to F_0 in the topology induced by the L^1 norm of the modulus $|\cdot|$. That is,*

(i) *for any $u \in L^1(\Omega; \mathbb{R}^2)$ and for any sequence $\{u_\varepsilon\}$ in $L^1(\Omega; \mathbb{R}^2)$,*

$$|u_\varepsilon| \rightarrow |u| \text{ in } L^1(\Omega) \text{ implies } \liminf_{\varepsilon \rightarrow \infty} F_\varepsilon(u_\varepsilon) \geq F_0(u), \quad (2.4)$$

and

(ii) *for each $u \in L^1(\Omega; \mathbb{R}^2)$ there exists a recovery sequence $\{w_\varepsilon\}$ in $L^1(\Omega; \mathbb{R}^2)$ satisfying*

$$|w_\varepsilon| \rightarrow |u| \text{ in } L^1(\Omega; \mathbb{R}^2) \quad \text{and} \quad \limsup_{\varepsilon \rightarrow \infty} F_\varepsilon(w_\varepsilon) \leq F_0(u). \quad (2.5)$$

In fact, we can construct the sequence $\{w_\varepsilon\}$ so that $w_\varepsilon \rightarrow u$ in L^1 .

Remark 2.2. *Regarding the asymptotic behavior of global minimizers, this result does not seem to address the possibility of a phase transition since there is no ‘incentive’ for a minimizer of F_ε to take on both 0 and \mathbb{S}^1 values. To encourage a phase transition for a minimizer, one could, for example, impose a mass constraint such as*

$$\int_\Omega |u_\varepsilon|^2 dx = m \quad \text{or} \quad \int_\Omega |u_\varepsilon| dx = m \quad \text{where } m \in (0, |\Omega|) \quad \text{with } |\Omega| = \text{Lebesgue measure of } \Omega.$$

Alternatively, one could impose a Dirichlet condition on $\partial\Omega$ such as $u_\varepsilon = g_\varepsilon$ where g_ε is \mathbb{S}^1 -valued on one portion of the boundary and then transitions smoothly down to 0 on the rest of

the boundary. Either of these alterations in the problem can be easily accommodated using what are by now standard techniques in Γ -convergence, see e.g. [27, 32, 37]. However, in order to present the main ideas without excessive technicalities, we formulate and prove a Γ -convergence theorem without either of these conditions, and merely remark that they could be incorporated if desired.

Though as indicated below (2.5), we can in fact establish Γ -convergence in the stronger topology $L^1(\Omega)$, it is not possible to obtain L^1 -compactness for an arbitrary energy bounded sequence due to the degeneracy of the well \mathbb{S}^1 . However, L^1 -compactness of $\{|u_\varepsilon|\}$ follows by a standard argument, cf. e.g. [37, Proposition 3].

Proposition 2.3. *Let $\{u_\varepsilon\}$ be a sequence of maps from Ω to \mathbb{R}^2 and assume that the sequence of energies $F_\varepsilon(u_\varepsilon)$ is uniformly bounded. Then there exists a subsequence $\{u_{\varepsilon_j}\}$ and $u \in L^1(\Omega; \mathbb{S}^1 \cup \{0\})$ such that $|u_{\varepsilon_j}| \rightarrow |u|$ in $L^1(\Omega)$.*

As observed in [31], this rather weak form of compactness is nonetheless sufficient to imply the existence of local minimizers of F_ε given a local minimizer of F_0 which is isolated in this weaker topology, by modifying an argument of [22]. For example, on a “dumbbell”-type domain, there always exist local minimizers of F_ε for ε sufficiently small, cf. [31, Theorems 4.2, 5.1].

Proof of the lower semi-continuity condition (2.4). Lower semi-continuity follows as in the Modica-Mortola setting since one simply ignores the divergence term. Since the argument is short, however, we present it here. The cases in which $\liminf_{\varepsilon \rightarrow 0} F_\varepsilon(u_\varepsilon) = \infty$ or $W(u) \neq 0$ on a set of positive measure are trivial. We therefore assume that $\liminf_{\varepsilon \rightarrow 0} F_\varepsilon(u_\varepsilon) = C < \infty$, and suppose that $|u_\varepsilon| \rightarrow |u|$ in $L^1(\Omega)$. Suppose also for now that $|u_\varepsilon| \leq 1$, an assertion we will justify later by means of a truncation procedure. In the argument below, we will make use of the function $\Phi(t) := \int_0^t \sqrt{V(s)} ds$. As $L_\varepsilon \geq 0$, we have

$$\begin{aligned} F_\varepsilon(u_\varepsilon) &= \frac{1}{2} \int_\Omega \left(\frac{1}{\varepsilon} W(u_\varepsilon) + \varepsilon |\nabla u_\varepsilon|^2 + L_\varepsilon (\operatorname{div} u_\varepsilon)^2 \right) dx \geq \int_\Omega \sqrt{V(|u_\varepsilon|)} |\nabla |u_\varepsilon|| dx \\ &\geq \int_\Omega |\nabla \Phi(|u_\varepsilon|)| dx. \end{aligned}$$

By the assumption that $\liminf F_\varepsilon(u_\varepsilon) = C < \infty$, we obtain a uniform bound on $\{\Phi(|u_\varepsilon|)\}_{\varepsilon > 0}$ in $BV(\Omega)$, implying the existence of a subsequence converging in L^1 to $\Phi(|u|)$. Therefore, by lower semi-continuity in BV ,

$$\begin{aligned} \liminf_{\varepsilon \rightarrow 0} F_\varepsilon(u_\varepsilon) &\geq \liminf_{\varepsilon \rightarrow 0} \int_\Omega |\nabla \Phi(|u_\varepsilon|)| dx \\ &\geq \int_\Omega |\nabla \Phi(|u|)| dx \\ &= c_0 \operatorname{Per}_\Omega(\{|u| = 1\}). \end{aligned}$$

This then completes the proof of (2.4) under the assumption that $|u_\varepsilon| \leq 1$.

If it does not hold that $|u_\varepsilon| \leq 1$ then we define

$$u_\varepsilon^*(x) := \begin{cases} u_\varepsilon(x) & \text{if } |u_\varepsilon(x)| \leq 1, \\ \frac{u_\varepsilon(x)}{|u_\varepsilon(x)|} & \text{if } |u_\varepsilon(x)| > 1. \end{cases}$$

We compute that

$$F_\varepsilon(u_\varepsilon) \geq \frac{1}{2} \int_\Omega \left(\frac{1}{\varepsilon} W(u_\varepsilon) + \varepsilon |\nabla u_\varepsilon|^2 \right) dx \geq \frac{1}{2} \int_\Omega \left(\frac{1}{\varepsilon} W(u_\varepsilon^*) + \varepsilon |\nabla u_\varepsilon^*|^2 \right) dx. \quad (2.6)$$

Finally, we have that

$$\| |u_\varepsilon^*| - |u| \|_{L^1(\Omega)} \leq \| |u_\varepsilon| - |u| \|_{L^1(\Omega)} \rightarrow 0,$$

so that we can combine the previous arguments with (2.6) to obtain lower semi-continuity for the original sequence $\{u_\varepsilon\}$. \square

Proof of the recovery sequence condition (2.5). Suppose we are given $u : \Omega \rightarrow \mathbb{S}^1 \cup \{0\}$ with $|u| \in BV(\Omega; \{0, 1\})$. We will construct a sequence $w_\varepsilon \in H^1(\Omega; \mathbb{R}^2)$ with $w_\varepsilon \rightarrow u$ in $L^1(\Omega; \mathbb{R}^2)$ such that $\limsup_{\varepsilon \rightarrow 0} F_\varepsilon(w_\varepsilon) \leq F_0(u)$. We first briefly discuss the main idea, in order to motivate the construction that follows. Suppose that u is smooth on the set, say N , where it is \mathbb{S}^1 -valued, except for finitely many singular points a_i , and suppose u carries degree d_i around each ‘‘vortex’’ a_i . Suppose also that ∂N is smooth. We would like to define w_ε using a boundary layer near ∂N which bridges the values of $u|_N$ near ∂N to 0 outside. In order to recover the correct Γ -limit with constant $2c_0$, we must define w_ε on a neighborhoods \mathcal{N}_ε of N so that

$$\frac{1}{2} \int_{\mathcal{N}_\varepsilon} \left(\frac{1}{\varepsilon} W(w_\varepsilon) + \varepsilon |\nabla w_\varepsilon|^2 + L_\varepsilon(\operatorname{div} w_\varepsilon)^2 \right) dx \rightarrow c_0 \operatorname{Per}_\Omega(\{|u| = 1\}).$$

As this is the least upper bound we could achieve even if $L_\varepsilon = 0$, we must therefore construct w_ε on \mathcal{N}_ε so that

$$\int_{\mathcal{N}_\varepsilon} L_\varepsilon(\operatorname{div} w_\varepsilon)^2 dx \rightarrow 0$$

and so that the gradient squared and potential terms give the correct asymptotic limit. Since there is no assumption on how fast the sequence $\{L_\varepsilon\}$ approaches zero, a natural construction to try is to define w_ε on \mathcal{N}_ε so that it is divergence-free there. This can be done by setting

$$w_\varepsilon = f_\varepsilon(d(x))(\nabla^\perp d)(x), \quad (2.7)$$

where $d(x)$ is the distance function to ∂N and f_ε is a suitably defined scalar function bridging the values 0 and 1. Then

$$\operatorname{div} w_\varepsilon = f'_\varepsilon(d)(\nabla d) \cdot \nabla^\perp d + f_\varepsilon(d) \operatorname{div}(\nabla^\perp d) = 0. \quad (2.8)$$

It is easy to check that if w_ε is a smooth, non-zero vector field tangent to level sets of d , as above, then its degree restricted to such a level set is 1. If, however, $\sum_i d_i \neq 1$, then degree considerations imply that it is impossible to define smooth w_ε which are non-zero and tangent to ∂N but equal to u in the interior of N away from the boundary. In addition, even if $\sum d_i = 1$, defining w_ε inside N by mollifying u could yield vortices which result in unbounded energy as $\varepsilon \rightarrow 0$; see Theorem 4.1.

To address these issues, it is instructive to consider the case in which Ω is the ball of radius 2 centered at the origin, $N := \{|u| = 1\}$ is the unit disk with $u \equiv \vec{e}_1$ there and u vanishes on the annulus $\{1 < |x| < 2\}$. As explained above, there is no smooth field tangent to the boundary of the

disk and equal to u inside the disk. However, suppose we alter the boundary of the disk by adding two small cusps. Then we can define a continuous vector field tangent to the modified boundary, except at the cusps, which has degree zero. This tangent vector field allows for the construction of a boundary layer similar to (2.7) which contributes a perimeter term differing from $F_0(u)$ by a negligible amount, and a second, \mathbb{S}^1 -valued boundary layer inside the disk which bridges the degree zero tangent field to the constant \vec{e}_1 . The energetic contribution of this second layer vanishes in the limit.

Our general construction utilizes this basic idea. Given any component of the nematic region N , we first approximate u there by a map with degree zero around any closed curve lying in that component. This allows us to avoid the creation of vortices which are energetically too expensive for the divergence term. Then, we add two cusps to the boundary components of the nematic regions; and finally, we use two boundary layers to bridge 0 to the values in the nematic regions. We should emphasize that the approximations will be close to the original function u in L^1 but of course will not be close in a stronger topology as that would violate basic properties of degree.

We now fix any $u : \Omega \rightarrow \mathbb{S}^1 \cup \{0\}$ such that $|u| \in BV(\Omega; \{0, 1\})$ and begin our construction of the recovery sequence. We first approximate u by vector fields u_n , then construct a recovery sequence for any u_n . A standard diagonal procedure will then imply the existence of a recovery sequence for u . We begin by showing that there exists an intermediate sequence of vector fields $\{v_n\} : \mathbb{R}^2 \rightarrow \mathbb{S}^1 \cup \{0\}$ such that

- (i) $\{|v_n| = 1\} =: \tilde{A}_n$ has C^2 boundary,
- (ii) v_n is smooth restricted to \tilde{A}_n ,
- (iii) for each n , there exists a non-empty arc $I_n \subset \mathbb{S}^1$ such that $v_n(x) \notin I_n$ for all $x \in \tilde{A}_n$,
- (iv) $\mathcal{H}^1(\partial\tilde{A}_n \cap \partial\Omega) = 0$ where \mathcal{H}^1 denotes one-dimensional Hausdorff measure,
- (v) $v_n \rightarrow u$ in L^1 , and
- (vi) $\text{Per}_\Omega(\tilde{A}_n \cap \Omega) \rightarrow \text{Per}_\Omega(\{|u| = 1\})$.

It is standard that there exist \tilde{A}_n such that (i), (iv), and (vi) hold and $\chi_{\tilde{A}_n} \rightarrow \chi_{\{|u|=1\}}$ in L^1 , see e.g. [16, Theorem 1.24]. Next, we define a sequence \tilde{v}_n by

$$\tilde{v}_n = \begin{cases} u(x) & \text{if } x \in \tilde{A}_n \cap \{|u| = 1\}, \\ \vec{e}_1 & \text{if } x \in \tilde{A}_n \setminus \{|u| = 1\}, \\ 0 & \text{if } x \notin \tilde{A}_n. \end{cases}$$

The choice of \vec{e}_1 is arbitrary, since any unit vector would suffice. From the convergence of $\chi_{\tilde{A}_n}$ to $\chi_{\{|u|=1\}}$ and the dominated convergence theorem, it follows that, up to a subsequence, $\tilde{v}_n \rightarrow u$ in $L^1(\Omega; \mathbb{R}^2)$. The sequence $\{\tilde{v}_n\}$ satisfies properties (i) and (iv)–(vi), so it remains to argue we can modify it so that (ii) and (iii) hold as well. For each n , we define for $1 \leq j \leq n$

$$C_j^n := \{x \in \Omega : \tilde{v}_n(x) \in (\cos([2\pi(j-1)/n, 2\pi j/n]), \sin([2\pi(j-1)/n, 2\pi j/n]))\},$$

and observe that for some j_n , $|C_{j_n}^n| \leq |\Omega|/n$, since $\sum_j |C_j^n| \leq |\Omega|$. Then for $x \in C_{j_n}^n$, we redefine $\tilde{v}_n(x)$ to be identically $(\cos(2\pi(j_n - 1)/n), \sin(2\pi(j_n - 1)/n))$, so that the \tilde{v}_n now avoids an arc

$I_n \subset \mathbb{S}^1$ of length $2\pi/n$. Now we can mollify \tilde{v}_n to obtain smooth v_n which also avoid I_n and satisfy (i)–(vi). Indeed, this can be done by choosing an interval $[a_n, b_n]$ in which to define the values of the phase of v_n and mollifying the phase function itself. We also point out that inside \tilde{A}_n , the degree of v_n around any simple, closed curve is zero, since v_n cannot take values in I_n .

Next, for each n , we add small cusps to the sets \tilde{A}_n and modify v_n to obtain u_n . For each connected component of $\partial\tilde{A}_n$, we add two cusps pointing into the isotropic region, which change the perimeter of \tilde{A}_n by at most $1/n$. We denote the resulting modification of \tilde{A}_n by A_n , and smoothly alter the values of the function v_n , yielding u_n . This procedure can be carried out in such a fashion so that properties (ii)–(vi) above still hold for the sequence $\{u_n\}$, and property (i), the smoothness of ∂A_n , holds except at the cusps. This completes the construction of the sequence $\{u_n\}$.

For each n , we now construct a recovery sequence $\{u_\varepsilon\}$, suppressing the dependence of $\{u_\varepsilon\}$ on n for ease of notation. Away from ∂A_n , u_ε will be identically equal to u_n . Near ∂A_n , we will use a boundary layer of the form $f_\varepsilon \vec{t}$, where \vec{t} is a unit vector field tangent to level sets of the signed distance function d to A_n and where f_ε solves a certain ODE. Away from the cusps, the level sets of the d are smooth, which will be enough for our purposes. For each connected component of ∂A_n , we define \vec{t} there by choosing a unit vector field tangent to that component and continuous on all of that component; see Fig. 2 below.

The fact that each component contains two cusps implies that for the field \vec{t} to be continuous, it must change the sense of tangency at every cusp. Thus on ∂A_n , \vec{t} is always equal to $\pm \nabla^\perp d$. From these observations it follows that the degree of \vec{t} around any connected component of ∂A_n is zero. We then extend \vec{t} to a continuous, unit vector field tangent to level sets of d for x such that $d(x)$ is small and positive and the nearest point projection x onto ∂A_n is not contained in any one of a union of rectangles near each cusp; see Fig. 3 below. To bridge the divergence free field $f_\varepsilon \vec{t}$ to the values of u_n inside A_n , there is a second boundary layer, which is defined via an \mathbb{S}^1 -valued homotopy between \vec{t} and the values of u_n inside A_n . This is only possible because \vec{t} has degree zero around ∂A_n , as does u_n around any simple, closed curve in A_n . The energy contribution from this layer in the limit will be zero, since $W(u_\varepsilon) = 0$ there.

We now specify u_ε in the first boundary layer, which contributes the perimeter term in the asymptotic limit. In the interior of A_n and in A_n^c at sufficient distances away from ∂A_n to be specified shortly, we set u_ε equal to u_n .

First, for some fixed $\delta > 0$, we consider the following ODE, similar to [6, Equation 3.2]:

$$\left(\frac{\partial}{\partial s} f_\varepsilon(s)\right)^2 = \frac{\delta + V(f_\varepsilon(s))}{\varepsilon^2 (f_\varepsilon(s))^2}.$$

As argued in [6], there exists a constant C , depending on δ , such that for every ε , there exist positive numbers C_ε and strictly decreasing solutions $f_\varepsilon : [0, C_\varepsilon] \rightarrow [0, 1]$ of this ODE such that

$$C_\varepsilon \leq C\varepsilon \tag{2.9}$$

and

$$f_\varepsilon(0) = 1 \text{ and } f_\varepsilon(C_\varepsilon) = 0.$$

Each f_ε in fact depends on δ , but we suppress this dependence. Next, we excise a small rectangle at each cusp. Let

$$m_\varepsilon := \max\{\varepsilon, L_\varepsilon\}. \tag{2.10}$$

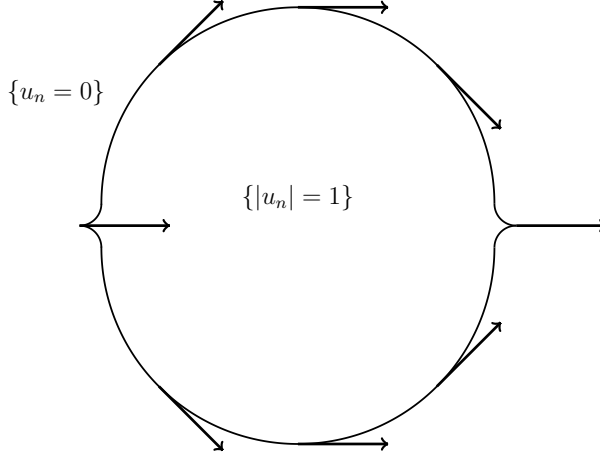


Figure 2: The Lipschitz vector field \vec{t} is tangent to this connected component of ∂A_n and has degree zero around it.

For each cusp c_i , consider a rectangle R_i^ε with one side of length $2C_\varepsilon$, centered at c_i , and perpendicular to the one-sided tangents at c_i , such that R_i^ε protrudes $m_\varepsilon^{2/3}$ into the isotropic set $\{u = 0\}$ in the other direction; see Fig. 3 below. We denote by \mathcal{R}_ε the union of all R_i^ε 's and then we define

$$u_\varepsilon(x) := \begin{cases} u_n(x) & \text{if } C_\varepsilon \leq d(x) \text{ or } d(x) \leq -m_\varepsilon^{2/3}, \\ f_\varepsilon(d(x))\vec{t}(x) & \text{if } 0 < d(x) < C_\varepsilon \text{ and } x \notin \mathcal{R}_\varepsilon. \end{cases}$$

In the definition above and in the remainder of the argument, we take d to denote the signed distance function to ∂A_n which is negative inside A_n . We will deal with u_ε on $\{x : -m_\varepsilon^{2/3} < d(x) \leq 0\}$ and on \mathcal{R}_ε at the end. It can be shown, by calculations similar to those preceding [31, Equation 3.33] that

$$\limsup_{\varepsilon \rightarrow 0} \frac{1}{2} \int_{\{0 \leq d(x) \leq C_\varepsilon\}} \left(\frac{1}{\varepsilon} W(u_\varepsilon) + \varepsilon |\nabla u_\varepsilon|^2 + L_\varepsilon (\operatorname{div} u_\varepsilon)^2 \right) dx \leq c_0 \operatorname{Per}_\Omega(A_n) + O(\sqrt{\delta}), \quad (2.11)$$

observing in the process the crucial fact that the divergence of u_ε on this set is zero, cf. (2.8). Furthermore,

$$\begin{aligned} & \frac{1}{2} \int_{\{C_\varepsilon \leq d(x) \text{ or } d(x) \leq -m_\varepsilon^{2/3}\}} \left(\frac{1}{\varepsilon} W(u_\varepsilon) + \varepsilon |\nabla u_\varepsilon|^2 + L_\varepsilon (\operatorname{div} u_\varepsilon)^2 \right) dx \\ &= \frac{1}{2} \int_{\{C_\varepsilon \leq d(x) \text{ or } d(x) \leq -m_\varepsilon^{2/3}\}} \left(\frac{1}{\varepsilon} W(u_n) + \varepsilon |\nabla u_n|^2 + L_\varepsilon (\operatorname{div} u_n)^2 \right) dx \xrightarrow{\varepsilon \rightarrow 0} 0, \end{aligned} \quad (2.12)$$

since $W(u_n) = 0$ and $|\nabla u_n|^2$ and $(\operatorname{div} u_n)^2$ are bounded functions independent of ε away from ∂A_n .

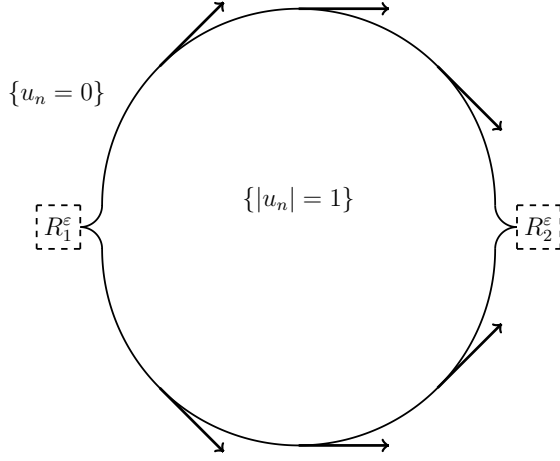


Figure 3: Each rectangle R_i^ϵ has length $m_\epsilon^{2/3}$ and height $2C_\epsilon$ and is perpendicular to the one-sided tangent vectors at the cusp c_i . For x near the interface and not in R_i^ϵ , we can extend the tangent field \vec{t} to be unit valued and tangent to level sets of the distance function to the interface.

It remains to define u_ϵ on the second boundary layer, $\{x : -m_\epsilon^{2/3} < d(x) \leq 0\}$, and on \mathcal{R}_ϵ . Let us first consider the second boundary layer. Because of the fact that u_ϵ defined thus far has degree zero around ∂A_n and $\{d(x) = -m_\epsilon^{2/3}\}$, there exist Lipschitz phases $\psi_1 : \partial A_n \rightarrow \mathbb{R}$, $\psi_2 : \{d(x) = -m_\epsilon^{2/3}\} \rightarrow \mathbb{R}$ such that $u_\epsilon = (\cos(\psi_1), \sin(\psi_1))$ on ∂A_n and $u_\epsilon = (\cos(\psi_2), \sin(\psi_2))$ on $\{d(x) = -m_\epsilon^{2/3}\}$. Then we can interpolate on the intermediate region using convex combinations of ψ_1 and ψ_2 so that $|\nabla u_\epsilon|^2$ and $(\operatorname{div} u_\epsilon)^2$ are both $O(m_\epsilon^{-4/3})$. Since u_ϵ is a unit vector field here, $W(u_\epsilon)$ is 0. Hence we can calculate

$$\begin{aligned} \frac{1}{2} \int_{\{x: -m_\epsilon^{2/3} < d(x) \leq 0\}} \left(\frac{1}{\epsilon} W(u_\epsilon) + \epsilon |\nabla u_\epsilon|^2 + L_\epsilon (\operatorname{div} u_\epsilon)^2 \right) dx &\lesssim |\{-m_\epsilon^{2/3} < d(x) \leq 0\}| (\epsilon m_\epsilon^{-4/3} + L_\epsilon m_\epsilon^{-4/3}) \\ &\leq O(m_\epsilon^{1/3}). \end{aligned} \quad (2.13)$$

So u_ϵ on the second boundary layer contributes nothing to the asymptotic limit.

Finally, we treat u_ϵ on the union \mathcal{R}_ϵ of rectangles R_i^ϵ . It suffices to demonstrate the construction on a single R_i^ϵ such that the cusp c_i contained on one of its sides is the origin and the isotropic phase is to the right of the x_2 -axis. Up to a translation, this is the situation depicted in Fig. 3 with R_2^ϵ . In these coordinates we may describe R_i^ϵ as the rectangle $[0, m_\epsilon^{2/3}] \times [-C_\epsilon, C_\epsilon]$. We set

$$u_\epsilon(x_1, x_2) = f_\epsilon(|x_2|)(1 - m_\epsilon^{-2/3} x_1) \vec{t}(0)$$

on R_i^ϵ , which ensures compatibility with u_ϵ as previously defined. We remark that $\vec{t}(0)$ is either plus or minus \vec{e}_1 . Then on R_i^ϵ , $(\operatorname{div} u_\epsilon)^2 \sim O(m_\epsilon^{-4/3})$, and $|\nabla u_\epsilon|^2 \sim O(\epsilon^{-2})$. Since the area of R_i^ϵ is $2C_\epsilon m_\epsilon^{2/3} \leq 2C_\epsilon m_\epsilon^{2/3}$ by (2.9) and (2.10), we have for small ϵ

$$\frac{1}{2} \int_{R_i^\epsilon} \left(\frac{1}{\epsilon} W(u_\epsilon) + \epsilon |\nabla u_\epsilon|^2 + L_\epsilon (\operatorname{div} u_\epsilon)^2 \right) dx \leq O(m_\epsilon^{2/3}). \quad (2.14)$$

Combining (2.11)–(2.14), we obtain

$$F_\varepsilon(u_\varepsilon) \rightarrow F_0(u_n) + O\sqrt{\delta}.$$

In addition, the u_ε converge in L^1 to u_n by virtue of the dominated convergence theorem, since they are bounded and the set where they differ from u_n has measure going to zero. Therefore, recalling that $\{u_\varepsilon\}$ depends on δ as well, we diagonalize over ε and δ to obtain a recovery sequence for u_n . Since u_n converge in L^1 to u and $F_0(u_n) \rightarrow F_0(u)$, a second diagonalization argument over n and ε yields a recovery sequence for u . \square

3 A model with large elastic disparity and singular phase boundaries

In the previous section we saw that disparity in the elastic energy density of the form

$$\varepsilon |\nabla u|^2 + L_\varepsilon (\operatorname{div} u)^2 \quad \text{with } \varepsilon \ll L_\varepsilon \rightarrow 0$$

is insufficient to induce a singular phase boundary between the isotropic state 0 and an \mathbb{S}^1 -valued nematic state in minimizers of the Γ -limit. We now introduce a model with still larger disparity, and it is this model we will work with for the remainder of the article.

To this end, for a positive constant L independent of ε we define

$$E_\varepsilon(u) := \frac{1}{2} \int_\Omega \left(\frac{1}{\varepsilon} W(u) + \varepsilon |\nabla u|^2 + L (\operatorname{div} u)^2 \right) dx, \quad (3.1)$$

where $W(u) = V(|u|)$ for some continuous $V : [0, \infty) \rightarrow [0, \infty)$ that vanishes only at 0 and 1. As always, our prototype is the potential given by $W_{CSH}(u) = |u|^2 (|u|^2 - 1)^2$, but in what follows we can allow for more general potentials vanishing at 0 and 1, provided that for some constant $c > 0$ one has the condition

$$H(t) := \min(t^2, |1 - t^2|) \leq c \sqrt{V(t)} \quad (3.2)$$

for any $t \in [0, \infty)$.

In light of the divergence term in E_ε , it is clear that energy-bounded sequences $\{u_\varepsilon\}$ will have divergences that converge weakly in $L^2(\Omega)$. As we will discuss in Section 3.3, under the assumption (3.2), an adaptation of the compactness techniques of [12] allows us to also establish that a subsequence of $\{u_\varepsilon\}$ will converge strongly in $L^2(\Omega)$ to a limit taking values in $\mathbb{S}^1 \cup \{0\}$. We will write $u_\varepsilon \xrightarrow{\wedge} u$ when both $\operatorname{div} u_\varepsilon \rightharpoonup \operatorname{div} u$ weakly in $L^2(\Omega)$ and $u_\varepsilon \rightarrow u$ strongly in $L^2(\Omega; \mathbb{R}^2)$. See Theorem 3.4.

These compactness results naturally lead us to consider the Hilbert space $H_{\operatorname{div}}(\Omega; \mathbb{R}^2)$ of L^2 vector fields having L^2 divergence, and more specifically $H_{\operatorname{div}}(\Omega; \mathbb{S}^1 \cup \{0\})$, in light of the assumed zero set of the potential W .

A vector field $u \in H_{\operatorname{div}}(\Omega; \mathbb{S}^1 \cup \{0\})$ that additionally lies in the space $BV(\Omega; \mathbb{S}^1 \cup \{0\})$ is known to have a countably 1-rectifiable jump set J_u off of which u is approximately continuous. In our pursuit of a possible candidate for the limit of the sequence $\{E_\varepsilon\}$ we will focus on functions lying in the intersection of these two spaces.

Mappings in BV have well-defined traces, say u_+ and u_- on either side of J_u and an easy application of the Divergence Theorem reveals that when H_{div} vector fields have jump discontinuities across J_u then necessarily the normal component is continuous, i.e.

$$u_+ \cdot \nu = u_- \cdot \nu \quad \mathcal{H}^1 \text{ a.e. on } J_u \quad (3.3)$$

where ν is the (approximate) normal to J_u .

This brings us to a crucial distinction when attempting to identify a limiting energy for the sequence $\{E_\varepsilon\}$ —a mapping $u \in (H_{\text{div}} \cap BV)(\Omega; \mathbb{S}^1 \cup \{0\})$ may undergo a jump between two \mathbb{S}^1 -valued states, in which case (3.3) is supplemented by the additional requirement that

$$u_+ \cdot \tau = -(u_- \cdot \tau) \quad \text{along } J_u, \quad (3.4)$$

where τ is the approximate tangent to J_u . We will refer to any component of J_u bridging two \mathbb{S}^1 -valued states as a *wall*. On the other hand, u may jump between an \mathbb{S}^1 -valued state, say u_+ , and $u_- = 0$, in which case (3.3) implies that u_+ must coincide with $\pm\tau$. We will refer to any such component of J_u as an *interface*. It is this tangency requirement along an interface that can induce singularities in the isotropic-nematic phase boundary.

3.1 A conjecture for the Γ -limit of E_ε

Our goal in this section is to make the case for a proposed Γ -limit of the sequence $\{E_\varepsilon\}$ defined in (3.1). While we do not at present have matching upper and lower asymptotic bounds for this sequence, we do have a construction leading to an asymptotic upper bound which we strongly suspect is sharp. We will begin with a description of this construction and then discuss various strategies for lower bounds, why the analogue of what works for the Ginzburg-Landau potential, cf. [17], apparently fails here and what the evidence is to support our conjecture on the sharpness of the upper bound.

We should say at the outset that our pursuit of the Γ -limit $E_0(u)$ begins with the assumption that $u \in (BV \cap H_{\text{div}})(\Omega; \mathbb{S}^1 \cup \{0\})$. While this is not the natural space from the standpoint of compactness, the identification of the correct limiting space is non-trivial and we do not attempt to address it here. We refer the reader to [3, 10, 24] for more discussion of this issue. We make the BV assumption here in order to speak sensibly about the 1-rectifiability of the jump set J_u , though for that part of J_u corresponding to interfaces, i.e. to $\partial\{|u| = 1\}$, as we will note below, this rectifiability comes easily from the fact that limits u of energy-bounded sequences satisfy $|u| \in BV(\Omega)$.

As noted above, for such a vector-valued function u , the jump set naturally splits into two types: walls and interfaces, though these two types of singular curves may well meet in junctions, see e.g. Theorem 3.13 and Fig. 4. An upper bound construction then rests on efficiently smoothing out these jump discontinuities, and in both cases, we rely on a one-dimensional type of resolution described formally below. The rigorous execution of these ideas follows the approach of [9] as adapted in [17].

To resolve an interface separating an isotropic region where $u = 0$ from a nematic region where $u \in \mathbb{S}^1$ we invoke a by-now standard Modica-Mortola type of heteroclinic connection in the *modulus*. More precisely, after mollifying the interface to smoothen it if necessary, we mollify u in the nematic region and make a boundary layer construction, say $\{w_\varepsilon\}$, of the form

$$w_\varepsilon(x) = h\left(\frac{\text{dist}(x, J_u)}{\varepsilon}\right)u(x) \quad (3.5)$$

where $\text{dist}(x, J_u)$ denotes the signed distance function to J_u and where $h : \mathbb{R} \rightarrow \mathbb{R}$ minimizes the 1d energy

$$\int_{-\infty}^{\infty} V(f) + |f'|^2 dt \quad \text{taken over } f \in H^1(\mathbb{R}) \text{ such that } f(-\infty) = 0, f(\infty) = 1. \quad (3.6)$$

This leads to the same ‘interfacial cost’ encountered in Section 2, namely

$$c_0 = \int_0^1 \sqrt{V(s)} ds,$$

multiplying the perimeter of the interface. Since

$$\text{div } w_\varepsilon(x) = h\left(\frac{\text{dist}(x, J_u)}{\varepsilon}\right) \text{div } u(x) + \frac{1}{\varepsilon} h'\left(\frac{\text{dist}(x, J_u)}{\varepsilon}\right) \nabla \text{dist}(x, J_u) \cdot u(x),$$

the term $L \int (\text{div } w_\varepsilon)^2$ in $E_\varepsilon(w_\varepsilon)$ will contribute nothing to such a boundary layer construction in the limit $\varepsilon \rightarrow 0$ since the first term is controlled by the fact that $u \in H_{\text{div}}$ and the second term is negligible due to the required tangency of u and J_u along an interface. We note that the ansatz (3.5) would fail for the sequence of functionals F_ε analyzed in Section 2 since there u is not required to lie in H_{div} and so the term $\nabla \text{dist}(x, J_u) \cdot u(x)$ will in general not vanish.

With appropriate care taken to treat issues of regularity, this can be made rigorous. What is more, this construction, based only on appropriate interpolation of the modulus between 0 and 1, gives a sharp upper bound on the interfacial energy, in light of the inequality

$$E_\varepsilon(u) \geq \left(\frac{1}{2} \int_{\Omega} \frac{1}{\varepsilon} V(|u|) + \varepsilon |\nabla |u||^2 \right) dx \quad \text{for any } u \in H^1(\Omega; \mathbb{R}^2). \quad (3.7)$$

Since this is the classical scalar Modica-Mortola functional in terms of the function $|u|$, when applied in a neighborhood of the interface it yields the matching lower bound of $c_0 \text{Per}_\Omega(\{|u| = 1\})$.

Our boundary layer construction in a neighborhood of a wall separating two \mathbb{S}^1 -valued states, say u_+ and u_- , is one-dimensional in a different sense. In light of the continuity of the normal component of u across a wall, cf. (3.3), a natural choice is to fix the value of $u \cdot \nu$ across the boundary layer and use a heteroclinic connection to bridge the value of $u_- \cdot \tau$ to $u_+ \cdot \tau$, that is, to bridge $-\sqrt{1 - (u \cdot \nu)^2}$ to $\sqrt{1 - (u \cdot \nu)^2}$ in light of (3.4).

At a point on the wall, such a choice leads to a cost per unit length given by the minimum of a heteroclinic connection problem that is a bit different from (3.6), namely

$$\inf_f \int_{-\infty}^{\infty} W(f\tau + (u \cdot \nu)\nu) + |f'|^2 dt = \inf_f \int_{-\infty}^{\infty} V\left(\sqrt{f^2 + (u \cdot \nu)^2}\right) + |f'|^2 dt,$$

taken over $f \in H^1(\mathbb{R})$ such that

$$f(-\infty) = (u_- \cdot \tau) = -\sqrt{1 - (u \cdot \nu)^2} \quad \text{and} \quad f(\infty) = (u_+ \cdot \tau) = \sqrt{1 - (u \cdot \nu)^2}.$$

One easily checks that this infimum is given by $K(u \cdot \nu)$ where we define

$$K(z) := \int_{-\sqrt{1-z^2}}^{\sqrt{1-z^2}} \sqrt{V\left(\sqrt{z^2 + y^2}\right)} dy, \quad (3.8)$$

which in the prototypical case of $W_{CSH}(u) := |u|^2 (|u|^2 - 1)^2$ takes the form

$$K(z) = \int_{-\sqrt{1-z^2}}^{\sqrt{1-z^2}} \sqrt{z^2 + y^2} (1 - z^2 - y^2) dy. \quad (3.9)$$

We point out that $c_0 = \frac{K(0)}{2}$ and also note that K is not a monotone function of z on $[0, 1]$, but rather increases to a unique maximum and then decreases down to zero at $z = 1$.

Such an upper bound construction leads us to our conjectured Γ -limit when $u \in (H_{\text{div}} \cap BV)(\Omega; \mathbb{S}^1 \cup \{0\})$, namely E_0 given by

$$E_0(u) = \frac{L}{2} \int_{\Omega} (\text{div } u)^2 dx + \frac{K(0)}{2} \text{Per}_{\Omega}(\{|u| = 1\}) + \int_{J_u \cap \{|u|=1\}} K(u \cdot \nu) d\mathcal{H}^1. \quad (3.10)$$

One should also impose upon competitors in the minimization of E_0 a boundary condition of the form (1.6) if one imposes the Dirichlet condition $u|_{\partial\Omega} = g$ for E_{ε} or an area constraint on the measure of the isotropic or nematic region within Ω if an integral constraint has been imposed on E_{ε} .

In particular, we can rigorously assert:

Theorem 3.1. *For any $u \in (H_{\text{div}} \cap BV)(\Omega, \mathbb{S}^1 \cup \{0\})$, there exists a sequence $\{w_{\varepsilon}\} \in H^1(\Omega; \mathbb{R}^2)$ with $w_{\varepsilon} \xrightarrow{\Delta} u$ such that*

$$\limsup_{\varepsilon \rightarrow 0} E_{\varepsilon}(w_{\varepsilon}) = E_0(u). \quad (3.11)$$

Furthermore, we state a conjecture:

Conjecture : Suppose W satisfies (3.2). Then for any $u \in (H_{\text{div}} \cap BV)(\Omega, \mathbb{S}^1 \cup \{0\})$ and any sequence $u_{\varepsilon} \xrightarrow{\Delta} u$ we have

$$\liminf_{\varepsilon \rightarrow 0} E_{\varepsilon}(u_{\varepsilon}) \geq E_0(u). \quad (3.12)$$

Proof. The proof of (3.11) is similar to the proof of [17, Theorem 3.2(ii)], which itself is an adaptation of the techniques laid out in [9] for Aviles-Giga recovery sequences, so we omit the details. The only difference between the argument here and the argument in [17] is that, as discussed above, in addition to walls, there are also interfaces now in which u jumps from a tangent \mathbb{S}^1 -valued state to 0. However, this does not pose a serious obstacle to the construction, as the important technical components are the rectifiability of the jump set J_u and the condition (3.3) satisfied along J_u at either a wall or interface, which goes to guarantee that the boundary layer constructions do not contribute asymptotically to the L^2 -norm of the divergence. \square

Remark 3.2. *We have not addressed in (3.10) or in Theorem 3.1 the issue of boundary conditions, so we describe now how to incorporate them. Suppose one were to fix Dirichlet data $g_{\varepsilon} \in H^{1/2}(\partial\Omega; \mathbb{R}^2)$ for admissible functions in E_{ε} . The functions g_{ε} could be \mathbb{S}^1 -valued, or could transition smoothly between \mathbb{S}^1 and $\{0\}$ if we are trying to induce a phase transition. Let us assume that $g_{\varepsilon} \rightarrow g$ in $L^2(\partial\Omega; \mathbb{R}^2)$ for some $g : \partial\Omega \rightarrow \mathbb{S}^1 \cup \{0\}$. We observe that for a sequence $\{u_{\varepsilon}\} \in H^1(\Omega; \mathbb{R}^2)$ satisfying $u_{\varepsilon} = g_{\varepsilon}$ on $\partial\Omega$ and so in particular $u_{\varepsilon} \cdot \nu_{\Omega} = g \cdot \nu_{\Omega}$, under the*

convergence $u_\varepsilon \xrightarrow{\wedge} u$ with $u \in (BV \cap H_{\text{div}}(\Omega; \mathbb{S}^1 \cap \{0\}))$, it follows from the divergence theorem and the convergence of g_ε to g that

$$u \cdot \nu_\Omega = g \cdot \nu_\Omega.$$

In this case, the limiting energy E_0 would also contain integrals around the portion of $\partial\Omega$ where $u \cdot \tau_\Omega \neq g \cdot \tau_\Omega$, and the cost along these portions would either be given by $K(0)/2$ or $K(u \cdot \nu_\Omega)$.

Remark 3.3. *An a priori sharper upper bound for the wall cost K could be obtained for these energies using the techniques of [33]. There, the author obtains an upper bound without assuming that the optimal profile is one-dimensional. Instead, the cost is defined via a cell problem. As the class of admissible functions for the cell problem is strictly larger than the class of 1d competitors, the cell problem yields what could in theory be a sharper upper bound. However, since we conjecture that the one-dimensional profile is optimal and since at present we see no way to analyze the abstract cell problem to make this comparison, we do not pursue the strategy from [33].*

Given the presence of arguments leading to matching lower bounds for one-dimensional constructions in the Aviles-Giga problem [5] and for the energy E_0 with the potential replaced by a Ginzburg-Landau potential $W_{GL}(v) := (1 - |v|^2)^2$, in [17], it behooves us to comment on why, at present, we have no such argument here. In [5] and in [17], the authors employ the celebrated Jin-Kohn entropy [20]. Defining

$$\Xi(v_1, v_2) = 2 \left(\frac{1}{3} v_2^3 + v_2 v_1^2 - v_2, \frac{1}{3} v_1^3 + v_1 v_2^2 - v_1 \right), \quad (3.13)$$

the version of these entropies well-suited to the situation where the jump set is parallel to one of the coordinate axes, one can then calculate

$$\text{div } \Xi(v_1, v_2) = 2(|v|^2 - 1)(\partial_{x_1} v_2 + \partial_{x_2} v_1) + 4v_1 v_2 \text{div } v. \quad (3.14)$$

In the divergence-free Aviles-Giga setting of [20], the last term drops out and an application of the inequality $a^2 + b^2 \geq 2ab$ allows one to bound the Aviles-Giga energy density from below by $\text{div } \Xi(v_1, v_2)$. When the divergence is possibly non-zero, as in [17], a slight modification yields

$$\text{div } \Xi(v_1, v_2) \leq \left(\varepsilon |\nabla v|^2 + \frac{1}{\varepsilon} (|v|^2 - 1)^2 + L(\text{div } v)^2 \right) + \text{error terms},$$

which is the crux of the argument.

Unfortunately, for most radial potentials that are not the Ginzburg-Landau potential W_{GL} , this technique does not seem to work. First, we note that

$$\Xi(v_1, v_2) = \left(\int_{-v_2}^{v_2} (v_1^2 + s^2 - 1) ds, \int_{-v_1}^{v_1} (s^2 + v_2^2 - 1) ds \right),$$

where the integrands are, up to signs, given by $\sqrt{W_{GL}}$. Therefore, to obtain a version of (3.14) with W_{GL} replaced by \sqrt{W} , where W is our potential vanishing on $\mathbb{S}^1 \cup \{0\}$, the natural choice for the vector field to replace Ξ would be

$$\Xi_W(v_1, v_2) = \left(\int_{-v_2}^{v_2} \sqrt{W(v_1, s)} ds, \int_{-v_1}^{v_1} \sqrt{W(s, v_2)} ds \right).$$

When we calculate the divergence of $\Xi_W(v_1, v_2)$, we get

$$\begin{aligned} \operatorname{div} \Xi(v_1, v_2) &= 2\sqrt{W(v)}(\partial_{x_1} v_2 + \partial_{x_2} v_1) + \partial_{x_1} v_1 \int_{-v_2}^{v_2} (\partial_{v_1} \sqrt{W(v_1, s)}) ds + \partial_{x_2} v_2 \int_{-v_1}^{v_1} (\partial_{v_2} \sqrt{W(v_2, s)}) ds. \end{aligned}$$

The only way for $\operatorname{div} v$ to factor out of the last two terms is if

$$\int_{-v_2}^{v_2} \partial_{v_1} \sqrt{W(v_1, s)} ds = \int_{-v_1}^{v_1} \partial_{v_2} \sqrt{W(v_2, s)} ds,$$

which holds for radial W when \sqrt{W} is linear in $|v|^2$. This cannot hold for any W that vanishes only at \mathbb{S}^1 and $\{0\}$.

We point out that a related problem that has resisted resolution for several decades is the determination of a sharp lower bound for the sequence of energies

$$\int_{\Omega} \frac{1}{\varepsilon} (|u|^2 - 1)^p + \varepsilon |\nabla u|^2 \quad \text{with } p < 2 \quad (3.15)$$

where competitors $u : \Omega \rightarrow \mathbb{R}^2$ must be divergence-free. Here too it is conjectured that the optimal lower bound for the wall cost is based on a one-dimensional ansatz, [3], but a proof has not been found, and in particular, no version of the Jin-Kohn entropy is evident. An abstract lower bound involving a cell problem for functionals of this type has been derived in [34], but has not yet to our knowledge been matched by a corresponding upper bound. The strategy in this and other papers involving a lower bound phrased in terms of a cell problem is based on a blow up procedure introduced in [15]. Such a lower bound of the form $\int_{J_u} \tilde{K}(u \cdot \nu) d\mathcal{H}^1$ for some $\tilde{K} : [0, \infty) \rightarrow [0, \infty)$ defined as the solution to a cell problem could be derived for our wall energy as well, but we do not include the argument since it does not provide much insight here.

On the other hand, for $p > 2$ in (3.15), as shown in [3], the one-dimensional ansatz is *not* optimal, with an oscillatory construction, often referred to as ‘microstructure,’ whose modulus hews close to \mathbb{S}^1 , yielding a lower asymptotic energy.

So what is the rationale behind our conjecture (3.12)? One key point is that for W given by W_{CSH} or more generally by a potential satisfying (3.2), the level of degeneracy of the \mathbb{S}^1 potential well is no flatter than that of W_{GL} where again it is known that walls follow a one-dimensional profile asymptotically. Thus, it seems unlikely that microstructure of the type emerging, for example, in (3.15) for $p > 2$ would appear here since for our model it is no more beneficial energetically to abandon one-dimensionality in order to be nearer to \mathbb{S}^1 across a wall than it was in (1.2).

Other evidence for our conjecture is numerical. Repeated numerical experiments in the form of gradient flow for E_ε with ε small in a variety of domains, for a variety of boundary conditions and for a wide range of L values have not indicated any lack of one-dimensionality in the wall structure. Were the transition to be truly $2d$, one might expect the wall to exhibit some oscillation or other instability. For example, in [17] while we prove that for (1.2)-(1.3) the wall cost is based on a one-dimensional construction, we also find that when minimizing (1.2) in a rectangle with \mathbb{S}^1 -valued Dirichlet data given by $(\pm a, \sqrt{1-a^2})$ for $a \in [0, 1)$ on the top and bottom respectively and periodic boundary conditions on the sides, there exists a parameter regime in L and in the box dimensions where the minimizer is not one-dimensional, cf. [17], Thm. 6.6. Indeed this

theorem is supported by numerics revealing the eventual instability of a horizontal wall and the emergence of so-called ‘cross-ties’ commonly arising in studies of micromagnetics such as [2]. On the other hand, as we discuss in Section 4.1, numerically we detect no such instability of a horizontal wall for E_ε under these boundary conditions. Then a numerical examination in Section 4.3 of wall structure for a version of our problem posed in a disk also indicates a one-dimensional heteroclinic connection for the wall structure. This gives us further confidence in the conjectured one-dimensionality of the wall cost.

3.2 Compactness

In this section we establish a compactness result for energy-bounded sequences. Recalling the assumption (3.2), we begin by observing that

$$E_\varepsilon(u) \geq \frac{1}{2} \int_{\Omega} \left(\frac{1}{\varepsilon c^2} H^2(|u|) + \varepsilon |\nabla u|^2 + L(\operatorname{div} u)^2 \right) dx. \quad (3.16)$$

Both the Ginzburg-Landau and the Chern-Simons-Higgs potentials satisfy this inequality and in [17] it is shown that for W given by the Ginzburg-Landau potential, the compactness result of [12] generalizes to E_ε . In this section, we show that this compactness approach generalizes to potentials also vanishing at the origin provided we assume (3.2).

Theorem 3.4. *Let $\{u_\varepsilon\}_{\varepsilon>0} \subset H^1(\Omega; \mathbb{R}^2)$ be a sequence such $E_\varepsilon(u_\varepsilon) \leq C$, with C independent of ε . Then there exists a subsequence (still denoted here by u_ε) and a function $u \in H_{\operatorname{div}}(\Omega; \mathbb{S}^1 \cup \{0\})$ with $|u| \in BV(\Omega; \{0, 1\})$ such that*

$$u_\varepsilon \rightharpoonup u \quad \text{in } H_{\operatorname{div}}(\Omega; \mathbb{R}^2), \quad (3.17)$$

$$u_\varepsilon \rightarrow u \quad \text{in } L^2(\Omega; \mathbb{R}^2). \quad (3.18)$$

The fact that for a subsequence of $\{u_\varepsilon\}$, one has $|u_\varepsilon| \rightarrow |u|$ in $L^1(\Omega)$ where $|u| \in BV(\Omega; \{0, 1\})$ follows from inequality (3.7) via the standard Modica-Mortola approach, cf. [27] or [37]. The proof of (3.17) follows immediately from the uniform bound on the L^2 norm of the divergences, so we turn to the proof of (3.18). The proof follows closely the proof in [12, Proposition 1.2], with the details suitably modified to account for the fact that the potential may now possibly vanish at 0 in addition to \mathbb{S}^1 . Below we outline the procedure and indicate which portions require changes from [12].

The proof relies on compensated compactness and a careful analysis of the Young measure $\{\mu_x\}_{x \in \Omega}$ generated by the sequence $\{u_\varepsilon\}$. One of the key tools in this analysis is the concept of an entropy, defined here as a mapping $\Phi \in C_0^\infty(\mathbb{R}^2; \mathbb{R}^2)$ such that

$$\Phi(0) = 0, \quad D\Phi(0) = 0 \quad \text{and for all } z \in \mathbb{R}^2 \text{ one has } z \cdot D\Phi(z) z^\perp = 0,$$

where $z^\perp = (-z_2, z_1)$, cf. [12, Definition 2.1]. A crucial property of any such entropy is that Φ satisfies a certain equation relating $\nabla \cdot [\Phi(u)]$ and $\nabla \cdot (1 - |u|^2)$ for any $u \in H^1(\Omega; \mathbb{R}^2)$. We state this equation precisely in (3.27), and refer the reader to [12, Lemmas 2.2, 2.3] for the proof, which is a straightforward calculation. In Lemma 3.5, we prove that the class of entropies is large enough for our purposes. Next, in Proposition 3.7, we prove the requisite compactness for the sequence

$\{u_\varepsilon\}$. We achieve this by first adapting the proof of [12, Proposition 1.2] using the aforementioned equation (3.27) to show that for any entropy Φ ,

$$\{\nabla \cdot [\Phi(u_\varepsilon)]\} \text{ is compact in } H^{-1}(\Omega).$$

This compactness then allows us to use the div-curl lemma of Murat and Tartar [29, 38] and the result of Lemma 3.5 to conclude that each μ_x is a Dirac measure. One can then quickly deduce, in the same fashion as in [12, page 843], that the sequence $\{u_\varepsilon\}$ is precompact in L^2 . We begin the proof with

Lemma 3.5. (cf. [12, Lemma 2.2]) *Let μ be a probability measure on \mathbb{R}^2 supported on $\mathbb{S}^1 \cup \{0\}$. Suppose it has the property*

$$\int \Phi \cdot \tilde{\Phi}^\perp d\mu = \int \Phi d\mu \cdot \int \tilde{\Phi}^\perp d\mu \text{ for all entropies } \Phi, \tilde{\Phi}. \quad (3.19)$$

Then μ is a Dirac measure.

Remark 3.6. *We point out that the proof of this lemma does not generalize to the case where the potential vanishes on a pair of circles that both have non-zero radius. As a consequence, this proof of Theorem 3.4 does not generalize to such situations.*

Proof. We begin by recalling the definition of “generalized entropy” from [12, Lemma 2.5]. These are functions Φ defined by

$$\Phi(z) = \begin{cases} |z|^2 e & \text{for } z \cdot e > 0 \\ 0 & \text{for } z \cdot e \leq 0 \end{cases}$$

for any fixed $e \in \mathbb{S}^1$. Any such Φ can be approximated closely enough by entropies Φ_n such that (3.19) holds for Φ as well. Using the fact that these generalized entropies vanish at the origin, we have

$$\int_{\mathbb{S}^1} \Phi \cdot \tilde{\Phi}^\perp d\mu = \int_{\mathbb{S}^1} \Phi d\mu \cdot \int_{\mathbb{S}^1} \tilde{\Phi}^\perp d\mu.$$

We rewrite this as

$$e \cdot \tilde{e}^\perp \mu(\{z \cdot e > 0\} \cap \{z \cdot \tilde{e} > 0\} \cap \mathbb{S}^1) = e \cdot \tilde{e}^\perp \mu(\{z \cdot e > 0\} \cap \mathbb{S}^1) \mu(\{z \cdot \tilde{e} > 0\} \cap \mathbb{S}^1) \text{ for all } e, \tilde{e} \in \mathbb{S}^1$$

or

$$\mu(\{z \cdot e > 0\} \cap \{z \cdot \tilde{e} > 0\} \cap \mathbb{S}^1) = \mu(\{z \cdot e > 0\} \cap \mathbb{S}^1) \mu(\{z \cdot \tilde{e} > 0\} \cap \mathbb{S}^1) \\ \text{for all } \tilde{e} \in \mathbb{S}^1 \setminus \{e, -e\} \text{ and all } e \in \mathbb{S}^1.$$

Letting \tilde{e} approach e , we obtain

$$\mu(\{z \cdot e > 0\} \cap \mathbb{S}^1) \leq \mu(\{z \cdot e > 0\} \cap \mathbb{S}^1) \mu(\{z \cdot e \geq 0\} \cap \mathbb{S}^1) \text{ for all } e \in \mathbb{S}^1$$

or

$$\mu(\{z \cdot e > 0\} \cap \mathbb{S}^1) = 0 \text{ or } \mu(\{z \cdot e \geq 0\} \cap \mathbb{S}^1) \geq 1 \text{ for all } e \in \mathbb{S}^1. \quad (3.20)$$

If $\mu(\{0\}) > 0$ then it cannot be that $\mu(\{z \cdot e \geq 0\} \cap \mathbb{S}^1) \geq 1$ for any $e \in \mathbb{S}^1$. In this case $\mu(\{z \cdot e > 0\} \cap \mathbb{S}^1) = 0$ for all \mathbb{S}^1 -valued e , and μ is clearly a Dirac measure concentrated at zero. So we may assume that $\mu(\{0\}) = 0$, implying that μ is a probability measure on \mathbb{S}^1 . In this case, we deduce from (3.20) that

$$\text{supp } \mu \subset \{z \cdot e \leq 0\} \cap \mathbb{S}^1 \text{ or } \text{supp } \mu \subset \{z \cdot e \geq 0\} \cap \mathbb{S}^1 \text{ for all } e \in \mathbb{S}^1.$$

As μ is a probability measure on \mathbb{S}^1 , this implies that μ is concentrated on a single point. \square

We can now prove the main result.

Proposition 3.7. (cf. [12, Proposition 1.2]) *Let $\Omega \subset \mathbb{R}^2$ be open and bounded. Let $\{u_\varepsilon\} \subset H^1(\Omega; \mathbb{R}^2)$ be such that*

$$\nabla \cdot u_\varepsilon \text{ are uniformly bounded in } L^2, \quad (3.21)$$

$$\|H(|u_\varepsilon|)\|_{L^2(\Omega)} \xrightarrow{\varepsilon \rightarrow 0} 0, \quad (3.22)$$

and

$$\|\nabla u_\varepsilon\|_{L^2} \|H(|u_\varepsilon|)\|_{L^2} \text{ are uniformly bounded.} \quad (3.23)$$

Then

$$\{u_\varepsilon\} \subset L^2(\Omega; \mathbb{R}^2) \text{ is relatively compact.} \quad (3.24)$$

Proof. First, we modify our sequence slightly for convenience. By choosing real numbers r_ε close enough to 1 and considering the sequence $\{r_\varepsilon u_\varepsilon\}$, we can without loss of generality assume that for each ε ,

$$\left| \left\{ x \in \Omega : |r_\varepsilon u_\varepsilon(x)| = \frac{1}{\sqrt{2}} \right\} \right| = 0. \quad (3.25)$$

In addition, we can choose r_ε so that $\{r_\varepsilon u_\varepsilon\}$ has uniformly bounded energies and is precompact in $L^2(\Omega; \mathbb{R}^2)$ if and only if $\{u_\varepsilon\}$ is as well. Henceforth we refer to the modified sequence as simply $\{u_\varepsilon\}$ and assume that these conditions hold for u_ε .

We aim to show for any entropy Φ that

$$\{\nabla \cdot [\Phi(u_\varepsilon)]\} \text{ is compact in } H^{-1}(\Omega). \quad (3.26)$$

Utilizing (3.21), (3.25) and [12, Lemmas 2.2, 2.3], we see that there exists $\Psi \in C_0^\infty(\mathbb{R}^2)^2$ and $\alpha \in C_0^\infty(\mathbb{R}^2)$ such that at a.e. point in Ω one has

$$\begin{aligned} -\alpha(u_\varepsilon) \text{div } u_\varepsilon + \nabla \cdot [\Phi(u_\varepsilon)] &= \Psi(u_\varepsilon) \cdot \nabla(1 - |u_\varepsilon|^2) = -\Psi(u_\varepsilon) \cdot \nabla(|u_\varepsilon|^2) \\ &= \text{sgn}(|u_\varepsilon| - 1/\sqrt{2}) \Psi(u_\varepsilon) \cdot \nabla H(|u_\varepsilon|). \end{aligned}$$

Before proceeding, we let $s : \mathbb{R} \rightarrow \mathbb{R}$ denote a smooth, increasing, bounded function with bounded derivative such that $s(z) \equiv -1$ for $z \leq \frac{1}{2\sqrt{2}}$ and $s(z) \equiv 1$ for $z \geq \frac{1}{2\sqrt{2}}$. We will utilize

the sequence $s(|u_\varepsilon|)$, and we remark that $\frac{1}{2\sqrt{2}}$ could readily be replaced by any number less than $\frac{1}{\sqrt{2}}$. Replacing $\text{sgn}(|u_\varepsilon| - 1/\sqrt{2})$ by $s(|u_\varepsilon|)$ as such allows us to maintain L^1 control on $\nabla s(|u_\varepsilon|)$ as opposed to having to analyze the distributional gradient of a sgn function, as will be necessary in a step at the end of the proof. Continuing from (3.27), we find that

$$-\alpha(u_\varepsilon)\text{div } u_\varepsilon + \nabla \cdot [\Phi(u_\varepsilon)] = s(|u_\varepsilon|)\Psi(u_\varepsilon) \cdot \nabla H(|u_\varepsilon|) + R_\varepsilon, \quad (3.27)$$

$$R_\varepsilon := \left(\text{sgn}(|u_\varepsilon| - 1/\sqrt{2}) - s(|u_\varepsilon|) \right) \Psi(u_\varepsilon) \cdot \nabla H(|u_\varepsilon|). \quad (3.28)$$

We claim the remainder terms R_ε are bounded uniformly in L^1 . Noticing that $s(|u_\varepsilon|) = \text{sgn}(|u_\varepsilon| - 1/\sqrt{2})$ if $\left| |u_\varepsilon| - 1/\sqrt{2} \right| \geq \frac{1}{2\sqrt{2}}$, we have

$$\int_{\Omega} |R_\varepsilon| \leq C \int_{\Omega} \chi_{\left\{ \left| |u_\varepsilon| - \frac{1}{2\sqrt{2}} \right| < \frac{1}{2\sqrt{2}} \right\}} |\nabla |u_\varepsilon|| \, dx.$$

Continuing now using Holder's inequality and the bound $\int_{\Omega} W(u_\varepsilon) \leq C\varepsilon$, we have

$$\begin{aligned} \int_{\Omega} |R_\varepsilon| &\leq C \|\nabla |u_\varepsilon|\|_{L^2} \cdot \text{meas} \left\{ \left| |u_\varepsilon| - \frac{1}{\sqrt{2}} \right| < \frac{1}{2\sqrt{2}} \right\}^{1/2} \\ &\leq C \frac{1}{\sqrt{\varepsilon}} \sqrt{\varepsilon} \\ &\leq C. \end{aligned}$$

To prove (3.26), we will prove that the sequence

$$\{\nabla \cdot [\Phi(u_\varepsilon) - s(|u_\varepsilon|)H(|u_\varepsilon|)\Psi(u_\varepsilon)]\} \text{ is compact in } H^{-1}(\Omega). \quad (3.29)$$

Since the energy bound implies that $s(|u_\varepsilon|)H(|u_\varepsilon|)\Psi(u_\varepsilon)$ converges to 0 in L^2 , the divergence of this sequence converges to 0 in H^{-1} . Thus (3.29) implies (3.26). Thanks to (3.27), we have that

$$\begin{aligned} \nabla \cdot [\Phi(u_\varepsilon) - sH(|u_\varepsilon|)\Psi(u_\varepsilon)] &= \nabla \cdot [\Phi(u_\varepsilon)] - \nabla \cdot [s\Psi(u_\varepsilon)]H(|u_\varepsilon|) - s\Psi(u_\varepsilon) \cdot \nabla [H(|u_\varepsilon|)] \\ &= R_\varepsilon + \alpha(u_\varepsilon)\text{div } u_\varepsilon - \nabla \cdot [s\Psi(u_\varepsilon)]H(|u_\varepsilon|) \end{aligned}$$

We will show the desired compactness by appealing to a lemma of [30], cf. [12, Lemma 3.1]. This entails verifying the following two claims:

(1) The sequence $\{\nabla \cdot [\Phi(u_\varepsilon) - sH(|u_\varepsilon|)\Psi(u_\varepsilon)]\}$ is uniformly bounded in $L^1(\Omega)$.

(2) The sequence $\{|\Phi(u_\varepsilon) - s(|u_\varepsilon|)H(|u_\varepsilon|)\Psi(u_\varepsilon)|^2\}_{\varepsilon>0}$ is uniformly integrable.

Proof of (1): We have shown that the R_ε are uniformly bounded in L^1 , and the boundedness of the function α along with the L^2 bound on $\text{div } u_\varepsilon$ yield that $\alpha(u_\varepsilon)\text{div } u_\varepsilon$ is uniformly bounded in L^1 . It remains to show that the last term, namely $\nabla \cdot [s(|u_\varepsilon|)\Psi(u_\varepsilon)]H(|u_\varepsilon|)$, is bounded in L^1 . We have

$$H(|u_\varepsilon|)\nabla \cdot [s\Psi(u_\varepsilon)] = H(|u_\varepsilon|) \left(s'(|u_\varepsilon|) \nabla |u_\varepsilon| \cdot \Psi(u_\varepsilon) + s(|u_\varepsilon|)\text{div } \Psi(u_\varepsilon) \right).$$

The desired L^1 bound follows from Cauchy-Schwarz along with the energy bound.

Proof of (2): This is clear from the fact that Φ , s , H , and Ψ are bounded functions.

We have now proved that $\{\nabla \cdot [\Phi(u_\varepsilon)]\}$ is compact in $H^{-1}(\Omega)$. The rest of the proof follows as in the second step of [12, Proposition 1.2]. \square

3.3 The Γ -limit of E_ε among 1d competitors

In this section we analyze Γ -convergence of E_ε where competitors $u_\varepsilon = (u_\varepsilon^{(1)}, u_\varepsilon^{(2)})$ are defined on an interval $[-H, H]$ for some $H > 0$ and are required to satisfy \mathbb{S}^1 -valued boundary conditions of the form

$$u(\pm H) = (\pm \sqrt{1 - a^2}, a) \quad \text{for some } a \in [0, 1). \quad (3.30)$$

Under the one-dimensional assumption, E_ε takes the form

$$E_\varepsilon^{1D}(u) := \begin{cases} \frac{1}{2} \int_{-H}^H \left(\frac{1}{\varepsilon} W(u) + \varepsilon |u'|^2 + L(u^{(2)'})^2 \right) dx_2 & \text{if } u \in H^1((-H, H); \mathbb{R}^2), \\ +\infty & \text{otherwise.} \end{cases} \quad (3.31)$$

In a manner similar to [17], Section 6, within this one-dimensional ansatz we can obtain a sharp compactness theorem for energy bounded sequences, a complete Γ -convergence result of the E_ε functionals and a complete characterization of minimizers of the Γ -limit. Since the proofs of the results in this section are completely analogous to those in [17, Section 6], we only sketch the arguments highlighting differences.

In Section 4.1, we present results of numerical simulations obtained via gradient flow for E_ε with $\varepsilon > 0$ for the two-dimensional problem in a rectangle $\Omega = (-1/2, 1/2) \times (-H, H)$, subject to the boundary conditions (3.30) on the top and bottom and periodic boundary conditions on the left and right sides. These computations suggest convergence in large time to configurations that resemble the one-dimensional minimizers of this section, lending further evidence to our conjecture (3.12). We emphasize that the initial data for these numerics were *not* restricted to be one-dimensional.

We continue making the assumption (3.2) on our potentials. Recall that we are writing $W(u) = V(|u|)$. We begin with a compactness result.

Theorem 3.8. *Let $u_\varepsilon = (u_\varepsilon^{(1)}, u_\varepsilon^{(2)}) \in H^1((-H, H); \mathbb{R}^2)$ with $E_\varepsilon^{1D}(u_\varepsilon) \leq C$. Then there exists $u = (u_1, u_2)$ with*

$$\Psi(u_1) := \int_{-u_1}^{u_1} \sqrt{V} \left(\sqrt{s^2 + 1 - u_1^2} \right) ds \in BV((-H, H); [0, 1])$$

such that up to a subsequence, $u_\varepsilon^{(1)} \rightarrow u_1$ in $L^2(-H, H)$. In addition, $u_2 \in H^1((-H, H); \mathbb{R})$, $u_\varepsilon^{(2)} \rightarrow u_2$ in $C^{0,\gamma}(-H, H)$ for all $\gamma < 1/2$, and $|(u_1, u_2)| = 1$ or 0 a.e.

Proof. Throughout the course of the proof, we repeatedly pass to further and further subsequences of ε converging to zero but suppress this from our notation. We notice that thanks to the uniform L^4 bound from (3.2), after passing to a subsequence,

$$u_\varepsilon \rightharpoonup u = (u_1, u_2) \text{ in } L^4. \quad (3.32)$$

Furthermore, this bound, along with the uniform L^2 bound on $(u_\varepsilon^{(2)})'$ yields after passing to a further subsequence that

$$u_\varepsilon^{(2)} \rightarrow u_2 \text{ in } H^1 \quad \text{and} \quad u_\varepsilon^{(2)} \rightarrow u_2 \text{ in } C^{0,\gamma}([-H, H]) \text{ for every } \gamma < 1/2. \quad (3.33)$$

Finally, from the bound on the potential, there exists $\rho \in L^2((-H, H); \{0, 1\})$ such that

$$|u_\varepsilon| \rightarrow \rho \text{ in } L^2. \quad (3.34)$$

It remains to upgrade the convergence of $u_\varepsilon^{(1)}$ from weak to strong convergence. An algebraic identity is used in the proof of [17, Theorem 6.1] to obtain strong convergence. Here, without an explicit expression for W , we proceed differently. As in [17], we utilize the “entropy” ψ defined by

$$\psi(u_\varepsilon) := \int_{-u_\varepsilon^{(1)}}^{u_\varepsilon^{(1)}} \sqrt{V}(|(s, u_\varepsilon^{(2)})|) ds = u_\varepsilon^{(1)} \int_{-1}^1 \sqrt{V}(|(u_\varepsilon^{(1)}t, u_\varepsilon^{(2)})|) dt. \quad (3.35)$$

We set $J_\varepsilon = \int_{-1}^1 \sqrt{V}(|(u_\varepsilon^{(1)}t, u_\varepsilon^{(2)})|) dt$, so that

$$u_\varepsilon^{(1)} J_\varepsilon = \psi(u_\varepsilon). \quad (3.36)$$

On the one hand,

$$J_\varepsilon = \int_{-1}^1 \sqrt{V} \left(\sqrt{(|u_\varepsilon|^2 - (u_\varepsilon^{(2)})^2)t^2 + (u_\varepsilon^{(2)})^2} \right) dt;$$

thus (3.33)-(3.34) yield that

$$J_\varepsilon \rightarrow \int_{-1}^1 \sqrt{V} \left(\sqrt{(\rho^2 - (u^{(2)})^2)t^2 + (u^{(2)})^2} \right) dt =: J \quad \text{a.e. in } (-H, H). \quad (3.37)$$

On the other hand, using (3.2) and a Cauchy-Schwarz argument completely analogous to that found in [17], we note that $\psi(u_\varepsilon)$ is bounded in BV . Upon passing to a subsequence, we conclude that $\{\psi(u_\varepsilon)\}$ converges in L^1 , and upon passing to a further subsequence, $\{\psi(u_\varepsilon)\}$ converges almost everywhere. Consequently, using (3.36) and (3.37), we find that $u_\varepsilon^{(1)}$ converges almost everywhere as well.

Finally, since $|u_\varepsilon^{(1)}| \leq |u_\varepsilon|$ and $|u_\varepsilon| \rightarrow \rho$ strongly in L^2 , we can apply the Lebesgue dominated convergence theorem to conclude that $u_\varepsilon^{(1)}$ converges strongly in L^2 to some limit. From (3.32), this limit is u_1 , and it follows that $|(u_1, u_2)| = 0$ or 1 a.e. and that the limit of $\psi(u_\varepsilon)$ is $\psi(u_1, u_2) \in BV$. Since ψ is 0 when $u_1 = 0$, we see that $\Psi(u_1) = \psi(u)$, which concludes the proof. \square

We turn next to Γ -convergence in this one-dimensional setting. The analogue of E_0 from (3.10) is the energy

$$E_0^{1D}(u) := \frac{L}{2} \int_{-H}^H (u^{(2)})^2 dx_2 + \sum_{x_2 \in J_{\rho(1)} \cap \{|u|=1\}} K(u^{(2)}(x_2)) + c_0 \mathcal{H}_{(-H,H)}^0(\partial(\{|u|=1\})). \quad (3.38)$$

One can establish the Γ -convergence of E_ε^{1D} to E_0^{1D} in a completely analogous manner to the proof of Theorem 6.2 in [17], so we omit the details.

Finally, as in Theorem 6.4 of [17], and with identical proofs, one can characterize the minimizers of (3.38) explicitly. When the boundary conditions (3.30) are different from $(\pm 1, 0)$ the

minimizer is unique and consists of a single wall occurring at $y = 0$, no interfaces and bulk contribution in the regions $\{y > 0\} \cup \{y < 0\}$: the function $u^{(2)}$ is piecewise linear and $u^{(1)}$ jumps from $\sqrt{1 - (u^{(2)})^2}$ to $-\sqrt{1 - (u^{(2)})^2}$ across $y = 0$. The optimal jump value is easily determined by optimizing over the bulk and jump contributions. Finally when the Dirichlet boundary conditions on the top and the bottom are given by $(\pm 1, 0)$, we find two parameter regimes similar to the situation in [17]. When L/H is smaller than a certain threshold, the minimizer is unique and has both bulk divergence and jump contributions. However for larger L/H values, the minimizer only has perimeter contribution, along with two interfaces, one connecting $(-1, 0)$ to $(0, 0)$ and the other connecting $(0, 0)$ to $(1, 0)$. These interfaces divide the interval into subintervals in each of which the minimizer is a constant. See Section 4.1 for numerical simulations.

3.4 Criticality conditions for E_0

In this section we will describe criticality conditions associated with critical points u of the conjectured Γ -limit E_0 given by (3.10). For $u \in (H_{\text{div}} \cap BV)(\Omega; \mathbb{S}^1 \cup \{0\})$, we recall the notation $K(u \cdot \nu)$, with K given by (3.8) or (3.9) in the case of the Chern-Simons-Higgs potential, for the cost per arclength of a jump from one \mathbb{S}^1 -valued state, say u_1 to another one, say u_2 across a jump set J_u , with ν denoting the unit normal pointing from the 1 side of a wall to the 2 side. We recall that for such a jump, an H_{div} vector field must satisfy the requirement

$$u_1 \cdot \nu = u_2 \cdot \nu \quad \text{along the jump set } J_u. \quad (3.39)$$

In light of (3.39), we will sometimes write just $u \cdot \nu$ when evaluating the normal component of u along J_u .

We also recall that for portions of J_u corresponding to a jump from the isotropic state 0 to an \mathbb{S}^1 -valued state u , the cost per unit arclength is given by $\frac{K(0)}{2}$ and condition (3.39) becomes simply $u \cdot \nu = 0$.

Parts of the argument follow the same lines as in the proof of Theorem 4.1 in [17] except that the cost in that paper is the one associated with a Ginzburg-Landau potential, namely $K_{GL}(u \cdot \nu)$ where

$$K_{GL}(z) := \int_{-\sqrt{1-z^2}}^{\sqrt{1-z^2}} (1 - z^2 - y^2) dy,$$

which can also be written as $\frac{4}{3} (1 - (u \cdot \nu)^2)^{3/2}$ or equivalently $\frac{1}{6} |u_- - u_+|^3$.

However, in the present context, we will need to distinguish between variations of the ‘walls’ separating two \mathbb{S}^1 -valued states and ‘interfaces’ separating the isotropic state from an \mathbb{S}^1 -valued state. We will also examine criticality conditions at a junction corresponding to the intersection of these two kinds of curves. We begin with:

Theorem 3.9. *(Variations that fix the jump set)*

Consider any $u \in BV(\Omega, \mathbb{S}^1 \cup \{0\}) \cap H_{\text{div}}(\Omega, \mathbb{S}^1 \cup \{0\})$ such that $u_{\partial\Omega} \cdot \nu_{\partial\Omega} = g \cdot \nu_{\partial\Omega}$ on $\partial\Omega$. Denote by J_u its jump set. Then if the first variation of E_0 evaluated at u vanishes when taken with respect to perturbations compactly supported in $\Omega \setminus J_u$, one has the condition

$$u^\perp \cdot \nabla \text{div } u = 0 \quad \text{holding weakly on } \Omega \setminus J_u, \quad (3.40)$$

where $u^\perp = (-u_2, u_1)$.

Now assume the first variation vanishes at u when taken with respect to perturbations that fix J_u and are supported within any ball $B(p, R)$ centered at a smooth point of $p \in J_u \cap \Omega$. If J_u separates the ball $B(p, R)$ into two regions where u is given by \mathbb{S}^1 -valued states u_1 and u_2 and if the traces $\operatorname{div} u_1$ and $\operatorname{div} u_2$ are sufficiently smooth, then one has the condition

$$K'(u \cdot \nu) = L[\operatorname{div} u] \text{ on } J_u \cap \Omega, \quad (3.41)$$

where $[\operatorname{div} u] = \operatorname{div} u_2 - \operatorname{div} u_1$ represents the jump in divergence across J_u and ν is the unit normal to J_u pointing from region 1 to region 2.

Remark 3.10. There is no natural boundary condition analogous to (3.41) for such variations taken about a point of J_u where J_u separates an isotropic state 0 from an \mathbb{S}^1 -valued state since the requirement of tangency in such a configuration is too rigid to allow for a rich enough class of perturbations.

Proof. To derive conditions (3.40) and (3.41) we assume that for some point $p \in \Omega$ and for some $R > 0$, either $B(p, R) \cap J_u = \emptyset$ or else $p \in J_u$ and the following conditions hold $B(p, R)$:

(i) The set $B(p, R) \cap J_u$ is a smooth curve, which we denote by Γ and which admits a smooth parametrization by arclength, which we denote by $r : [-s_0, s_0] \rightarrow \Omega$ for some $s_0 > 0$ with $r(0) = p$.

(ii) On either side of Γ the critical point u and $\operatorname{div} u$ possess smooth traces on J_u . We will denote the two components of $B(p, R) \setminus \Gamma$ by Ω_1 and Ω_2 and we denote u on these two sets by $u_j : \Omega_j \rightarrow \mathbb{S}^1$, for $j = 1, 2$.

We will present the argument for case (ii), indicating how the easier case (i) follows from the same analysis.

To define an allowable perturbation u^t of the critical point u given by u_1 and u_2 , we must maintain the property of being \mathbb{S}^1 -valued, so to that end we introduce smooth functions $\phi_j : B(p, R) \times (-T, T) \rightarrow \mathbb{R}$ for some $T > 0$ such that the perturbations of u_1 and u_2 take the form

$$u_j^t(x) := u_j(x) e^{it\phi_j(x,t)}, \quad (3.42)$$

shifting just for the moment to complex notation. Introducing $\phi_j(x) := \phi_j(x, 0)$, expanding (3.42) and reverting back to an \mathbb{R}^2 -valued description of u_j^t we find that for $x \in \Omega_j^t$ one has

$$u_j^t(x) \sim u_j(x) + t\phi_j(x)u_j(x)^\perp. \quad (3.43)$$

Along J_u , we must also be sure to preserve to $O(t)$ the H_{div} condition (3.39), namely

$$u_1^t \cdot \nu = u_2^t \cdot \nu \quad \text{along } \Gamma. \quad (3.44)$$

Invoking (3.39) for the unperturbed critical point, along with (3.43) we find that $u_1^t \cdot \nu = u_2^t \cdot \nu$ to $O(t)$ provided

$$\phi_1 u_1^\perp \cdot \nu = \phi_2 u_2^\perp \cdot \nu.$$

However, since

$$u_j^\perp \cdot \nu = u_j \cdot \tau \quad \text{and} \quad u_1 \cdot \tau = -u_2 \cdot \tau \neq 0 \quad (3.45)$$

along the jump set J_u bridging \mathbb{S}^1 -valued states, it follows that we must require

$$\phi_1(x) = \phi_2(x) \quad \text{for } x \in \Gamma. \quad (3.46)$$

For later use, we also record that from (3.43) and (3.45) one has along Γ the expansion

$$u^t \cdot \nu \sim u_1 \cdot \nu + t\phi_1(u_1 \cdot \tau) + o(t). \quad (3.47)$$

Now we calculate

$$\begin{aligned} \frac{d}{dt}\Big|_{t=0} E_0(u^t) &= \frac{d}{dt}\Big|_{t=0} \left\{ \frac{L}{2} \sum_{j=1}^2 \int_{\Omega_j} (\operatorname{div} u_j^t)^2 dx \right\} + \frac{d}{dt}\Big|_{t=0} \int_{\Gamma} K(u^t \cdot \nu) ds \\ &= \frac{d}{dt}\Big|_{t=0} \left\{ \sum_{j=1}^2 \frac{L}{2} \int_{\Omega_j} (\operatorname{div} (u_j(x) + t\phi_j(x)u_j(x)^\perp))^2 dx \right\} + \\ &\quad \frac{d}{dt}\Big|_{t=0} \int_{\Gamma} K(u_1 \cdot \nu + t\phi_1(u_1 \cdot \tau)) ds \end{aligned}$$

Taking the t -derivatives and evaluating at $t = 0$ we obtain

$$\begin{aligned} \frac{d}{dt}\Big|_{t=0} E_0(u^t) &= \left\{ L \sum_{j=1}^2 \int_{\Omega_j} (\operatorname{div} u_j)(\operatorname{div} (\phi_j u_j^\perp)) dx \right\} \\ &\quad \int_{\Gamma} K'(u \cdot \nu)(u_1 \cdot \tau) ds. \end{aligned}$$

Integrating by parts, a vanishing first variation of this type leads to the condition

$$\begin{aligned} -L \sum_{j=1}^2 \int_{\Omega_j} \nabla(\operatorname{div} u_j \cdot \phi_j u_j^\perp) dx + L \int_{\Gamma} \{(\operatorname{div} u_1)\phi_1 u_1^\perp \cdot \nu - (\operatorname{div} u_2)\phi_2 u_2^\perp \cdot \nu\} ds \\ + \int_{\Gamma} K'(u \cdot \nu)(u_1 \cdot \tau) ds = 0. \end{aligned} \quad (3.48)$$

Now by taking the functions ϕ_j to be supported off of J_u we arrive at condition (3.40). This also handles case (i) where $B(p, R) \cap J_u = \emptyset$. Then, in light of (3.40), along with (3.45) and (3.46) we find that

$$\int_{\Gamma} \{K'(u \cdot \nu)(u_1 \cdot \tau) + L(\operatorname{div} u_1 - \operatorname{div} u_2)\}(u_1 \cdot \tau) \phi_1 ds = 0.$$

Since $u_1 \cdot \tau \neq 0$ along the jump set and ϕ_1 is arbitrary, we arrive at (3.41). \square

Corollary 3.11. (cf. [17], Cor. 4.2). *Suppose u is smooth and critical for E_0 in the sense of (3.40). Then writing u locally in terms of a lifting as $u(x) = e^{i\theta(x)}$ and defining the scalar $v := \operatorname{div} u$ one has that (3.40) is equivalent to the following system for the two scalars θ and v :*

$$-\sin \theta \theta_{x_1} + \cos \theta \theta_{x_2} = v \quad (3.49)$$

$$-\sin \theta v_{x_1} + \cos \theta v_{x_2} = 0. \quad (3.50)$$

Consequently, starting from any initial curve in Ω parametrized via $s \mapsto (x_1^0(s), x_2^0(s))$ along which θ and v take values $\theta_0(s)$ and $v_0(s)$ respectively, the characteristic curves, say $t \mapsto (x_1(s, t), x_2(s, t))$, are given by

$$x_1(s, t) = \frac{1}{v_0(s)} [\cos(v_0(s)t + \theta_0(s)) - \cos \theta_0(s)] + x_1^0(s), \quad (3.51)$$

$$x_2(s, t) = \frac{1}{v_0(s)} [\sin(v_0(s)t + \theta_0(s)) - \sin \theta_0(s)] + x_2^0(s), \quad (3.52)$$

whenever $v_0(s) \neq 0$. The corresponding solutions $\theta(s, t)$ and $v(s, t)$ are given by

$$\theta(s, t) = v_0(s)t + \theta_0(s), \quad v(s, t) = v_0(s), \quad (3.53)$$

so that the characteristics are circular arcs of curvature $v_0(s)$ and carry constant values of the divergence. In case the divergence vanishes somewhere along the initial curve, i.e. $v_0(s) = 0$, then the characteristic is a straight line.

We also consider the implications of criticality with respect to perturbations of the jump set itself.

Theorem 3.12. (*Variations of the jump set*)

Under the same assumptions on u as in the previous theorem, suppose in addition to the criticality with respect to perturbations that fix the location of J_u , one also assumes the vanishing of the first variation of E_0 , evaluated at u , allowing for local perturbations of the jump set $J_u \cap \Omega$ itself. Then along any points of J_u where u jumps between two \mathbb{S}^1 -valued maps u_1 and u_2 , a vanishing first variation leads to the condition

$$\frac{L}{2} \left((\operatorname{div} u_1)^2 - (\operatorname{div} u_2)^2 \right) - L(\operatorname{div} u_1 + \operatorname{div} u_2)' (u_1 \cdot \tau) - L(\operatorname{div} u_1 + \operatorname{div} u_2) (u_1 \cdot \tau)' - K(u \cdot \nu) \kappa = 0, \quad (3.54)$$

at any point $p \in J_u$ such that J_u , u_1 and u_2 are sufficiently smooth in some ball centered at p . Here κ denotes the curvature of J_u , τ denotes the unit tangent to J_u and ν is the unit normal to J_u pointing from the u_1 side of J_u to the u_2 side. The notation $(\cdot)'$ refers to the tangential derivative along the jump set.

For portions of J_u separating an \mathbb{S}^1 -valued state u^* from the isotropic state 0, criticality takes the form

$$\frac{L}{2} (\operatorname{div} u^*)^2 - L(\operatorname{div} u^*)' (u^* \cdot \tau) + \frac{K(0)}{2} \kappa = \lambda, \quad (3.55)$$

where λ is a Lagrange multiplier that is present only if E_0 is considered subject to an area constraint on the measure of the isotropic phase 0. Also, since $u \in H_{\operatorname{div}}(\Omega)$ requires that $u^* \cdot \nu = 0$ along such a portion of J_u , we note that in (3.55) one either has $u^* \cdot \tau \equiv 1$ or $u^* \cdot \tau \equiv -1$.

Proof. To derive condition (3.54) assume that for some point $p \in J_u$ the following conditions hold in a ball $B(p, R)$ for some radius R :

(i) The set $B(p, R) \cap J_u$ is a smooth curve, which we denote by Γ and which admits a smooth parametrization by arclength, which we denote by $r : [-s_0, s_0] \rightarrow \Omega$ for some $s_0 > 0$ with $r(0) = p$.

(ii) On either side of Γ the critical point u is C^2 with C^1 traces on J_u . We will denote the two components of $B(p, R) \setminus \Gamma$ by Ω_1 and Ω_2 and we denote u on these two sets by $u_j : \Omega_j \rightarrow \mathbb{S}^1$, for $j = 1, 2$. Again, our convention for the unit normal ν is that it points out of Ω_1 into Ω_2 .

For the calculation it will be convenient to assume that for $j = 1, 2$, u_j has been smoothly extended so as to be defined in an open neighborhood of Γ . We take this extension to be executed so that u_1 is constant along ν and so that u_2 is constant along $-\nu$.

In order to effect a smooth perturbation of Γ , u_1 and u_2 we now introduce a vector field $X \in C_0^1(B(p, R); \mathbb{R}^2)$. For convenience we will assume that $X(x)$ is parallel to $\nu(x)$ for $x \in \Gamma$ and so we introduce the scalar function $h : [-s_0, s_0] \rightarrow \mathbb{R}$ such that

$$X(r(s)) = h(s)\nu(s) \quad \text{for } s \in [-s_0, s_0], \quad (3.56)$$

where $h(\pm s_0) = 0$. Here we have written $\nu(s)$ for the composition $\nu(r(s))$. Then let $\Psi : B(p, R) \times (-T, T) \rightarrow \Omega$ solve

$$\frac{\partial \Psi}{\partial t} = X(\Psi) \quad \Psi(x, 0) = x, \quad (3.57)$$

for some $T > 0$. Expanding in t we find that

$$D\Psi(\cdot, t) \sim I + t\nabla X + o(t), \quad (3.58)$$

so that in particular one has the identity

$$J\Psi(x, t) := \det D\Psi \sim 1 + t\operatorname{div} X(x) + o(1). \quad (3.59)$$

Throughout this proof, the symbol \sim refers to an equivalence up to terms that are $o(t)$.

Now we define the evolution of the curve Γ via the vector field X by $\Gamma^t := \Psi(\Gamma, t)$ with corresponding parametrization

$$r^t(s) := \Psi(r(s), t) \sim r(s) + X(r(s))t \sim r(s) + th(s)\nu(s), \quad (3.60)$$

in light of (3.56). A simple calculation goes to show that the normal ν^t to Γ^t takes the form

$$\nu^t(s) \sim \nu(s) - th'(s)\tau(s), \quad (3.61)$$

where we have introduced the notation τ for the unit tangent $r'(s)$ to Γ . We caution that the parameter s used to parametrize Γ^t is not an arclength parametrization on this deformed curve. Indeed one finds through an application of the Frenet equation that

$$r^{t'}(s) = r'(s) + th'(s)\nu(s) + th\nu'(s) = (1 - th(s)\kappa(s))\tau(s) + th'(s)\nu(s)$$

where κ denotes the curvature of Γ , so that

$$|r^{t'}(s)| \sim 1 - th(s)\kappa(s). \quad (3.62)$$

Similarly, we define the deformation of the two sets Ω_1 and Ω_2 via

$$\Omega_j^t := \Psi(\Omega_j, t) \quad \text{for } j = 1, 2. \quad (3.63)$$

To define the allowable evolution of the critical point u given by u_1 and u_2 requires a little more care. Firstly, we must maintain the property of being \mathbb{S}^1 -valued, so to that end we introduce smooth functions $\phi_j : B(p, R) \times (-\tau, \tau) \rightarrow \mathbb{R}$ such that the perturbations of u_1 and u_2 take the form

$$u_j^t(x) := u_j(x)e^{it\phi_j(x,t)}, \quad (3.64)$$

shifting just for the moment to complex notation. Introducing $\phi_j(x) := \phi_j(x, 0)$, expanding (3.64) and reverting back to an R^2 -valued description of u_j^t we find that for $x \in \Omega_j^t$ one has

$$u_j^t(x) \sim u_j(x) + t\phi_j(x)u_j(x)^\perp. \quad (3.65)$$

As before $(a, b)^\perp = (-b, a)$.

Secondly, we must preserve to $O(t)$ the H_{div} condition (3.39), namely

$$u_1^t \cdot \nu^t = u_2^t \cdot \nu^t \quad \text{along } \Gamma^t. \quad (3.66)$$

To this end, we observe that along Γ^t one has

$$\begin{aligned} u_j^t(r^t(s)) &\sim u_j^t(r(s) + th(s)\nu(s)) + t\phi_j(r(s) + th(s)\nu(s))u_j^\perp(r(s) + th(s)\nu(s)) \\ &\sim u_j(r(s)) + t\phi_j(r(s))u_j^\perp(r(s)). \end{aligned} \quad (3.67)$$

It is here that we require the slight extensions of the original functions u_j that are constant along the normal direction of ν to make (3.65) well-defined in $\Omega_j^t \setminus \Omega_j$ and to make (3.67) correct to $O(t)$.

Then once we apply (3.61) and (3.67) to (3.66) we arrive at the requirement that

$$(u_1 + t\phi_1 u_1^\perp) \cdot (\nu - th'\tau) \sim (u_2 + t\phi_2 u_2^\perp) \cdot (\nu - th'\tau) \quad \text{along } \Gamma. \quad (3.68)$$

Equating terms at $O(t)$ and using (3.45), we find that necessarily,

$$h'(s) = \frac{1}{2}(\phi_1(r(s)) + \phi_2(r(s))) \quad \text{for } s \in [-s_0, s_0]. \quad (3.69)$$

For later use we also record that fact, based on expanding the left hand side of (3.68), that

$$u_1^t(r^t(s)) \cdot \nu^t(s) \sim u(r(s)) \cdot \nu(s) + t(\phi_1(r(s)) - h'(s))(u_1 \cdot \tau) \quad \text{for } s \in [-s_0, s_0]. \quad (3.70)$$

With these preliminaries taken care of, we are now ready to proceed with the calculation of the first variation $\frac{d}{dt}|_{t=0} E_0(u^t)$. We begin with the variation of the divergence term in the energy taken over Ω_j^t for $j = 1, 2$. We observe that

$$\begin{aligned} \int_{\Omega_j^t} (\text{div } u_j^t)^2 dx &\sim \int_{\Omega_j^t} (\text{div } u_j + t \text{div } (\phi_j u_j^\perp))^2 dx \\ &\sim \int_{\Omega_j} \left[\text{div } u_j(\Psi(y, t)) + t \text{div } \phi_j(\Psi(y, t))u_j^\perp(\Psi(y, t)) \right]^2 (1 + t \text{div } X(y)) dy, \end{aligned}$$

where we have utilized the change of variables $x = \Psi(y, t)$ and invoked (3.59) to obtain the leading order behavior of the Jacobian of the change of variables. Then, since $\Psi \sim y + tX(y)$ we find

$$\begin{aligned} \frac{d}{dt}|_{t=0} \int_{\Omega_j^t} (\text{div } u_j^t)^2 dx &= \\ \int_{\Omega_j} \left[(\text{div } u_j(y))^2 \text{div } X + 2 \text{div } u_j(y) \text{div } (\phi_j(y)u_j^\perp(y)) + \frac{\partial}{\partial t}|_{t=0} \left(\text{div } u_j(y + tX(y)) \right)^2 \right] dy &= \\ \int_{\Omega_j} \left[(\text{div } u_j(y))^2 \text{div } X + 2 \text{div } u_j(y) \text{div } (\phi_j(y)u_j^\perp(y)) + 2 \text{div } u_j(y) \nabla \text{div } u_j(y) \cdot X(y) \right] dy &= \\ \int_{\Omega_j} \left[\text{div} \left((\text{div } u_j)^2 X \right) + 2 \text{div } u_j(y) \text{div} (\phi_j(y)u_j^\perp(y)) \right] dy & \end{aligned}$$

(3.71)

Applying the divergence theorem, and invoking (3.40) along with the compact support of X within the ball $B(p, R)$, we conclude that

$$\begin{aligned} \frac{d}{dt} \Big|_{t=0} \frac{L}{2} \left(\int_{\Omega_1^t} (\operatorname{div} u_1^t)^2 dx + \int_{\Omega_2^t} (\operatorname{div} u_2^t)^2 dx \right) &= \\ \frac{L}{2} \int_{\Gamma} \left\{ ((\operatorname{div} u_1)^2 - (\operatorname{div} u_2)^2) h + 2 (\operatorname{div} u_1) \phi_1 u_1^\perp \cdot \nu - 2 (\operatorname{div} u_2) \phi_2 u_2^\perp \cdot \nu \right\} ds &= \\ \frac{L}{2} \int_{\Gamma} \left\{ ((\operatorname{div} u_1)^2 - (\operatorname{div} u_2)^2) h + 2 (\phi_1 \operatorname{div} u_1 + \phi_2 \operatorname{div} u_2) (u_1 \cdot \tau) \right\} ds, \end{aligned} \quad (3.72)$$

where in the last line we used (3.45).

We turn now to the variation of the jump energy. By (3.70) we have

$$\begin{aligned} K(u'(r'(s)) \cdot \nu'(s)) &\sim K(u(r(s)) \cdot \nu(s) + t(\phi_1(r(s)) - h'(s))(u_1(r(s)) \cdot \tau(s))) \\ &\sim K(u \cdot \nu) + tK'(u \cdot \nu)(\phi_1 - h')(u_1 \cdot \tau), \end{aligned}$$

where all terms in the last line are evaluated along Γ , that is, evaluated at $x = r(s)$. Then we can appeal to (3.62) to calculate that

$$\begin{aligned} \frac{d}{dt} \Big|_{t=0} \int_{\Gamma^t} K(u^t \cdot \nu^t) ds &= \\ \frac{d}{dt} \Big|_{t=0} \int_{-s_0}^{s_0} \left\{ (K(u(r(s)) \cdot \nu(s)) + tK'(u(r(s)) \cdot \nu(s))(\phi_1(r(s)) - h'(s))(u_1(r(s)) \cdot \tau(s))) \right\} \left\{ 1 - th(s)\kappa(s) \right\} ds &= \\ = \int_{\Gamma} K'(u \cdot \nu)(\phi_1 - h')(u_1 \cdot \tau) - K(u \cdot \nu) h \kappa ds &= \\ = \int_{\Gamma} L(\operatorname{div} u_2 - \operatorname{div} u_1)(\phi_1 - h')(u_1 \cdot \tau) - K(u \cdot \nu) h \kappa ds, \end{aligned} \quad (3.73)$$

where in the last line we have used the criticality condition (3.41).

Combining (3.72) and (3.73) we obtain

$$\begin{aligned} \frac{d}{dt} \Big|_{t=0} E_0(u^t) &= \\ \int_{\Gamma} \left\{ \frac{L}{2} \left((\operatorname{div} u_1)^2 - (\operatorname{div} u_2)^2 \right) - K(u \cdot \nu) \kappa \right\} h ds &+ \\ + L \int_{\Gamma} \left\{ (\phi_1 + \phi_2) \operatorname{div} u_2 + (\operatorname{div} u_1 - \operatorname{div} u_2) h' \right\} (u_1 \cdot \tau) ds &= \\ = \int_{\Gamma} \left\{ \frac{L}{2} \left((\operatorname{div} u_1)^2 - (\operatorname{div} u_2)^2 \right) - K(u \cdot \nu) \kappa \right\} h ds &+ \\ + L \int_{\Gamma} (\operatorname{div} u_1 + \operatorname{div} u_2) (u_1 \cdot \tau) h' ds, \end{aligned}$$

in light of (3.69). Integrating by parts in the last integrals, and using that $h(-s_0) = h(s_0) = 0$ we finally obtain

$$\frac{d}{dt}|_{t=0} E_0(u^t) = \int_{\Gamma} \left\{ \frac{L}{2} ((\operatorname{div} u_1)^2 - (\operatorname{div} u_2)^2) - L(\operatorname{div} u_1 + \operatorname{div} u_2)' (u_1 \cdot \tau) - L(\operatorname{div} u_1 + \operatorname{div} u_2) (u_1 \cdot \tau)' - K(u \cdot \nu) \kappa \right\} h ds.$$

Since criticality implies that this last integral must vanish for all h , we obtain (3.54).

The derivation of (3.55) follows along similar lines so we omit the details. One difference to note, however, is that in the presence of an area constraint on the measure of $\{u \equiv 0\}$, the normal component h of the vector field X along Γ must additionally satisfy the requirement

$$\int_{-s_0}^{s_0} h(s) ds = 0$$

so that the perturbed jump set preserves area to $O(t)$. This condition leads to the appearance of the Lagrange multiplier in (3.55). \square

Our last consequence of criticality for a vector field u with respect to the functional E_0 concerns the possible presence in Ω of a junction point P such that for some $R > 0$, the set $B(p, R) \cap J_u$ consists of four curves meeting at p . We wish to focus on the configuration where two of these curves, which we label as Γ_{01} and Γ_{03} , are interfaces separating an isotropic region, which we label as Ω_0 , from two disjoint regions, Ω_1 and Ω_3 , where u is given by $u_1 : \Omega_1 \rightarrow \mathbb{S}^1$ and $u_3 : \Omega_3 \rightarrow \mathbb{S}^1$, respectively. Wedged between Ω_1 and Ω_3 we assume there exists a set Ω_2 where u takes on another \mathbb{S}^1 -valued state u_2 . The dashed curve separating Ω_1 from Ω_2 , representing the wall across which u jumps from u_1 to u_2 we denote by Γ_{12} , and the dashed curve separating Ω_2 from Ω_3 , representing the wall across which u jumps from u_2 to u_3 we denote by Γ_{12} . We write τ_{ij} and ν_{ij} for the unit tangent and unit normal to the curve Γ_{ij} where each τ_{ij} points away from the junction P and ν_{ij} points from the region Ω_i into the region Ω_j . See Fig. 4.

Our reason for focusing on this particular configuration is predicated on the belief that it is somehow quite generic behavior in a neighborhood of a singular point on the isotropic-nematic phase boundary; see the discussion in Section 4.4. This belief is grounded in the findings of numerous numerical experiments we have conducted and examples we have constructed for this model, some of which appear in the last section of this article. Our hope is that the condition derived in Theorem 3.13 below will be of use in constructing particular candidates for minimizers of E_0 as well as perhaps being of use in ruling out certain junction configurations that are found to violate (5.19).

To state the next result we must introduce the notation τ_{ij} for the unit tangent on Γ_{ij} oriented so as to point away from P , and ν_{ij} for the unit normal to Γ_{ij} , pointing from region Ω_i into Ω_j .

Theorem 3.13. *(Criticality conditions at a junction). Assume a configuration in a neighborhood of a point $P \in \Omega$ as described above and as depicted in Fig. 4. Assume that in a neighborhood of P the functions u_j and their divergences $\operatorname{div} u_j$ for $j = 1, 2, 3$ are all smooth in the closure of Ω_j including at the junction point P . Assume further that the four curves $\Gamma_{01}, \Gamma_{12}, \Gamma_{23}$ and Γ_{03} are*

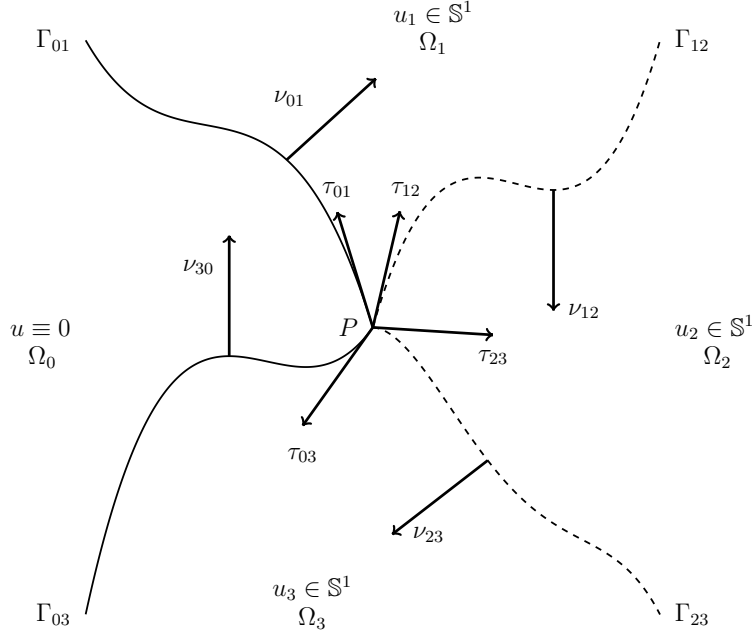


Figure 4: A configuration with a junction point P at which two components of the interface, Γ_{01} and Γ_{03} meet two components of the wall Γ_{12} and Γ_{23} .

all smooth near P . Then criticality of E_0 with respect to variations of P , the four curves Γ_{ij} and the three functions u_j leads to the condition

$$\begin{aligned}
& \frac{K(0)}{2}(\tau_{01} + \tau_{03}) + K(u_1 \cdot \nu_{12})\tau_{12} + K(u_2 \cdot \nu_{23})\tau_{23} \\
& = L \left\{ (\operatorname{div} u_1)(u_1 \cdot \tau_{01})\nu_{01} + (\operatorname{div} u_3)(u_3 \cdot \tau_{03})\nu_{03} \right\} \\
& - L \left\{ (\operatorname{div} u_1 + \operatorname{div} u_2)(u_1 \cdot \tau_{12})\nu_{12} + (\operatorname{div} u_2 + \operatorname{div} u_3)(u_2 \cdot \tau_{23})\nu_{23} \right\} \quad (3.74)
\end{aligned}$$

where all quantities above are evaluated at P .

The proof of Theorem 3.13 can be found in the appendix.

4 Examples: Analytical constructions for large L and some numerics

We conclude with an exploration of possible morphologies for our limiting energy E_0 , which we recall is given by

$$E_0(u) = \frac{L}{2} \int_{\Omega} (\operatorname{div} u)^2 dx + \frac{K(0)}{2} \operatorname{Per}_{\Omega}(\{|u| = 1\}) + \int_{J_u \cap \{|u|=1\}} K(u \cdot \nu) d\mathcal{H}^1,$$

with the cost K given by (3.8). After describing in Section 4.1 some numerics that complement our rigorous work in Section 3.3 for the case where Ω is a rectangle, we will focus on two main settings: (i) the case where Ω is a disk and competitors must satisfy a boundary condition in the sense of (1.6) where g has degree $k \in \mathbb{Z}$; and (ii) the case of an island of isotropic phase, generated by an area constraint, lying inside a nematic whose far field is given by \vec{e}_1 .

For both settings (i) and (ii) we will not work directly with E_0 but rather with a problem that at least formally can be viewed as the large L limit of E_0 , namely

$$E_0^\infty(u) := \frac{K(0)}{2} \text{Per}_\Omega(\{|u| = 1\}) + \int_{J_u \cap \{|u|=1\}} K(u \cdot \nu) d\mathcal{H}^1, \quad (4.1)$$

defined for $u \in (BV \cap H_{\text{div}})(\Omega, \mathbb{S}^1 \cup \{0\})$ such that

$$\text{div } u = 0 \quad \text{in } \Omega, \quad (4.2)$$

and perhaps supplemented by the condition $u_{\partial\Omega} \cdot \nu_{\partial\Omega} = g \cdot \nu_{\partial\Omega}$ on $\partial\Omega$ if one wishes to specify Dirichlet data $g : \partial\Omega \rightarrow \mathbb{S}^1 \cup \{0\}$, or such that $|\{u = 0\}| = \text{const}$ or $|\{|u| = 1\}| = \text{const}$ if one wishes to specify an area constraint. We also note that the H_{div} requirement still enforces the condition that competitors have trace from the nematic side that is tangent to any interface, i.e. (3.4) where $u_- = 0$.

We will construct critical points for E_0^∞ that we expect to be local or even globally minimal and we observe that these divergence-free vector fields are competitors in the minimization of E_0 for finite L . Thus, we expect that they may well be close to critical points or *perhaps* even minimizers of E_0 when L is large. As we shall see, this expectation is supported by simulations on the gradient flow for E_ε where L is large but fixed and then ε is taken to be small.

Regarding all simulations in this section, we obtain critical points for the energy E_ε by simulating gradient flow for E_ε using the software package COMSOL [1]. Unless specified otherwise, we do not claim that solutions that we obtain are minimizers of E_ε or prove that these solutions converge to critical points of the limiting energy. We will infer such convergence in cases where we are able to show via an analytical construction that a similar looking critical point of E_0 does exist.

We consider E_0^∞ rather than E_0 here in part because, as we will describe below, the divergence-free condition (4.2) provides a rigidity that simplifies the search for critical points. We hasten to add, however, that to us minimization of E_0^∞ is a fascinating and nontrivial problem in its own right that one might view as a version of the Aviles-Giga limiting problem which allows for phase transitions, i.e. isotropic regions, as well as walls. Of course this entire project represents just an initial investigation of E_ε and E_0 that we hope will generate interest in future analysis of critical points and minimization of these functionals for L finite. In that vein, we hope the work in this section provides intuition and techniques that can be generalized, and that the criticality conditions derived in Section 3.4 provide some tools.

So what does criticality mean for E_0^∞ ? Within the nematic region where $|u| = 1$, but away from the jump set J_u , if we locally describe a competitor u via $u(x) = (\cos \theta(x), \sin \theta(x))$, then (4.2) implies that

$$\nabla \theta \cdot (-\sin \theta, \cos \theta) = 0.$$

Defining the characteristic direction via $x'_1 = -\sin \theta$, $x'_2 = \cos \theta$ we see that θ and therefore u is constant along characteristics and further that u is orthogonal to characteristics and so one

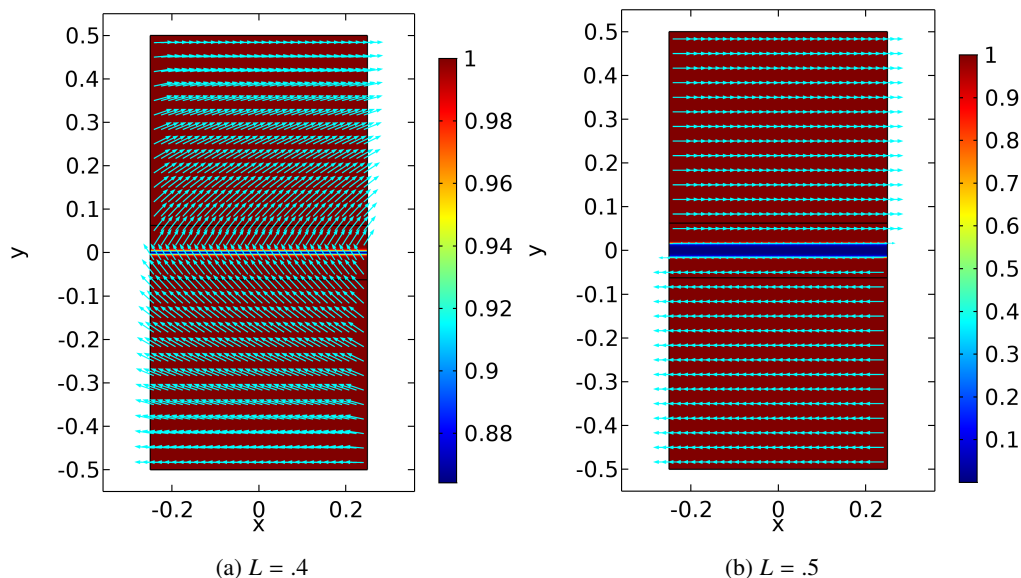


Figure 5: Critical points of E_ε in the rectangle. Here $\varepsilon = 0.001$.

concludes in particular that:

Characteristics for E_0^∞ must be straight lines along which u is orthogonal and constant. (4.3)

This rigidity, familiar to those who work on Aviles-Giga, is what will allow us to carry out some of the analytical constructions in this section.

On the other hand, this amount of rigidity limits one's ability build a rich class of variations of E_0^∞ and so we will not attempt to directly compute $L = \infty$ analogues of the ODE's (3.54) or (3.55) or the junction condition (3.74).

4.1 Critical points of E_0 in a rectangle.

Here we take Ω to be the rectangle $(-0.2, 0.2) \times (-0.5, 0.5)$ and we seek critical points of the energy E_0 which satisfy the boundary conditions $u(\cdot, \pm 1/2) = \pm \vec{e}_1 = (\pm 1, 0)$ and satisfy periodic boundary conditions on the sides $x = \pm \frac{1}{2}$.

As discussed in Section 3.3, when restricting minimization of E_ε to one-dimensional competitors which in this case are functions of y , we obtain full Γ -convergence of the one-dimensional analog of E_ε to that of E_0 . Further, the behavior of minimizers of E_0 among one-dimensional competitors is determined by the value of L . When L exceeds a certain threshold, the bulk divergence contribution vanishes and the energy of a critical point is associated solely with a wall along the x -axis that separates the regions of zero divergence. When L falls below the threshold value, the bulk divergence contribution is present along with a cost of the wall associated with the jump set of the minimizer. When L tends to zero, the wall disappears and the energy minimizing vector field is essentially a linear interpolation of the boundary data.

Figs. 5-6 present the results of simulations for the gradient flow for E_ε in the rectangle. It is evident that, even though the simulations are fully two-dimensional, the critical points obtained in this way are one-dimensional and conform to the picture described in the previous paragraph. Two main observations follow from these figures. First, the results seem to indicate that the wall cost is indeed one-dimensional as we conjectured earlier in the paper. Second, in all simulations done in the rectangle, the critical points we observe are always one-dimensional, even for large values of L . This is in contrast to the results in [17] for the version of the problem with the Ginzburg-Landau instead of the Chern-Simons-Higgs potential. In that work, one-dimensional critical points are found to be unstable with respect to formation of cross-tie configurations for large L —such instability does not seem to be present here, at least numerically.

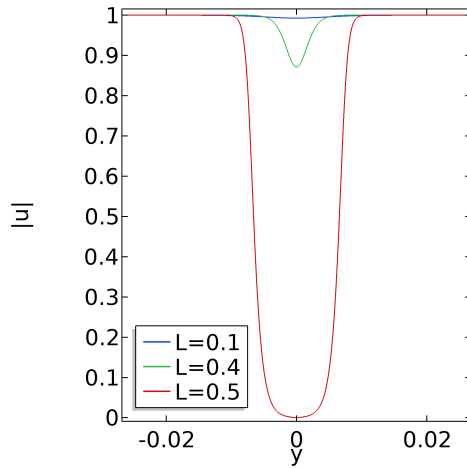


Figure 6: Cross-section of the wall for a critical point of E_ε in the rectangle. The y -axis is as shown in Fig. 5 and $\varepsilon = 0.001$. When $L \geq 0.5$, the profile is independent of L (not shown).

4.2 Degrees other than 0 or 1 are too costly

Before we begin the constructions and numerics pertaining to E_0^∞ , we first present a theorem which will elucidate the behavior of certain critical points for E_0 and provide an explanation for some of the morphology to come. The theorem yields a lower bound for the L^2 -norm of the divergence, in the spirit of analogous lower bound results of Jerrard [19] and Sandier [36] for the Ginzburg-Landau energy. The proofs of the Jerrard/Sandier results rely crucially on the fact that the square of the gradient of a function is a sum of squares of its components, a feature that is not shared by the square of the divergence of a vector field. We overcome this difficulty by working in Fourier space.

Theorem 4.1. Fix $0 < \rho < \rho' \leq 1$, set $A := \{x \in \mathbb{R}^2 : \rho < |x| < \rho'\}$ and let C_t be a circle of radius t centered at the origin. Suppose that $u \in C^1(\bar{A}; \mathbb{R}^2)$ is such that $|u| \geq 1/2$ on A and $\deg(u, C_t) = d \neq 0, 1$ for any $t \in [\rho, \rho']$. Then

$$\int_A (\operatorname{div} u)^2 dx \geq |\pi d \log(\rho'/\rho) + 4|, \quad d < 0, \quad (4.4)$$

$$\int_A (\operatorname{div} u)^2 dx \geq |\pi(d-1) \log(\rho'/\rho) - 4|, \quad d > 1. \quad (4.5)$$

Remark 4.2. By majorizing $\int_A (\operatorname{div} u)^2$ by $\int_A |\nabla u|^2$ in (4.4)-(4.5), it follows from results for $|\nabla u|^2$ that the scaling in ρ'/ρ is optimal. Note that there is no similar lower bound when $d = 1$ due to existence of the divergence-free vector field \vec{e}_θ .

Proof. The proof of this result proceeds using Fourier series.

1. Developing u in a Fourier series, given by

$$u \sim \sum_{n \in \mathbb{Z}} u_n(r) e^{in\theta},$$

we first derive a formula for the degree of u in terms of its Fourier coefficients. Denoting by u' the restriction of u to C_r , and writing $u_n = f_n + ig_n$, we compute

$$\begin{aligned} d := \deg(u', C_r) &= \frac{1}{2\pi} \int_{C_r} u' \times u'_r d\mathcal{H}^1 \\ &= \frac{1}{2\pi} \int_{C_r} \sum_n n \begin{pmatrix} f_n \cos n\theta - g_n \sin n\theta \\ f_n \sin n\theta + g_n \cos n\theta \end{pmatrix} \times \begin{pmatrix} -f_n \sin n\theta - g_n \cos n\theta \\ f_n \cos n\theta - g_n \sin n\theta \end{pmatrix} \\ &= \sum_{n \in \mathbb{Z}} n (|f_n(t)|^2 + |g_n(t)|^2) \end{aligned} \quad (4.6)$$

$$= \sum_{n \in \mathbb{Z}} n |u_n(t)|^2, \quad (4.7)$$

where in the last line we have used orthogonality.

2. As in the proof of Thm. 5.1 in [17], we find

$$\operatorname{div} u = \sum_{n \in \mathbb{Z}} \operatorname{div} V_n,$$

in L^2 , where we have

$$\begin{aligned} \operatorname{div} V_1 &= \left(f'_1(r) + \frac{f_1(r)}{r} \right), \\ \operatorname{div} V_n &= \left(f'_n(r) + \frac{nf_n(r)}{r} \right) \cos(n-1)\theta - \left(g'_n(r) + \frac{ng_n(r)}{r} \right) \sin(n-1)\theta. \quad n \neq 1. \end{aligned}$$

It follows that

$$\begin{aligned} \frac{1}{\pi} \int_A (\operatorname{div} u)^2 &= 2 \int_\rho^{\rho'} \left(f'_1 + \frac{f_1}{r} \right)^2 r dr + \sum_{n \neq 1} \int_\rho^{\rho'} \left(\left(f'_n + \frac{nf_n(r)}{r} \right)^2 + \left(g'_n + \frac{ng_n(r)}{r} \right)^2 \right) r dr \\ &\geq \int_\rho^{\rho'} \left[2 \frac{f_1^2}{r} + \sum_{n \neq 1} \frac{n^2 (f_n(r)^2 + g_n(r)^2)}{r} \right] dr \\ &\quad + \int_\rho^{\rho'} \left[4 f_1(r) f'_1(r) + \sum_{n \in \mathbb{Z}, n \neq 1} 2n (f_n(r) f'_n(r) + g_n(r) g'_n(r)) \right] dr \end{aligned}$$

$$:= I + II.$$

We estimate the integrals I and II separately as follows, beginning with II . From Eqn. (4.6) and the assumption that $\deg(u, C_t) = d$ for each $t \in [\rho, \rho']$, we obtain that for each r

$$\begin{aligned} II &= \int_{\rho}^{\rho'} \frac{\partial}{\partial r} \left[2f_1^2 + \sum_{n \in \mathbb{Z}, n \neq 1} n(f_n^2 + g_n^2) \right] dr \\ &= \int_{\rho}^{\rho'} \frac{\partial}{\partial r} \left[f_1^2 - g_1^2 + \sum_{n \in \mathbb{Z}} n(f_n^2 + g_n^2) \right] dr \\ &= \int_{\rho}^{\rho'} \frac{\partial}{\partial r} [f_1^2 - g_1^2 + d] dr \\ &= f_1(\rho')^2 - f_1(\rho)^2 + g_1(\rho)^2 - g_1(\rho')^2. \end{aligned} \quad (4.8)$$

Using now the definition of f_1, g_1 , and the fact that $|u| \leq 1$, we find that $\|f_1\|_{\infty}, \|g_1\|_{\infty} \leq 1$. It follows that

$$|II| \leq 4. \quad (4.9)$$

We next turn to estimating I . Let us first suppose $d > 1$. We have

$$\begin{aligned} I &\geq \int_{\rho}^{\rho'} \left(\frac{f_1(r)^2}{r} + \sum_{n \in \mathbb{Z}, n \neq 1} \frac{n^2(f_n(r)^2 + g_n(r)^2)}{r} \right) dr \\ &= \int_{\rho}^{\rho'} \left(\frac{f_1(r)^2}{r} + \sum_{n \in \mathbb{Z}, n \neq 1} \frac{(n^2 - n)(f_n(r)^2 + g_n(r)^2)}{r} + \frac{n(f_n(r)^2 + g_n(r)^2)}{r} \right) dr \\ &\geq \int_{\rho}^{\rho'} \left(\frac{f_1(r)^2}{r} + \sum_{n \in \mathbb{Z}, n \neq 1} \frac{n(f_n(r)^2 + g_n(r)^2)}{r} \right) dr \end{aligned} \quad (4.10)$$

$$= \int_{\rho}^{\rho'} \frac{d - g_1^2(r)}{r} dr \quad (4.11)$$

$$\geq \int_{\rho}^{\rho'} \frac{d - 1}{r} dr \quad (4.12)$$

$$= (d - 1) \log(\rho'/\rho). \quad (4.13)$$

In going from (4.10) to (4.11) we have used (4.13) while in going from (4.11) to (4.12) we have used that $g_1^2 \leq 1$. This completes the proof of the theorem when $d > 1$, so we turn our attention to when $d < 0$. In this case, we have

$$\begin{aligned} I &\geq \int_{\rho}^{\rho'} \left(\frac{f_1(r)^2}{r} + \sum_{n \in \mathbb{Z}, n \neq 1} \frac{n^2(f_n(r)^2 + g_n(r)^2)}{r} \right) dr \\ &= \int_{\rho}^{\rho'} \left(\frac{f_1(r)^2}{r} + \sum_{n \in \mathbb{Z}, n \neq 1} \frac{(n^2 + n)(f_n(r)^2 + g_n(r)^2)}{r} - \frac{n(f_n(r)^2 + g_n(r)^2)}{r} \right) dr \end{aligned}$$

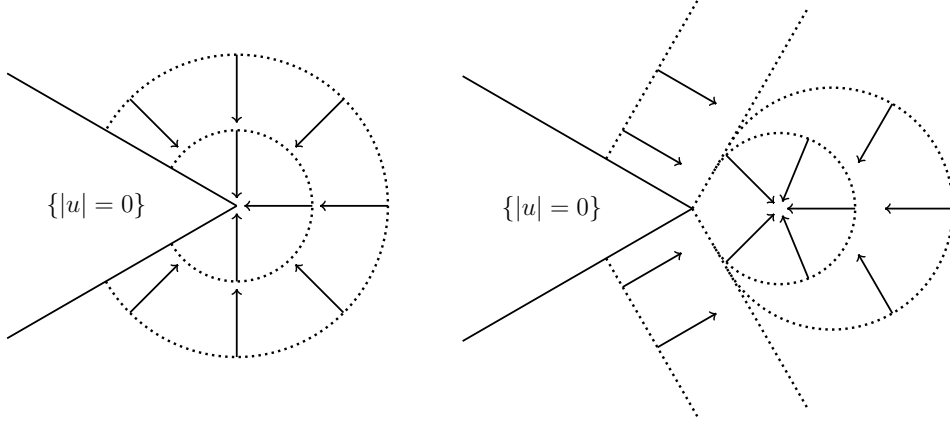


Figure 7: Corner on an interface at which u changes tangency: If there are no walls, a Ginzburg-Landau vortex forms in one of two ways, resulting in infinite E_0 energy. The dotted lines represent characteristics, and the arrows represent the \mathbb{S}^1 -valued director, which is perpendicular to the characteristics.

$$\begin{aligned}
&\geq \int_{\rho}^{\rho'} \sum_{n \in \mathbb{Z}} -n \frac{f_n^2(r) + g_n^2(r)}{r} dr \\
&\geq -d \int_{\rho}^{\rho'} \frac{1}{r} dr \\
&= -d \log(\rho'/\rho) = |d| \log(\rho'/\rho).
\end{aligned}$$

□

It also is worth mentioning that among degree 1 singularities, the L^2 -norm of the divergence can vary greatly and may or may not satisfy a lower bound of the type in the previous theorem. For example, for a Ginzburg-Landau vortex $\frac{x}{|x|}$, the L^2 -norm of the divergence taken over an annulus centered at the origin blows up logarithmically as the inner radius approaches 0. However, an \vec{e}_θ vortex, given by $\frac{x^\perp}{|x|}$, is divergence free. This observation is relevant to our model, especially at corner-type defects on the phase boundary. In many of our examples, the director u , which must be tangent to the phase boundary, switches the sense of tangency at a corner. If such a switch occurs at a corner of the phase boundary in the interior of the domain, then walls must intersect the defect in order to avoid infinite energy from the bulk divergence term; see Fig. 7. Conversely, if u does not change its sense of tangency at a corner on the interface, then the singularity can be locally resolved by the formation of a partial \vec{e}_θ vortex in which an infinite family of characteristics emanate from the defect.

4.3 Critical points of E_0 and E_0^∞ in a disk.

In this section we consider critical points of the energy E_0^∞ in the disk Ω of radius R among competitors satisfying the boundary condition

$$u\left(R \cos \frac{s}{R}, R \sin \frac{s}{R}\right) \cdot \nu_{\partial\Omega} = (\cos(ks + \alpha), \sin(ks + \alpha)) \cdot \nu_{\partial\Omega} \quad \text{for } s \in [0, 2\pi R), \quad (4.14)$$

where $k \in \mathbb{Z}$, $\alpha \in \mathbb{R}$, and the boundary is parametrized with respect to arc-length.

The simplest cases to consider are $(k, \alpha) = (1, \pi/2)$ and when $k = 0$ for which minimizers of E_0 are the divergence-free vortex

$$u_0 = \vec{e}_\theta = \left(\frac{-y}{\sqrt{x^2 + y^2}}, \frac{x}{\sqrt{x^2 + y^2}} \right),$$

and the constant state

$$u_0 = (\cos \alpha, \sin \alpha),$$

respectively. Indeed, trivially, in both cases $E_0(u_0) = \min E_0 = 0$. Hence our principal interest in this section will be to understand the behavior of critical points for other choices of (k, α) .

We begin by considering the case where k is a negative integer and $\alpha = \pi$. To gain some insight into how these boundary conditions influence the morphology of interfaces and walls, we present in Figure 8 the large-time asymptotics for gradient flow dynamics for the energy E_ε with boundary conditions $u|_{\partial\Omega} = -(\cos ks, \sin ks)$ for two values of L . Then in Figure 9 we present simulations for data with degrees -2 and -3 . Although we do *not* impose an area constraint in these simulations in order to induce a phase transition, these numerics nonetheless indicate a substantial presence of the isotropic phase in the form of an island with $2|k| + 2$ boundary singularities. Generally speaking, these islands appear to grow in size as $|k|$ grows, and for $k < -1$, both configurations with a single or multiple vortices are possible. Studies on vortices using the Ginzburg-Landau potential such as [8] or—more appropriately to this study—the Chern-Simons-Higgs potential with $L = 0$ in the elastic energy [23] tempt one to think of these islands for $\varepsilon > 0$ as “defects” arising from the negative degree boundary condition. However, the numerics and Theorem 4.1 indicate that the cores of the defects do not shrink in the $\varepsilon \rightarrow 0$ limit. Indeed, from Theorem 4.1 it follows that a defect with a negative degree must either be inside an isotropic region or have walls originating from the defect. The latter situation was, in fact, observed in [17] for the degree -1 defects while the Ginzburg-Landau potential considered in [17] did not allow for presence of interfaces.

We now provide some analytical evidence that supports the observations in Figs. 8-9. Motivated by the gradient flow simulations, we construct critical points for E_0^∞ and so divergence-free competitors for E_0 . These constructions will have only interface, but no walls, with singular points of the interface always touching the boundary of the disk, though of course the numerics suggest that for L finite, there should exist walls branching off the phase boundary singularities and attaching to $\partial\Omega$.

Example 4.3. In this example, $\Omega = B(0, 1)$, and we are interested in competitors which exhibit the symmetry

$$u\left(e^{\pi i/(k+1)} x\right) = e^{-\pi k i/(k+1)} u(x) \quad \text{for } k \in \mathbb{N}. \quad (4.15)$$

This is the symmetry exhibited by the configurations in Figs. 8-9. The construction will proceed by issuing characteristics off $\partial\Omega$ and by adhering to the condition (4.3).

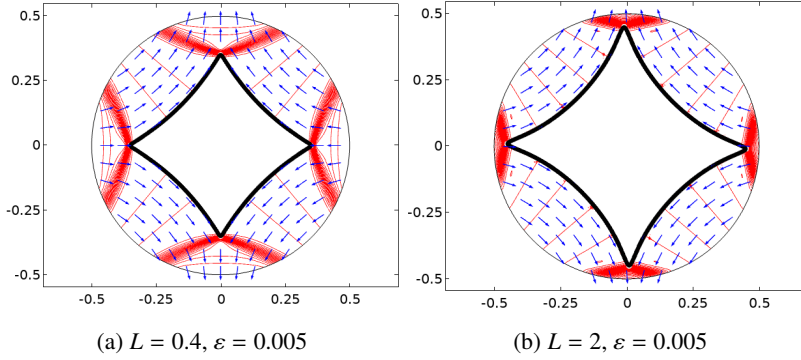


Figure 8: Critical points of E_ε for $(k, \alpha) = (-1, \pi)$. The red curves represent level sets of $\operatorname{div} u$ while $|u| = 0.5$ on the black curves that enclose the isotropic phase.

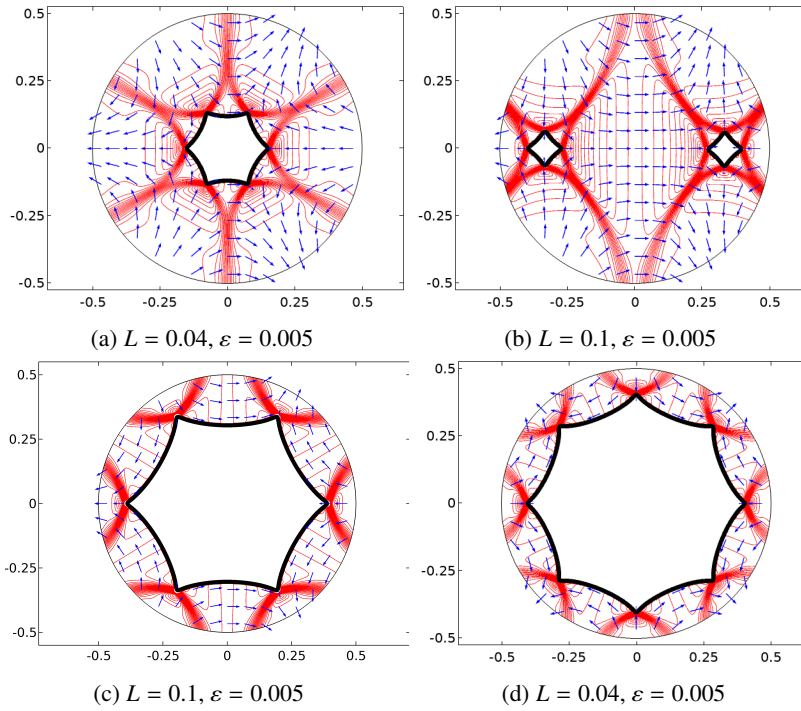


Figure 9: Critical points of E_ε for (a-c): $(k, \alpha) = (-2, \pi)$ and (d): $(k, \alpha) = (-3, \pi)$. The red curves represent level sets of $\operatorname{div} u$ while $|u| = 0.5$ on the black curves that enclose the isotropic phase. The configurations (b) and (c) are obtained starting from different initial conditions. Configuration (b) has slightly lower energy in E_ε .

Owing to the condition (4.15), we construct a critical point of E_0^∞ in the sector S corresponding to $[0, \pi/(k+1)]$ and then extend the construction to the rest of the domain by symmetry. Shifting out of complex notation and parametrizing $\partial\Omega \cap \partial S$ by $(\cos s, \sin s)$ for $s \in [0, \pi/(k+1)]$, we will insist that $u|_{\partial\Omega} = (-\cos ks, \sin ks)$, rather than just having agreement between the normal component of u and that of the data.

Integrating the characteristic equations then yields

$$(x_1(s, t), x_2(s, t)) = (\cos s, \sin s) - t(\sin ks, \cos ks) \quad (4.16)$$

$$u(x_1(s, t), x_2(s, t)) = (-\cos ks, \sin ks), \quad (4.17)$$

with $s \in [0, \pi/(k+1)]$, $t \geq 0$. We represent the interface in the form

$$(p(s), q(s)) := (x_1(s, t(s)), x_2(s, t(s)))$$

for an appropriate arrival time $t(s) \geq 0$. Here, for each s , a characteristic arrives at the interface at the time $t(s)$ and we require that u at the point of arrival is tangent to the interface, that is

$$(p'(s), q'(s)) = \alpha (u(p(s)), u(q(s))) \text{ for some } \alpha \in \mathbb{R}.$$

Using this expression in (4.16), we find that

$$\begin{aligned} x_1'(s, t(s)) &= -\sin s - t'(s) \sin ks - kt(s) \cos ks = -\alpha \cos ks, \\ x_2'(s, t(s)) &= \cos s - t'(s) \cos ks + kt(s) \sin ks = \alpha \sin ks. \end{aligned}$$

Upon rearrangement, we have

$$\begin{aligned} -\sin s + \alpha \cos ks - kt(s) \cos ks &= t'(s) \sin ks, \\ \cos s - \alpha \sin ks + kt(s) \sin ks &= t'(s) \cos ks. \end{aligned}$$

Multiplying these equations by $\sin ks$ and $\cos ks$, respectively, and adding the results gives

$$t' = -\sin s \sin ks + \cos s \cos ks = \cos(k+1)s.$$

Integration then yields

$$t(s) = \frac{1}{k+1} \sin(k+1)s + c.$$

Motivated by numerics, we seek an interface that meets $\partial\Omega$ at $(1, 0)$, so that $t(0) = 0$. Then $c = 0$, so that $t(s) = \frac{1}{k+1} \sin(k+1)s$. The parametric equation of the interface in the sector S is now given by

$$p(s) = \cos s - \frac{1}{k+1} \sin(k+1)s \sin ks = \left(1 - \frac{1}{2(k+1)}\right) \cos s + \frac{1}{2(k+1)} \cos(2k+1)s, \quad (4.18)$$

$$q(s) = \sin s - \frac{1}{k+1} \sin(k+1)s \cos ks = \left(1 - \frac{1}{2(k+1)}\right) \sin s - \frac{1}{2(k+1)} \sin(2k+1)s. \quad (4.19)$$

Extending the interface to all of Ω via the symmetry condition (4.15), we obtain a closed curve with $2(k+1)$ evenly-spaced cusps. When $k = 1$ one checks that $p(s) = \cos^3 s$ and $q(s) = \sin^3 s$

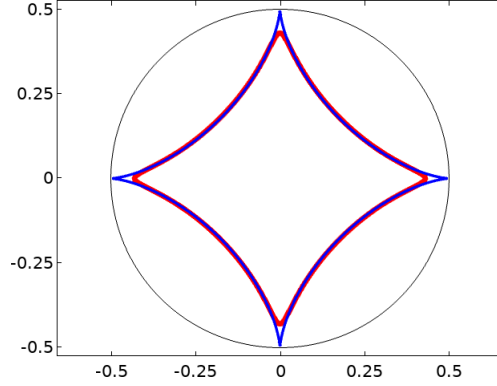


Figure 10: Contour line $|u| = 0.5$ for the critical point with $(k, \alpha) = (-1, \pi)$ obtained via gradient flow (red) and the plot of $x_1^{2/3} + x_2^{2/3} = 1$ (blue). Here $L = 2$ and $\varepsilon = 0.005$.

and the interface satisfies the equation $x_1^{2/3} + x_2^{2/3} = 1$. In Fig. 10 we compare the graph of this curve with the contour line $|u| = 0.5$ for the critical point obtained numerically via gradient flow when $L = 2$. It is clear that the two curves are very close to each other, which is quite striking since one might only expect a strong connection between the critical points of E_ε and E_0^∞ for L large.

One can also check that for the construction obtained above, the area of the isotropic island increases with $|k|$. In fact, a calculation that we omit goes to show that in the $k \rightarrow \infty$ limit, the isotropic region fills the entire disk!

The preceding calculation can also be used in the case of $L < \infty$ in order to reconstruct parts of critical points of E_0 . Recall that, in this case, by Corollary 3.11, the characteristics are circular arcs of finite radii that may run directly from the interface to $\partial\Omega$. In Fig. 8, for example, red curves correspond to level sets of $\operatorname{div} u$ and thus the characteristics for u connect large portions of the interface to the boundary. In order to fully reproduce the critical point of E_0 completely, however, one needs to allow for the presence of walls, as evidenced by the gradient flow numerics in Fig. 8. Although a similar approach yielded critical points of (1.3) for degree -1 boundary data in [17], such a construction will be more elaborate here and we do not pursue this issue further in the present paper.

We conclude this section by considering the boundary data in (4.14) corresponding to k positive and $\alpha = 0$. The results of the gradient flow simulations are shown in Fig. 11. Not surprisingly, when L is small for $k = 2$, the stable configuration consists of two degree one vortices looking locally like \vec{e}_θ , see Fig. 11a. As L increases, however, these vortices collapse onto and spread along $\partial\Omega$ while forming two walls along the upper and lower halves of the boundary, respectively, cf. Fig. 11b. Indeed this simulation suggests that for E_0 with L large, the preferred state is $u \equiv \vec{e}_1$. In fact, if one tries to construct a competitor u having a ‘boundary wall’ for this boundary data, that is, a unit vector field such that the normal component of the data is met but the tangential component switches sign, then one finds

$$u \cdot \nu_{\partial\Omega} = (\cos 2s, \sin 2s) \cdot (\cos s, \sin s) = \cos s = \vec{e}_1 \cdot (\cos s, \sin s)$$

and

$$u \cdot \tau_{\partial\Omega} = -(\cos 2s, \sin 2s) \cdot (-\sin s, \cos s) = -\sin s = \vec{e}_1 \cdot (-\sin s, \cos s).$$

Thus such a competitor u must have trace \vec{e}_1 along $\partial\Omega$ and there is no need then to accumulate divergence inside the disk by varying from constancy.

In the case of a degree 3 boundary data, cf. Figure 11c, the behavior is more complex—the degree 3 vortex appears to split into four degree 1 vortices and one degree -1 vortex. The four $+1$ vortices approach the boundary of the domain with an increasing L while the degree -1 vortex remains at the center of the disk.

We use the simulations in the case of $(k, \alpha) = (2, 0)$ to test Conjecture (3.12) on the one-dimensional character of the wall cost. The walls in this example turn out to be significantly deeper than in other cases that we considered and it is therefore easier to compare the numerically computed wall profiles with the corresponding heteroclinic connection. Consider the critical point for E_ε depicted in Fig. 11b. For a large value of L the defects present inside Ω for small ε spread along the boundary to form two boundary walls. Due to symmetry, it is sufficient to consider the wall in the first quadrant. Then along each ray emanating at angle θ from the origin, the wall connects the vector $\vec{e}_1 = (1, 0)$ to the vector $(\cos 2\theta, \sin 2\theta)$. Because the normal to the boundary/interface is $(\cos \theta, \sin \theta)$, the normal component of the vector field is continuous across the wall, while the tangential component reverses sign. The jump in the tangential component across the wall grows as θ changes from 0 to $\pi/2$. In Fig. 12a we plot cross-sections of $|u|$ for the critical point of E_ε shown in Fig. 11b, where the cross-sections are shown along several rays $\theta = \text{const}$. In Fig. 12b, the same scaled and translated profiles are shown together with the corresponding solutions of the ODE that describes a heteroclinic connection associated with E_ε , assuming one-dimensional cost. As Fig. 12b demonstrates, the graphs are close to each other for all respective values of θ —this is in agreement with our conjecture that the cost is one-dimensional.

4.4 Examples for Degree Zero Boundary Data

In this section, we analytically and numerically construct an example with an isotropic tactoid which exhibits two defects on the phase boundary. Let us describe a key feature of this example. Recall that at a nematic-isotropic interface for E_0 , the trace of a $BV \cap H_{\text{div}}$ competitor u from the nematic region is tangent to the interface, cf. (3.4). If, for example, u is smooth and does not change the sense of tangency along the interface, then the degree of u around any connected component of the interface is 1. If we specify a degree 0 boundary condition around $\partial\Omega$ or at infinity, this mismatch can be rectified by the presence of two defects along the interface, similar to the construction of the recovery sequence in Section 2. This is the effect we will see in the following example.

We begin with some numerics. Fig. 15a shows the result of gradient flow simulation in a large rectangular domain with constant boundary data \vec{e}_1 . We observe in Fig. 15a that (i) the interface surrounds a single isotropic island, (ii) there appear to be two walls which intersect the two defects on the interface, and (iii) the solutions possess the symmetries

$$(u_1(x_1, x_2), u_2(x_1, x_2)) = (u_1(x_1, -x_2), -u_2(x_1, -x_2))$$

and

$$(u_1(x_1, x_2), u_2(x_1, x_2)) = (u_1(-x_1, x_2), -u_2(x_1, -x_2)).$$

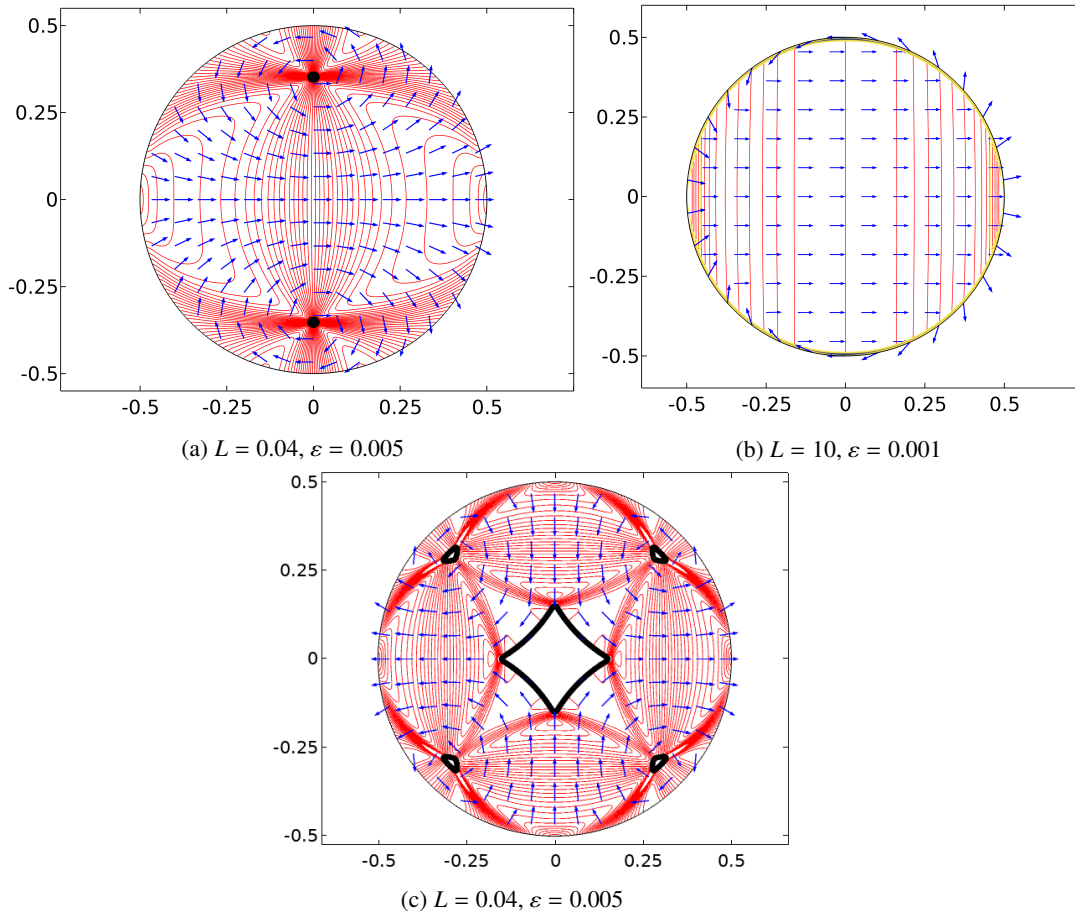


Figure 11: Critical points of E_ε for (a-b): $(k, \alpha) = (2, 0)$ and (c): $(k, \alpha) = (3, 0)$. The red curves represent level sets of $\operatorname{div} u$ while $|u| = 0.5$ on the black curves that enclose the isotropic phase. The wall adjacent to the boundary in plot (b) is indicated in yellow.

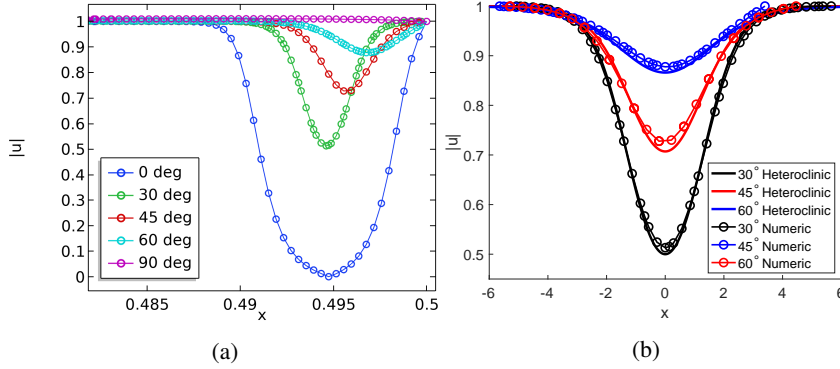


Figure 12: Wall cost is one-dimensional for the critical point shown in Fig. 11b. (a) Cross-sections of Fig. 11b in the direction of angle θ . Only parts of cross-sections closest to the boundary are shown; (b) Comparison between the numerical and analytical wall profiles.

Furthermore, in Fig. 15a we see that (iv) the walls divide the plane into three regions, with

$$u \equiv \vec{e}_1 \text{ in the two regions not containing the isotropic tactoid.} \quad (4.20)$$

This simulation, though depicting transient behavior, leads us to seek a critical point of E_0^∞ satisfying (i)-(iv) consisting of an isotropic tactoid in an infinite sea of nematic, where in the far field, $u \rightarrow \vec{e}_1$. To induce a static—and presumably stable—critical point having an isotropic phase, we will enforce an area constraint of the form $|\{u = 0\}| = \text{const}$.

The complication here—and it is a significant one—is that an interface and a wall are rigidly linked via the straight-line characteristics lying in between them, and the requirement of tangency of u along the interface and agreement of the normal component of u with that of \vec{e}_1 along the wall make the construction rather daunting.

Somewhat surprisingly, we are able to achieve this construction by deriving a formula of the form

$$E_0^\infty(u) = \int_{\partial\{|u|=1\}} f(\theta) d\mathcal{H}^1 \quad (4.21)$$

for an explicit f , for competitors u satisfying (i)–(iv), where θ is the angle the tangent vector to $\partial\{|u|=1\}$ makes with the horizontal. For such u , the energy E_0^∞ therefore only depends on the interface, a reflection of the afore-mentioned rigidity of this problem. We then consider variations of the interface to derive an ODE (4.45) for θ along with the junction condition (4.46) at the intersection of walls and interfaces. Numerically integrating this ODE yields a configuration which closely resembles the results of the simulations shown in Figure 15a, cf. Figure 15b.

The Role of Walls: Before embarking on this construction, let us comment on the role of walls in this example. A natural question is: given these conditions, namely an area constraint on the isotropic region and the requirement that $u \equiv \vec{e}_1$ in the far field, is it necessary for a critical point to have walls? While we do not as yet have a proof, we believe the answer is yes. Let us present some heuristic arguments to this effect. Working within the symmetry assumption (iii), consider the possibility of constructing a competitor without walls. Then one of the two configurations

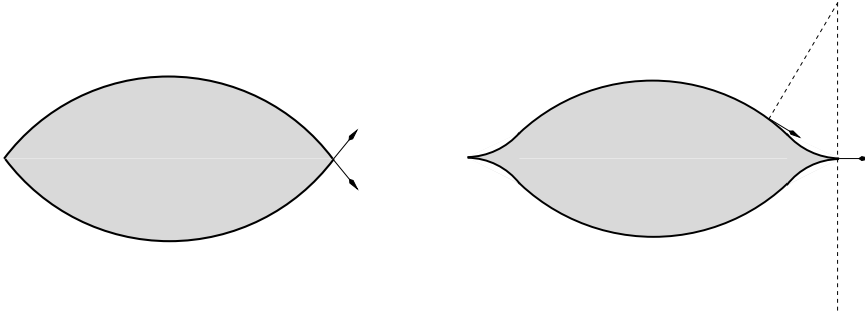


Figure 13: An isotropic island (marked in gray) surrounded by the nematic medium in \mathbb{R}^2 without wall singularities and satisfying $u = \vec{e}_1$ at infinity. The vector field is tangent to the boundary of the island and switches the sense of tangency at the boundary singularities. Left: the island has a corner and thus an infinite energy E_0 due to the bulk divergence term—cf. Fig. 7. Right: the island has a cusp—impossible without a wall since the characteristics will intersect. Characteristics are indicated by the dashed lines.

depicted in Fig. 13 are possible where the isotropic island either has two corners and no walls or it has two cusps and no walls. In the former case, one can show that partial vortices should form near the corners in the nematic phase, causing the divergence contribution to the energy to blow up; see Fig. 7 above. If there are two cusps and no walls, Fig. 13 demonstrates that this is not possible as the characteristics emanating from the interface would have to intersect non-tangentially. In light of these observations, junctions between interfaces and walls appear to be fairly generic, making in particular the junction condition (3.74) potentially important when analyzing candidates for possible critical points or minimizers when L is finite.

Example 4.4. For this calculation, by (iii), it suffices to consider the problem in the first quadrant Q_1 . Let us assume that $\partial\{|u| = 1\} \cap Q_1$ is smooth and can be parametrized by $r(\sigma)$ where $r : [0, L] \rightarrow Q_1$, with $r(0)$ on the x_1 -axis and $r(L)$ on the x_2 -axis; see Figure 14. We do not assume that the interface is parametrized by the arclength variable s in this derivation. Then

$$r'(\sigma)/|r'(\sigma)| = \tau(\sigma) = (\cos \theta(\sigma), \sin \theta(\sigma)) = -u(r(\sigma)). \quad (4.22)$$

Let us define

$$\rho(\sigma) = |r'(\sigma)|,$$

and the normal vector

$$\nu(\sigma) = (\sin \theta(\sigma), -\cos \theta(\sigma)).$$

We now deduce the location of the wall, which we will see is determined by the interface. Recall that in light of (4.3), u is perpendicular to the straight characteristics, which themselves intersect the interface perpendicularly, so we can parametrize the wall by shooting characteristics off of the interface until they hit the wall. We can write a parametrized path \tilde{r} for the wall then as

$$\tilde{r}(\sigma) := r(\sigma) + t(\sigma)\nu(\sigma). \quad (4.23)$$

Hence by (4.22) the trace of u on the wall from the left, denoted here by \tilde{u} , is given by

$$\tilde{u}(\sigma) = -(\cos \theta(\sigma), \sin \theta(\sigma)). \quad (4.24)$$

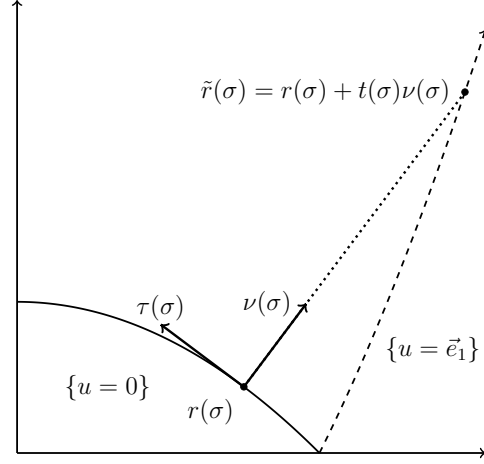


Figure 14: The isotropic island is surrounded by the nematic region. The dotted line represents a straight line characteristic, and the dashed line represents the wall.

We define a function ψ by the equation

$$\tilde{r}'(\sigma) = |\tilde{r}'(\sigma)|(\cos \psi(\sigma), \sin \psi(\sigma)).$$

Then the tangent and normal vectors to the wall are given by

$$\tilde{\tau} = (\cos \psi, \sin \psi) \quad \text{and} \quad \tilde{\nu} = (\sin \psi, -\cos \psi). \quad (4.25)$$

Next, we collect some relations between several of the above quantities which will be useful in the following calculations. From the continuity of the normal traces across a wall, we have

$$\tilde{u} \cdot \tilde{\nu} = \tilde{e}_1 \cdot \tilde{\nu},$$

which we rewrite using (4.24), (4.25), and the angle subtraction identity for sin as

$$\sin(\theta - \psi) = \sin \psi. \quad (4.26)$$

Similarly, the condition $\tilde{u} \cdot \tilde{\tau} = -\tilde{e}_1 \cdot \tilde{\tau}$ for the tangential components across a wall, cf. (3.4), can be expressed as

$$\cos(\theta - \psi) = \cos \psi. \quad (4.27)$$

From (4.26), (4.27) it follows that $\psi = \theta/2 + k\pi$ for some integer k , and k is in fact 0 since at $\sigma = 0$, $\psi(0) \leq \theta(0) \leq \psi(0) + \pi/2$. Thus

$$\psi = \theta/2. \quad (4.28)$$

We can now write the energy $E_0(u, Q_1)$ in the first quadrant as

$$E_0(u, Q_1) = \frac{K(0)}{2} \text{Per}_{Q_1}(\{|u| = 1\}) + \int_{J_u \cap \{|u|=1\}} K(u \cdot \nu) d\mathcal{H}^1$$

$$= \int_0^L \left(\frac{K(0)}{2} |r'(\sigma)| + K(\vec{e}_1 \cdot \tilde{\nu}(\sigma)) |\tilde{r}'(\sigma)| \right) d\sigma. \quad (4.29)$$

One can use (4.23) and the orthogonality of τ and ν to easily calculate

$$|\tilde{r}'| = \left((\rho + t\theta')^2 + (t')^2 \right)^{1/2}.$$

Substituting this and

$$\vec{e}_1 \cdot \nu = \sin \psi = \sin(\theta/2)$$

into (4.29) yields

$$\begin{aligned} E_0(u, Q_1) &= \int_0^L \left(\frac{K(0)}{2} |r'| + K(\sin(\theta/2)) \left((\rho + t\theta')^2 + (t')^2 \right)^{1/2} \right) d\sigma \\ &= \int_{\partial\{|u|=1\}} \frac{K(0)}{2} d\mathcal{H}^1 + \int_0^L \left(K(\sin(\theta/2)) \left((\rho + t\theta')^2 + (t')^2 \right)^{1/2} \right) d\sigma. \end{aligned} \quad (4.30)$$

In order to obtain a formula for E_0 depending only on the interface, it remains to simplify

$$\left((\rho + t\theta')^2 + (t')^2 \right)^{1/2}. \quad (4.31)$$

We begin this simplification by finding an expression for t in terms of θ and ρ . Using the definitions (4.22), (4.23), and (4.25) for r , \tilde{r} , and $\tilde{\nu}$, respectively, along with (4.28), we calculate

$$\begin{aligned} 0 &= \tilde{r}' \cdot \tilde{\nu} \\ &= (r' + t'\nu + t\nu') \cdot \tilde{\nu} \\ &= [\rho(\cos \theta, \sin \theta) + t'(\sin \theta, -\cos \theta) + t\theta'(\cos \theta, \sin \theta)] \cdot (\sin(\theta/2), -\cos(\theta/2)). \end{aligned} \quad (4.32)$$

Expanding out (4.32) and using the angle subtraction formulae for sine and cosine eventually gives

$$t' \cos(\theta/2) - (\rho + t\theta') \sin(\theta/2) = 0. \quad (4.33)$$

Now we observe from our symmetry assumption on u that $u \equiv \vec{e}_1$ on the x_2 -axis, so that $\theta(L) = \pi$. If we assume that $\theta(\sigma)$ does not reach π until $\theta(L) = \pi$, which in terms of the interface means that

$$\textit{the tangent vector to the interface is not horizontal in the interior of } Q_1, \quad (4.34)$$

then we can divide (4.33) by $\cos(\theta/2)$. This results in the following ODE for t :

$$t' - \frac{\sin(\theta/2)}{\cos(\theta/2)} \theta' t = \rho \tan(\theta/2). \quad (4.35)$$

Multiplying both sides of (4.35) by the integrating factor

$$M = \exp \left(-2 \int \frac{\sin(\theta/2)}{\cos(\theta/2)} \frac{\theta'}{2} \right) = \exp(2 \ln(\cos(\theta/2))) = \cos^2(\theta/2)$$

results in

$$(t \cos^2(\theta/2))' = \rho \sin(\theta/2) \cos(\theta/2) = \frac{1}{2} \rho \sin \theta.$$

Integrating both sides, dividing by $\cos^2(\theta/2)$, and using the half angle formula for cosine, we obtain

$$t = \frac{1}{2\cos^2(\theta/2)} \int_0^\sigma \rho(y) \sin \theta(y) dy = \frac{1}{1 + \cos \theta} \int_0^\sigma \rho \sin \theta dy. \quad (4.36)$$

Finally, let us record the identity

$$\rho + t\theta' = t' \frac{\cos(\theta/2)}{\sin(\theta/2)}, \quad (4.37)$$

which follows from rearranging (4.33).

We now use the formula (4.36) for t to calculate (4.31), the quantity we set out to simplify. Let us assume that $t' > 0$, which means that

$$\text{the length of characteristics connecting the interface to the wall increases in } \sigma. \quad (4.38)$$

Then plugging in (4.37) for (4.31) and using the assumptions (4.34) and (4.38), namely $\theta/2 \leq \pi/2$ and $t' > 0$, we write

$$\left((\rho + t\theta')^2 + (t')^2 \right)^{1/2} = \left((t')^2 \frac{\cos^2(\theta/2)}{\sin^2(\theta/2)} + (t')^2 \right)^{1/2} = \frac{t'}{\sin(\theta/2)}.$$

Utilizing the formula (4.36) to calculate t' and then a half angle formula for cosine and a double angle formula for sine, we arrive at

$$\begin{aligned} \left((\rho + t\theta')^2 + (t')^2 \right)^{1/2} &= \frac{1}{\sin(\theta/2)} \left[\frac{\rho \sin \theta}{1 + \cos \theta} + \frac{\theta' \sin \theta}{(1 + \cos \theta)^2} \int_0^\sigma \rho \sin \theta dy \right] \\ &= \frac{\sin \theta}{2 \sin(\theta/2)(1 + \cos \theta)} \left[\rho + \frac{\theta'}{1 + \cos \theta} \int_0^\sigma \rho \sin \theta dy \right] \\ &= \frac{2 \sin(\theta/2) \cos(\theta/2)}{2 \sin(\theta/2) \cos^2(\theta/2)} \left[\rho + \frac{\theta'}{1 + \cos \theta} \int_0^\sigma \rho \sin \theta dy \right] \\ &= \frac{1}{\cos(\theta/2)} \left[\rho + \frac{\theta'}{1 + \cos \theta} \int_0^\sigma \rho \sin \theta dy \right]. \end{aligned} \quad (4.39)$$

Now we are ready to use the expression (4.39) for (4.31) in the E_0 energy (4.30). We have

$$\begin{aligned} E_0(u, Q_1) &= E_0(\rho, \theta) \\ &= \int_{\partial\{|u|=1\}} \frac{K(0)}{2} d\mathcal{H}^1 + \int_0^L \left(\frac{K(\sin(\theta/2))}{\cos(\theta/2)} \left[\rho + \frac{\theta'}{1 + \cos \theta} \int_0^\sigma \rho \sin \theta dy \right] \right) d\sigma. \end{aligned}$$

We focus on the term

$$\int_0^L \left(\frac{K(\sin(\theta/2))}{\cos(\theta/2)} \frac{\theta'}{1 + \cos \theta} \int_0^\sigma \rho \sin \theta dy \right) d\sigma. \quad (4.40)$$

Let us define the function $H(v)$ by the equations

$$H'(v) = \frac{K(v)}{(1 - v^2)^2}, \quad H(0) = 0.$$

It follows from (3.8) that H remains finite as v approaches 1 so long as $V(t)$ approaches 0 as $t \nearrow 1$ at least as fast as $c(1-t^2)^p$ for some $p > 1$ and $c > 0$, an assumption which is satisfied by W_{CSH} . A straightforward calculation, which we omit, using the chain rule, the definition of H' , and some trigonometric identities yields

$$(H(\sin(\theta/2)))' = \frac{K(\sin(\theta/2))\theta'}{\cos(\theta/2)(1 + \cos \theta)}. \quad (4.41)$$

Inserting this expression into the last integral in (4.40), that term becomes

$$\int_0^L (H(\sin(\theta/2)))' \left(\int_0^\sigma \rho \sin \theta dy \right) d\sigma, \quad (4.42)$$

which we integrate by parts to obtain

$$\left[H(\sin(\theta/2)) \int_0^\sigma \rho \sin \theta dy \right]_0^L - \int_0^L H(\sin(\theta/2)) \rho \sin \theta d\sigma.$$

Note that by our symmetry assumptions, $\theta(L) = \pi$, so that

$$\begin{aligned} & \left[H(\sin(\theta/2)) \int_0^\sigma \rho \sin \theta dy \right]_0^L - \int_0^L H(\sin(\theta/2)) \rho \sin \theta d\sigma \\ &= H(1) \int_0^L \rho \sin \theta d\sigma - \int_0^L H(\sin(\theta/2)) \rho \sin \theta d\sigma. \end{aligned} \quad (4.43)$$

We combine (4.41)–(4.43) to rewrite (4.40):

$$\int_0^L \left(\frac{K(\sin(\theta/2))}{\cos(\theta/2)} \frac{\theta'}{1 + \cos \theta} \int_0^\sigma \rho \sin \theta dy \right) d\sigma = \int_0^L (H(1) - H(\sin(\theta/2))) \rho \sin \theta d\sigma. \quad (4.44)$$

Using the right hand side of (4.44) for (4.40), we finally have

$$\begin{aligned} E_0(u, Q_1) &= E_0(\rho, \theta) \\ &= \int_{\partial\{|u|=1\}} \frac{K(0)}{2} d\mathcal{H}^1 + \int_0^L \left(\frac{K(\sin(\theta/2))}{\cos(\theta/2)} \left[\rho + \frac{\theta'}{1 + \cos \theta} \int_0^\sigma \rho \sin \theta dy \right] \right) d\sigma \\ &= \int_{\partial\{|u|=1\}} \frac{K(0)}{2} d\mathcal{H}^1 + \int_0^L \left(\frac{K(\sin(\theta/2))}{\cos(\theta/2)} + (H(1) - H(\sin(\theta/2))) \sin \theta \right) \rho d\sigma \\ &=: \int_{\partial\{|u|=1\}} f(\theta) d\mathcal{H}^1. \end{aligned}$$

Thus we arrive at (4.21).

We turn now to the criticality conditions for θ . For any u with smooth interface, we parametrize the interface of length l by arclength s . Then the standard derivation [4] gives the following condition on the interface

$$(f''(\theta) + f(\theta))\theta' + \lambda = 0. \quad (4.45)$$

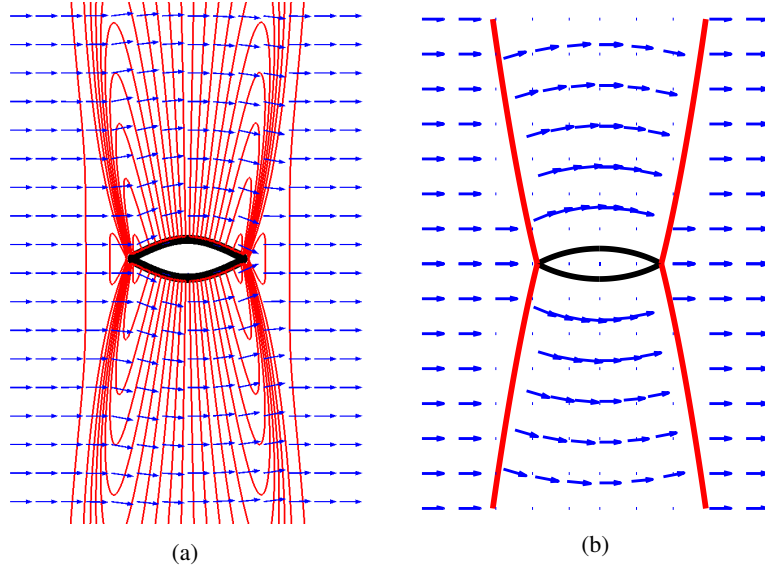


Figure 15: Isotropic island in \mathbb{R}^2 with $u = \vec{e}_1$ at infinity: (a) Gradient flow simulation in a large domain intended to represent \mathbb{R}^2 . The isotropic region is shrinking and the solution shown is a transient. Here $L = 10$, $\varepsilon = 0.02$; (b) Solution of (4.45)-(4.46) for $\lambda = 1$.

along with the the junction condition

$$f'(\theta) \sin \theta - f(\theta) \cos \theta = 0 \quad (4.46)$$

at $s = 0$, the intersection of $\partial\{|u| = 1\}$ with the x_1 -axis.

The solution of (4.45)-(4.46) for $\lambda = 1$ is depicted in Fig. 15b and bears a strong resemblance to a configuration observed in gradient flow dynamics shown in Fig. 15a.

5 Appendix

We present here the proof of Theorem 3.13. See Fig. 4 for a guide to the notation.

Proof. The derivation of (5.19) follows the same general lines as those appearing in the proof of Theorem 3.12. However, a major complicating consideration is that it is no longer possible to assume that the deforming vector field X is normal to all four curves Γ_{ij} since they all meet at p . Instead we will have to incorporate tangential components of X along these four curves as well.

To this end, we assume simply that $X \in C_0^1(B(p, R); \mathbb{R}^2)$ and again introduce the map Ψ via (3.57). We assume that each Γ_{ij} is smoothly parametrized by arclength through a map $r_{ij} : [0, s_0] \rightarrow \Gamma_{ij}$ for some $s_0 > 0$ with $r_{ij}(0) = p$. Then we replace (3.56) by

$$X(r_{ij}(s)) = h_{ij}^x(s) \tau_{ij}(s) + h_{ij}^y(s) \nu_{ij}(s) \quad \text{for } s \in [0, s_0], \quad (5.1)$$

where

$$h_{ij}^{\tau} := X(r_{ij}(s)) \cdot \tau_{ij}(s) \quad \text{and} \quad h_{ij}^{\nu}(s) := X(r_{ij}(s)) \cdot \nu_{ij}(s).$$

As a consequence of the compact support of X , we have that

$$h_{ij}^{\tau}(s_0) = h_{ij}^{\nu}(s_0) = 0 \quad \text{for all functions } h_{ij}^{\tau} \text{ and } h_{ij}^{\nu} \quad (5.2)$$

but we stress that none of these functions is assumed to vanish at $s = 0$, namely at the location of the junction P .

We now deform each region Ω_j , for $j = 0, 1, 2, 3$ by the map Ψ to form four contiguous regions $\Omega_j^t := \Psi(\Omega_j, t)$ and we deform the four boundary curves Γ_{ij} to form four new boundary curves $\Gamma_{ij}^t := \Psi(\Gamma_{ij}, t)$. Of course the junction point P is also carried along by this flow.

The four curves Γ_{ij}^t are parametrized by $s \mapsto \Psi(r_{ij}(s), t)$ which we denote by $r_{ij}^t(s)$ though s no longer represents arclength. Indeed one calculates that

$$r_{ij}^t(x) \sim r_{ij}(s) + t(h_{ij}^{\tau}(s)\tau_{ij}(s) + h_{ij}^{\nu}(s)\nu_{ij}(s)) \quad (5.3)$$

from which it follows that

$$\left| r_{ij}^t{}'(s) \right| \sim 1 + t(h_{ij}^{\tau}{}'(s) - h_{ij}^{\nu}(s)\kappa_{ij}(s)), \quad (5.4)$$

where $\kappa_{ij}(s)$ denotes the curvature of Γ_{ij} at $r_{ij}(s)$ (compare with (3.62)) and we have invoked the Frenet relations $\tau_{ij}' = \kappa_{ij}\nu_{ij}$ and $\nu_{ij}' = -\kappa_{ij}\tau_{ij}$. A related calculation goes to show that the unit normal ν_{ij}^t to Γ_{ij}^t is given by

$$\nu_{ij}^t \sim \nu_{ij} - t(h_{ij}^{\nu}{}'(s) + \kappa_{ij}h_{ij}^{\tau}(s))\tau_{ij}. \quad (5.5)$$

Now in the ball $B(p, R)$ the unperturbed critical point is given by

$$u(x) = \begin{cases} 0 & \text{for } x \in \Omega_0, \\ u_1(x) & \text{for } x \in \Omega_1, \\ u_2(x) & \text{for } x \in \Omega_2, \\ u_3(x) & \text{for } x \in \Omega_3 \end{cases}$$

and we wish to perturb it into a new function u^t given by

$$u^t(x) = \begin{cases} 0 & \text{if } x \in \Omega_0^t, \\ u_1^t(x) & \text{for } x \in \Omega_1^t, \\ u_2^t(x) & \text{for } x \in \Omega_2^t, \\ u_3^t(x) & \text{for } x \in \Omega_3^t \end{cases}.$$

To carry this out, as in the previous proof, we extend the domain of definition of u_j to a neighborhood of Ω_j in such a way that the extension is constant along the normals to the boundary of its original domain of definition. Then we introduce three functions ϕ_1, ϕ_2 and ϕ_3 such that

$$u_j^t(x) \sim u_j(x) + t\phi_j(x)u_j(x)^{\perp} \quad \text{for } x \in \Omega_j^t \text{ and for } j = 1, 2, 3 \quad (5.6)$$

so as to preserve the required \mathbb{S}^1 -valued nature of u_j^t .

We must also take care to preserve the property $u^t \in H_{\text{div}}$ in the sense of (3.39) and this requires that the following four conditions hold to $O(t)$ along $\Gamma_{01}, \Gamma_{12}, \Gamma_{23}$ and Γ_{03} respectively:

$$u_1^t(r_{01}^t(s)) \cdot \nu_{01}^t(s) = 0, \quad u_1^t(r_{12}^t(s)) \cdot \nu_{12}^t(s) = u_2^t(r_{12}^t(s)) \cdot \nu_{12}^t(s),$$

$$u_2^t(r_{23}^t(s)) \cdot \nu_{23}^t(s) = u_3^t(r_{23}^t(s)) \cdot \nu_{23}^t(s), \quad \text{and} \quad u_3^t(r_{03}^t(s)) \cdot \nu_{03}^t(s) = 0 \text{ for } s \in [0, s_0]. \quad (5.7)$$

We note that the first and last of these conditions implies at $t = 0$ that either $u_1 \equiv \tau_{01}$ or $\equiv -\tau_{01}$ along Γ_{01} and likewise either $u_3 \equiv \tau_{03}$ or $\equiv -\tau_{03}$ along Γ_{03} .

Substituting (5.3) and (5.5) into the four conditions of (5.7), and expanding to $O(t)$, a tedious but straight-forward calculation leads to the following requirements relating the traces of the ϕ_j to h_{ij}^y ':

$$\phi_1(r_{01}(s)) = h_{01}^y{}'(s), \quad (5.8)$$

$$\frac{1}{2}(\phi_1(r_{12}(s)) + \phi_2(r_{12}(s))) = h_{12}^y{}'(s), \quad (5.9)$$

$$\frac{1}{2}(\phi_2(r_{23}(s)) + \phi_3(r_{23}(s))) = h_{23}^y{}'(s), \quad (5.10)$$

$$\phi_3(r_{03}(s)) = h_{03}^y{}'(s), \quad (5.11)$$

for $s \in [0, s_0]$.

With the perturbations of the four curves Γ_{ij} and three functions u_j^t defined, we are ready to compute the variation of E_0 in a neighborhood of the junction point P . Carrying out the calculation (3.71) in Ω_j for $j = 1, 2, 3$ and then applying the divergence theorem we find with the aid of (3.40) that

$$\begin{aligned} & \frac{d}{dt}\Big|_{t=0} \sum_{j=1}^3 \left(\int_{\Omega_j^t} (\operatorname{div} u_j^t)^2 dx \right) = \\ & - \int_{\Gamma_{01}} \left((\operatorname{div} u_1)^2 h_{01}^y + 2(\operatorname{div} u_1)(u_1 \cdot \tau_{01})\phi_1 \right) ds \\ & + \int_{\Gamma_{12}} \left((\operatorname{div} u_1)^2 h_{12}^y + 2(\operatorname{div} u_1)(u_1 \cdot \tau_{12})\phi_1 \right) ds \\ & - \int_{\Gamma_{12}} \left((\operatorname{div} u_2)^2 h_{12}^y + 2(\operatorname{div} u_2)(u_2 \cdot \tau_{12})\phi_2 \right) ds \\ & + \int_{\Gamma_{23}} \left((\operatorname{div} u_2)^2 h_{23}^y + 2(\operatorname{div} u_2)(u_2 \cdot \tau_{23})\phi_2 \right) ds \\ & - \int_{\Gamma_{23}} \left((\operatorname{div} u_3)^2 h_{23}^y + 2(\operatorname{div} u_3)(u_3 \cdot \tau_{23})\phi_3 \right) ds \\ & - \int_{\Gamma_{03}} \left((\operatorname{div} u_3)^2 h_{03}^y + 2(\operatorname{div} u_3)(u_3 \cdot \tau_{03})\phi_3 \right) ds. \end{aligned}$$

where we have used the fact that $u_1^\perp \cdot \nu_{01} = u_1 \cdot \tau_{01}$, $u_1^\perp \cdot \nu_{12} = u_1 \cdot \tau_{12}$, etc.

Now we appeal to the relations (5.8)–(5.11), along with the conditions $u_2 \cdot \tau_{12} = -u_1 \cdot \tau_{12}$ and $u_3 \cdot \tau_{23} = -u_2 \cdot \tau_{23}$ and perform an integration by parts to find

$$\frac{d}{dt}\Big|_{t=0} \sum_{j=1}^3 \left(\int_{\Omega_j^t} (\operatorname{div} u_j^t)^2 dx \right) =$$

$$\begin{aligned}
& \int_{\Gamma_{01}} \left\{ -(\operatorname{div} u_1)^2 + 2(\operatorname{div} u_1)'(u_1 \cdot \tau_{01}) \right\} h_{01}^\nu ds + \\
& \int_{\Gamma_{12}} \left\{ \left((\operatorname{div} u_1)^2 - (\operatorname{div} u_2)^2 - 4[(\operatorname{div} u_2)'(u_1 \cdot \tau_{12}) + (\operatorname{div} u_2)(u_1 \cdot \tau_{12})'] \right) h_{12}^\nu + 2(\operatorname{div} u_1 - \operatorname{div} u_2)(u_1 \cdot \tau_{12})\phi_1 \right\} ds \\
& \int_{\Gamma_{23}} \left\{ \left((\operatorname{div} u_2)^2 - (\operatorname{div} u_3)^2 - 4[(\operatorname{div} u_3)'(u_2 \cdot \tau_{23}) + (\operatorname{div} u_3)(u_2 \cdot \tau_{23})'] \right) h_{23}^\nu + 2(\operatorname{div} u_2 - \operatorname{div} u_3)(u_2 \cdot \tau_{23})\phi_2 \right\} ds \\
& \int_{\Gamma_{03}} \left\{ -(\operatorname{div} u_3)^2 + 2(\operatorname{div} u_3)'(u_3 \cdot \tau_{03}) \right\} h_{03}^\nu ds + \\
& + 2(\operatorname{div} u_1(p))(u_1(p) \cdot \tau_{01}(0))h_{01}^\nu(0) - 4 \operatorname{div} u_2(p)(u_1(p) \cdot \tau_{12}(0))h_{12}^\nu(0) \\
& - 4 \operatorname{div} u_3(p)(u_2(p) \cdot \tau_{23}(0))h_{23}^\nu(0) + 2(\operatorname{div} u_3(p))(u_3(p) \cdot \tau_{03}(0))h_{03}^\nu(0). \tag{5.12}
\end{aligned}$$

We turn now to calculating the variations of the four jump energies. We begin by invoking (5.4) to compute

$$\begin{aligned}
& \frac{d}{dt} \Big|_{t=0} \left(\int_{\Gamma_{01}^t} 1 ds + \int_{\Gamma_{03}^t} 1 ds \right) \\
& = \frac{d}{dt} \Big|_{t=0} \left(\int_0^{s_0} |r_{01}'(s)| ds + \int_0^{s_0} |r_{03}'(s)| ds \right) \\
& = \frac{d}{dt} \Big|_{t=0} \left(\int_0^{s_0} 1 + t(h_{01}^\tau)'(s) - h_{01}^\nu(s)\kappa_{01}(s) ds + \int_0^{s_0} 1 + t(h_{03}^\tau)'(s) - h_{03}^\nu(s)\kappa_{03}(s) ds \right) \\
& \int_0^{s_0} (h_{01}^\tau)'(s) - h_{01}^\nu(s)\kappa_{01}(s) ds + \int_0^{s_0} (h_{03}^\tau)'(s) - h_{03}^\nu(s)\kappa_{03}(s) ds
\end{aligned}$$

Thus,

$$\begin{aligned}
& \frac{d}{dt} \Big|_{t=0} \frac{K(0)}{2} \left(\mathcal{H}^1(\Gamma_{01}^t) + \mathcal{H}^1(\Gamma_{03}^t) \right) = \\
& - \frac{K(0)}{2} \left(\int_{\Gamma_{01}} h_{01}^\nu \kappa_{01} ds + \int_{\Gamma_{03}} h_{03}^\nu \kappa_{03} ds + h_{01}^\tau(0) + h_{03}^\tau(0) \right). \tag{5.13}
\end{aligned}$$

To compute the variation in the jump energies over Γ_{12}^t and Γ_{23}^t requires an expansion to $O(t)$ of the quantities $u^t \cdot \nu_{12}^t$ and $u^t \cdot \nu_{23}^t$. Substituting the expression for r_{12}^t from (5.3) into the formula for u_1^t from (5.6) and Taylor expanding in t we find with the use of (5.5) that along Γ_{12}^t we have

$$u^t \cdot \nu_{12}^t \sim \left(u_1(r_{12}^t(s)) + t u_1^\perp(r_{12}(s))\phi_1(r_{12}(s)) \right) \cdot \nu_{12}^t \sim \tag{5.14}$$

$$\begin{aligned}
& \left(u_1(r_{12} + t[h_{12}^\tau \tau_{12} + h_{12}^\nu \nu_{12}]) + t\phi_1(r_{12})u_1^\perp(r_{12}) \right) \cdot \left(\nu_{12} - t(h_{12}^\nu)' + \kappa_{12}h_{12}^\tau \tau_{12} \right) \\
& \sim u_1 \cdot \nu_{12} + t \left[\left(\phi_1 - h_{12}^\nu' - \kappa_{12}h_{12}^\tau \right) (u_1 \cdot \tau_{12}) + h_{12}^\tau (u_1' \cdot \nu_{12}) \right], \tag{5.15}
\end{aligned}$$

where u_1 and ϕ_1 in the expression above are evaluated at $x = r_{12}(s)$ and $u_1' = \frac{d}{ds}u_1(r_{12}(s))$. In the last line we have also used that our extension of u_1 was constant along ν_{12} to eliminate the term $\nabla u_1 \cdot \nu_{12}$ that would otherwise have been present upon Taylor expanding.

Similarly, we calculate that along Γ_{23} we have

$$u^t \cdot v'_{23} \sim u_2 \cdot v_{23} + t \left[(\phi_2 - h_{23}^y)' - \kappa_{23} h_{23}^\tau \right] (u_2 \cdot \tau_{23}) + h_{23}^\tau (u'_2 \cdot v_{23}). \quad (5.16)$$

From (5.15) and (5.16), along with (5.4) we can compute that

$$\begin{aligned} & \frac{d}{dt} \Big|_{t=0} \left(\int_{\Gamma_{12}} K(u^t \cdot v'_{12}) ds + \int_{\Gamma_{23}} K(u^t \cdot v'_{23}) ds \right) \\ &= \frac{d}{dt} \Big|_{t=0} \left(\int_0^{s_0} K(u^t(r'_{12}(s)) \cdot v'_{12}(s)) |r'_{12}'(s)| ds + \int_0^{s_0} K(u^t(r'_{23}(s)) \cdot v'_{23}(s)) |r'_{23}'(s)| ds \right) \\ &= \int_{\Gamma_{12}} K(u_1 \cdot v_{12}) (h_{12}^\tau)' - h_{12}^y \kappa_{12} ds + \\ & \int_{\Gamma_{12}} K'(u_1 \cdot v_{12}) \left((\phi_1 - h_{12}^y)' - h_{12}^\tau \kappa_{12} \right) (u_1 \cdot \tau_{12}) + h_{12}^\tau (u'_1 \cdot v_{12}) ds + \\ & \int_{\Gamma_{23}} K(u_2 \cdot v_{23}) (h_{23}^\tau)' - h_{23}^y \kappa_{23} ds + \\ & \int_{\Gamma_{23}} K'(u_2 \cdot v_{23}) \left((\phi_2 - h_{23}^y)' - h_{23}^\tau \kappa_{23} \right) (u_2 \cdot \tau_{23}) + h_{23}^\tau (u'_2 \cdot v_{23}) ds. \end{aligned}$$

Now since

$$\frac{d}{ds} [K(u_1 \cdot v_{12})] = (u'_1 \cdot v_{12}) - \kappa_{12} (u_1 \cdot \tau_{12})$$

and

$$\frac{d}{ds} [K(u_2 \cdot v_{23})] = (u'_2 \cdot v_{23}) - \kappa_{23} (u_2 \cdot \tau_{23}),$$

we have that

$$K(u_1 \cdot v_{12}) h_{12}^\tau' + K'(u_1 \cdot v_{12}) ((u'_1 \cdot v_{12}) - \kappa_{12} (u_1 \cdot \tau_{12})) h_{12}^\tau = \frac{d}{ds} [K(u_1 \cdot v_{12}) h_{12}^\tau]$$

and

$$K(u_2 \cdot v_{23}) h_{23}^\tau' + K'(u_2 \cdot v_{23}) ((u'_2 \cdot v_{23}) - \kappa_{23} (u_2 \cdot \tau_{23})) h_{23}^\tau = \frac{d}{ds} [K(u_2 \cdot v_{23}) h_{23}^\tau].$$

Using these last two identities in (5.17) and integrating by parts implies that

$$\begin{aligned} & \frac{d}{dt} \Big|_{t=0} \left(\int_{\Gamma_{12}} K(u^t \cdot v'_{12}) ds + \int_{\Gamma_{23}} K(u^t \cdot v'_{23}) ds \right) \\ &= - \int_{\Gamma_{12}} K(u_1 \cdot v_{12}) h_{12}^y \kappa_{12} ds + \int_{\Gamma_{12}} K'(u_1 \cdot v_{12}) (\phi_1 - h_{12}^y)' (u_1 \cdot \tau_{12}) ds \\ & - \int_{\Gamma_{23}} K(u_2 \cdot v_{23}) h_{23}^y \kappa_{23} ds + \int_{\Gamma_{23}} K'(u_2 \cdot v_{23}) (\phi_2 - h_{23}^y)' (u_2 \cdot \tau_{23}) ds \\ & - K(u_1(p) \cdot v_{12}(0)) h_{12}^\tau(0) - K(u_2(p) \cdot v_{23}(0)) h_{23}^\tau(0). \end{aligned} \quad (5.17)$$

Then invoking the criticality condition (3.41) from Theorem 3.9 and integrating by parts we can rewrite this identity as

$$\frac{d}{dt} \Big|_{t=0} \left(\int_{\Gamma_{12}} K(u^t \cdot v'_{12}) ds + \int_{\Gamma_{23}} K(u^t \cdot v'_{23}) ds \right)$$

$$\begin{aligned}
&= - \int_{\Gamma_{12}} K(u_1 \cdot \nu_{12}) h_{12}^\nu \kappa_{12} ds + L \int_{\Gamma_{12}} (\operatorname{div} u_2 - \operatorname{div} u_1) (\phi_1 - h_{12}^\nu)' (u_1 \cdot \tau_{12}) ds \\
&- \int_{\Gamma_{23}} K(u_2 \cdot \nu_{23}) h_{23}^\nu \kappa_{23} ds + L \int_{\Gamma_{23}} (\operatorname{div} u_3 - \operatorname{div} u_2) (\phi_2 - h_{23}^\nu)' (u_2 \cdot \tau_{23}) ds \\
&- K(u_1(p) \cdot \nu_{12}(0)) h_{12}^\tau(0) - K(u_2(p) \cdot \nu_{23}(0)) h_{23}^\tau(0) \\
&= \int_{\Gamma_{12}} \left\{ L(\operatorname{div} u_2 - \operatorname{div} u_1)' (u_1 \cdot \tau_{12}) + L(\operatorname{div} u_2 - \operatorname{div} u_1) (u_1 \cdot \tau_{12})' - K(u_1 \cdot \nu_{12}) \kappa_{12} \right\} h_{12}^\nu ds \\
&+ L \int_{\Gamma_{12}} (\operatorname{div} u_2 - \operatorname{div} u_1) (u_1 \cdot \tau_{12}) \phi_1 ds \\
&\int_{\Gamma_{23}} \left\{ L(\operatorname{div} u_3 - \operatorname{div} u_2)' (u_2 \cdot \tau_{23}) + L(\operatorname{div} u_3 - \operatorname{div} u_2) (u_2 \cdot \tau_{23})' - K(u_2 \cdot \nu_{23}) \kappa_{23} \right\} h_{23}^\nu ds \\
&+ L \int_{\Gamma_{23}} (\operatorname{div} u_3 - \operatorname{div} u_2) (u_2 \cdot \tau_{23}) \phi_2 ds \\
&- K(u_1(p) \cdot \nu_{12}(0)) h_{12}^\tau(0) + L(\operatorname{div} u_2(p) - \operatorname{div} u_1(p)) (u_1(p) \cdot \tau_{12}(0)) h_{12}^\nu(0) \\
&- K(u_2(p) \cdot \nu_{23}(0)) h_{23}^\tau(0) + L(\operatorname{div} u_3(p) - \operatorname{div} u_2(p)) (u_2(p) \cdot \tau_{23}(0)) h_{23}^\nu(0). \tag{5.18}
\end{aligned}$$

Now we can combine (5.12), (5.13) and (5.18), and through a use of the criticality conditions (3.54) and (3.55) of Theorem 3.12 we find that all integrals over the four curves Γ_{ij} drop, leaving only

$$\begin{aligned}
&\frac{d}{dt}\Big|_{t=0} E_0(u^t) = \\
&- \frac{K(0)}{2} (h_{01}^\tau(0) + h_{03}^\tau(0)) - K(u_1(p) \cdot \nu_{12}(0)) h_{12}^\tau - K(u_2(p) \cdot \nu_{23}(0)) h_{23}^\tau \\
&+ L \left\{ \operatorname{div} u_1(p) (u_1(p) \cdot \tau_{01}(0)) h_{01}^\nu(0) + \operatorname{div} u_3(p) (u_3(p) \cdot \tau_{03}(0)) h_{03}^\nu(0) \right\} \\
&- L \left\{ (\operatorname{div} u_1(p) + \operatorname{div} u_2(p)) (u_1(p) \cdot \tau_{12}(0)) h_{12}^\nu + (\operatorname{div} u_2(p) + \operatorname{div} u_3(p)) (u_2(p) \cdot \tau_{23}(0)) h_{23}^\nu \right\}
\end{aligned}$$

Recall now that $h_{01}^\tau(0) = X(p) \cdot \tau_{01}(0)$, $h_{01}^\nu(0) = X(p) \cdot \nu_{01}(0)$, etc. Thus, the arbitrary value of the vector $X(p)$, implies that a vanishing first variation $\frac{d}{dt}\Big|_{t=0} E_0(u^t) = 0$ leads to the necessary condition at a junction P of the form

$$\begin{aligned}
&\frac{K(0)}{2} (\tau_{01} + \tau_{03}) + K(u_1 \cdot \nu_{12}) \tau_{12} + K(u_2 \cdot \nu_{23}) \tau_{23} \\
&= L \left\{ \operatorname{div} u_1 (u_1 \cdot \tau_{01}) \nu_{01} + \operatorname{div} u_3 (u_3 \cdot \tau_{03}) \nu_{03} \right\} \\
&- L \left\{ (\operatorname{div} u_1 + \operatorname{div} u_2) (u_1 \cdot \tau_{12}) \nu_{12} + (\operatorname{div} u_2 + \operatorname{div} u_3) (u_2 \cdot \tau_{23}) \nu_{23} \right\} \tag{5.19}
\end{aligned}$$

where all quantities above are evaluated at the junction P .

□

Acknowledgments. PS, MR and RV acknowledge the support from NSF DMS-1362879 and a Simons Collaboration grant 585520. RV also acknowledges the support from an Indiana University College of Arts and Sciences Dissertation Year Fellowship. The research of RV was also partially supported by the Center for Nonlinear Analysis at Carnegie Mellon University and by NSF DMS-1411646. DG acknowledges the support from NSF DMS-1729538.

References

- [1] COMSOL Multiphysics® v. 5.3. <http://www.comsol.com/>. COMSOL AB, Stockholm, Sweden.
- [2] ALOUGES, F., RIVIÈRE, T., AND SERFATY, S. Néel and cross-tie wall energies for planar micro-magnetic configurations. *ESAIM Control Optim. Calc. Var.* 8 (2002), 31–68. A tribute to J. L. Lions.
- [3] AMBROSIO, L., DE LELLIS, C., AND MANTEGAZZA, C. Line energies for gradient vector fields in the plane. *Calc. Var. Partial Differential Equations* 9, 4 (1999), 327–255.
- [4] ANGENENT, S., AND GURTIN, M. E. Multiphase thermomechanics with interfacial structure 2. Evolution of an isothermal interface. *Arch. Ration. Mech. Anal.* 108, 3 (Nov 1989), 323–391.
- [5] AVILES, P., AND GIGA, Y. On lower semicontinuity of a defect energy obtained by a singular limit of the Ginzburg-Landau type energy for gradient fields. *Proc. Roy. Soc. Edinburgh Sect. A* 129, 1 (1999), 1–17.
- [6] BALDO, S. Minimal interface criterion for phase transitions in mixtures of Cahn-Hilliard fluids. *Ann. Inst. H. Poincaré Anal. Non Linéaire* 7, 2 (1990), 67–90.
- [7] BAUMAN, P., PARK, J., AND PHILLIPS, D. Analysis of nematic liquid crystals with disclination lines. *Arch. Ration. Mech. Anal.* 205, 3 (2012), 795–826.
- [8] BETHUEL, F., BREZIS, H., AND HÉLEIN, F. *Ginzburg-Landau vortices*, vol. 13 of *Progress in Nonlinear Differential Equations and their Applications*. Birkhäuser Boston, Inc., Boston, MA, 1994.
- [9] CONTI, S., AND DE LELLIS, C. Sharp upper bounds for a variational problem with singular perturbation. *Math. Ann.* 338, 1 (2007), 119–146.
- [10] DE LELLIS, C., AND OTTO, F. Structure of entropy solutions to the eikonal equation. *J. Eur. Math. Soc. (JEMS)* 5, 2 (2003), 107–145.
- [11] DEBENEDICTIS, A., AND ATHERTON, T. J. Shape minimisation problems in liquid crystals. *Liquid Crystals* 43, 13-15 (2016), 2352–2362.
- [12] DESIMONE, A., KOHN, R. V., MÜLLER, S., AND OTTO, F. A compactness result in the gradient theory of phase transitions. *Proc. Roy. Soc. Edinburgh Sect. A* 131, 4 (2001), 833–844.
- [13] FANG, J., TEER, E., KNOBLER, C. M., LOH, K.-K., AND RUDNICK, J. Boojums and the shapes of domains in monolayer films. *Phys. Rev. E* 56 (Aug 1997), 1859–1868.

- [14] FONSECA, I. The wulff theorem revisited. *Proceedings: Mathematical and Physical Sciences* 432, 1884 (1991), 125–145.
- [15] FONSECA, I., AND MÜLLER, S. Quasi-convex integrands and lower semicontinuity in L^1 . *SIAM J. Math. Anal.* 23, 5 (1992), 1081–1098.
- [16] GIUSTI, E. *Minimal surfaces and functions of bounded variation*, vol. 80 of *Monographs in Mathematics*. Birkhäuser Verlag, Basel, 1984.
- [17] GOLOVATY, D., STERNBERG, P., AND VENKATRAMAN, R. A Ginzburg-Landau type problem for highly anisotropic nematic liquid crystals. *To appear in SIAM J. Math. Anal.* (2018).
- [18] IGNAT, R. Singularities of divergence-free vector fields with values into \mathbb{S}^1 or \mathbb{S}^2 . Applications to micromagnetics. *Confluentes Math.* 4, 3 (2012), 1230001, 80.
- [19] JERRARD, R. L. Lower bounds for generalized Ginzburg-Landau functionals. *SIAM J. Math. Anal.* 30, 4 (1999), 721–746.
- [20] JIN, W., AND KOHN, R. V. Singular perturbation and the energy of folds. *J. Nonlinear Sci.* 10, 3 (2000), 355–390.
- [21] KIM, Y.-K., SHIYANOVSKII, S. V., AND LAVRETOVICH, O. D. Morphogenesis of defects and tactoids during isotropic-nematic phase transition in self-assembled lyotropic chromonic liquid crystals. *Journal of Physics: Condensed Matter* 25, 40 (2013), 404202.
- [22] KOHN, R. V., AND STERNBERG, P. Local minimisers and singular perturbations. *Proc. Roy. Soc. Edinburgh Sect. A* 111, 1-2 (1989), 69–84.
- [23] KURZKE, M., AND SPIRN, D. Gamma limit of the nonself-dual Chern-Simons-Higgs energy. *J. Funct. Anal.* 255, 3 (2008), 535–588.
- [24] LAMY, X., AND OTTO, F. On the regularity of weak solutions to Burgers’ equation with finite entropy production. *Calc. Var. PDE* 57, 4 (2018), Art. 94, 19.
- [25] LORENT, A. A simple proof of the characterization of functions of low Aviles Giga energy on a ball via regularity. *ESAIM Control Optim. Calc. Var.* 18, 2 (2012), 383–400.
- [26] LORENT, A. A quantitative characterisation of functions of low Aviles Giga energy in convex domains. *Ann. Sc. Norm. Super. Pisa Cl. Sci. (5)* 13, 1 (2014), 1–66.
- [27] MODICA, L. The gradient theory of phase transitions and the minimal interface criterion. *Arch. Ration. Mech. Anal.* 98, 2 (1987), 123–142.
- [28] MOTTRAM, N. J., AND NEWTON, C. J. Introduction to Q-tensor theory. *arXiv preprint arXiv:1409.3542* (2014).
- [29] MURAT, F. Compacité par compensation. *Ann. Scuola Norm. Sup. Pisa Cl. Sci. (4)* 5, 3 (1978), 489–507.
- [30] MURAT, F. L’injection du cône positif de H^{-1} dans $W^{-1,q}$ est compacte pour tout $q < 2$. *J. Math. Pures Appl. (9)* 60, 3 (1981), 309–322.

- [31] NOVACK, M. R. Dimension reduction for the Landau-de Gennes model: the vanishing nematic correlation length limit. *To appear in SIAM J. Math. Anal.* (2018).
- [32] OWEN, N. C., RUBINSTEIN, J., AND STERNBERG, P. Minimizers and gradient flows for singularly perturbed bi-stable potentials with a Dirichlet condition. *Proc. Roy. Soc. London Ser. A* 429, 1877 (1990), 505–532.
- [33] POLIAKOVSKY, A. On the Γ -limit of singular perturbation problems with optimal profiles which are not one-dimensional. Part I: The upper bound. *Differential Integral Equations* 26, 9-10 (2013), 1179–1234.
- [34] POLIAKOVSKY, A. On the Γ -limit of singular perturbation problems with optimal profiles which are not one-dimensional. Part II: The lower bound. *Israel J. Math.* 210, 1 (2015), 359–398.
- [35] RUDNICK, J., AND BRUINSMA, R. Shape of domains in two-dimensional systems: Virtual singularities and a generalized wulff construction. *Phys. Rev. Lett.* 74 (Mar 1995), 2491–2494.
- [36] SANDIER, E. Lower bounds for the energy of unit vector fields and applications. *J. Funct. Anal.* 152, 2 (1998), 379–403.
- [37] STERNBERG, P. The effect of a singular perturbation on nonconvex variational problems. *Arch. Ration. Mech. Anal.* 101, 3 (1988), 209–260.
- [38] TARTAR, L. Compensated compactness and applications to partial differential equations. In *Nonlinear analysis and mechanics: Heriot-Watt Symposium, Vol. IV*, vol. 39 of *Res. Notes in Math.* Pitman, Boston, Mass.-London, 1979, pp. 136–212.
- [39] VAN BIJNEN, R. M. W., OTTEN, R. H. J., AND VAN DER SCHOOT, P. Texture and shape of two-dimensional domains of nematic liquid crystals. *Phys. Rev. E* 86 (Nov 2012), 051703.